Programa de Doctorado en Bioingeniería
Universidad Miguel Hernández de Elche

Estudio de los roles de INCURVATA11 y CUPULIFORMIS2 como proteínas accesorias del Polycomb Repressive Complex 2 de Arabidopsis

Riad Nadi

Director de la tesis
José Luis Micol Molina

Elche, 2024

Estudio de los roles de INCURVATA11 y CUPULIFORMIS2 como proteínas accesorias del Polycomb Repressive Complex 2 de Arabidopsis

Trabajo realizado por el Ingeniero Riad Nadi, en la Unidad de Genética del Instituto de Bioingeniería de la Universidad Miguel Hernández de Elche, para optar al grado de Doctor.

Elche, 19 de febrero de 2024

La presente Tesis Doctoral, titulada “Estudio de los roles de INCURVATA11 y CUPULIFORMIS2 como proteínas accesorias del Polycomb Repressive Complex 2 de Arabidopsis”, se presenta bajo la modalidad de **tesis por compendio** de las siguientes **publicaciones**:

Nadi, R., Mateo-Bonmatí, E., Juan-Vicente, L., y Micol, J.L. (2018). The 2OGD superfamily: emerging functions in plant epigenetics and hormone metabolism. *Molecular Plant* **11**,1222-1224.

Nadi, R., Juan-Vicente, L., Mateo-Bonmatí, E., Micol, J.L. (2023). The unequal functional redundancy of Arabidopsis *INCURVATA11* and *CUPULIFORMIS2* is not dependent on genetic background. *Frontiers in Plant Science* **14**, 1239093.

JOSÉ LUIS MICOL MOLINA, Catedrático de Genética de la Universidad Miguel Hernández de Elche (UMH)

HAGO CONSTAR:

Que el presente trabajo ha sido realizado bajo mi dirección y recoge fielmente la labor desarrollada por el Ingeniero Riad Nadi para optar al grado de Doctor. Las investigaciones reflejadas en esta memoria se han desarrollado íntegramente en la Unidad de Genética del Instituto de Bioingeniería de la UMH, según los términos y condiciones definidos en el Plan de Investigación del doctorando, y cumpliendo los objetivos inicialmente previstos de forma satisfactoria y lo establecido en el Código de Buenas Prácticas de la UMH.

José Luis Micol Molina

Elche, 19 de febrero de 2024

PIEDAD NIEVES DE AZA MOYA, Coordinadora del Programa de Doctorado en Bioingeniería de la Universidad Miguel Hernández de Elche por Resolución Rectoral 02976/2022, de 11 de noviembre de 2022

HACE CONSTAR:

Que da su conformidad a la presentación de la Tesis Doctoral de Don Riad Nadi, titulada "Estudio de los roles de INCURVATA11 y CUPULIFORMIS2 como proteínas accesorias del Polycomb Repressive Complex 2 de Arabidopsis", que se ha desarrollado en el Programa de Doctorado en Bioingeniería bajo la dirección del profesor José Luis Micol Molina.

Lo que firmo en Elche, a instancias del interesado y a los efectos oportunos, a diecinueve de febrero de dos mil veinticuatro.

Profesora PIEDAD NIEVES DE AZA MOYA
Coordinadora del Programa de Doctorado en Bioingeniería

A mis padres Saad y Dalila y mi hermano Racim

A mi mujer Karima Irekti

A mi hijo Malik

ÍNDICE DE MATERIAS

ÍNDICE DE FIGURAS II

ÍNDICE DE TABLAS II

I.- PREFACIO 1

II.- RESUMEN 2

III.- SUMMARY 5

IV.- INTRODUCCIÓN 8
IV.1.- Componentes y funciones de la maquinaria epigenética de las plantas 8
IV.1.1.- La epigenética de las plantas 8
IV.1.2.- Los complejos represores Polycomb y sus interactores 10
IV.2.- Funciones epigenéticas de las dioxigenasas dependientes de 2-oxoglutarato y Fe^{2+} 16
IV.3.- Antecedentes y objetivos 17
IV.3.1.- Una disección genética del desarrollo foliar 17
IV.3.2.- Componentes de la maquinaria epigenetica de Arabidopsis estudiados en el laboratorio de J.L. Micol 18
IV.3.3.- Estudios previos de las proteínas de la familia CUPULIFORMIS 19
IV.3.3.1.- INCURVATA11 y CUPULIFORMIS2 son componentes de la maquinaria epigenética 19
IV.3.3.2.- ICU11 es muy probablemente una proteína accesoria del PRC2 21
IV.3.4.- Objetivos de esta Tesis 22

V.- MATERIALES Y MÉTODOS 25

VI.- RESULTADOS Y DISCUSIÓN 27

VII.- CONCLUSIONES Y PERSPECTIVAS 30

VIII.- BIBLIOGRAFÍA DE LOS APARTADOS IV-VII 33

IX.- PUBLICACIONES 42

X.- OTRAS PUBLICACIONES 67

XI.- AGRADECIMIENTOS 116

ÍNDICE DE FIGURAS

Figura 1.- Proteínas del PcG conservadas en *Drosophila melanogaster*, *Homo sapiens* y *Arabidopsis thaliana* 14
Figura 2.- Modificación de la cromatina por el PRC1 y el PRC2..... 15
Figura 3.- Evidencias genéticas de la redundancia funcional de *ICU11* y *CP2* 20

ÍNDICE DE TABLAS

Tabla 1.- Componentes principales y proteínas accesorias del PRC2 de Arabidopsis 11
Tabla 2.- Componentes principales y proteínas accesorias del PRC1 de Arabidopsis 12

I.- PREFACIO

I.- PREFACIO

Siguiendo la normativa de la Universidad Miguel Hernández de Elche para la "Presentación de Tesis Doctorales por compendio de publicaciones", este documento se ha dividido en las partes siguientes:

I.- Este *Prefacio*.

II.- Un *Resumen* en español.

III.- Un *Summary* en inglés.

IV.- Una *Introducción*, en la que se presenta el tema de la Tesis y los antecedentes y objetivos del trabajo realizado.

V.- Un resumen de los *Materiales y métodos* de las publicaciones de la Tesis.

VI.- Un resumen de los *Resultados y discusión* de las publicaciones de la Tesis.

VII.- Un resumen de las *Conclusiones y perspectivas* del trabajo realizado.

VIII.- Una *Bibliografía de los apartados IV-VII*; algunas de las referencias que incluye se repiten en las bibliografías de los artículos incluidos en esta memoria.

IX.- Un apartado de *Publicaciones,* que incluye las tres siguientes.

Nadi, R., Mateo-Bonmatí, E., Juan-Vicente, L., y Micol, J.L. (2018). The 2OGD superfamily: emerging functions in plant epigenetics and hormone metabolism. *Molecular Plant* **11**, 1222-1224 [FI: 12,084].

Nadi, R., Juan-Vicente, L., Mateo-Bonmatí, E., y Micol, J.L. (2023). The unequal functional redundancy of Arabidopsis *INCURVATA11* and *CUPULIFORMIS2* is not dependent on genetic background. *Frontiers in Plant Science* **14**, 1239093 [FI: 5,6].

Nadi, R., Juan-Vicente, L., Lup, S.D., Fernández, Y., Rubio, V., y Micol, J.L. Overlapping roles of Arabidopsis INCURVATA11 and CUPULIFORMIS2 as Polycomb Repressive Complex 2 accessory proteins. Pendiente de aceptación.

Los "Supplemental Datasets" de este último artículo no se han incluido en esta memoria por su gran longitud. Las correspondientes hojas de cálculo se remitirán a los miembros del tribunal en formato electrónico.

X.- Un apartado de *Agradecimientos*.

Con el fin de reducir redundancias innecesarias e inconvenientes, se han mencionado en los apartados VI y VII solo los resultados y conclusiones más relevantes obtenidos en esta Tesis. El apartado IX recoge íntegramente el trabajo realizado.

II.- RESUMEN

II.- RESUMEN

Como primera parte de esta tesis se hizo una revisión de las publicaciones sobre la superfamilia de las dioxigenasas dependientes de 2-oxoglutarato (también denominado 2-cetoglutarato o α-cetoglutarato) y Fe^{2+} (2OGD), que son enzimas oxidativas cuyo sitio activo incluye dos histidinas y en la mayoría de los casos un residuo de ácido aspártico o glutámico. Este motivo conservado cataliza reacciones de desmetilación, desmetilenación, hidroxilación, halogenación, desaturación, ruptura o cierre de anillos, y epimerización. El genoma de Arabidopsis contiene más de 150 genes que codifican proteínas 2OGD, a las que se ha clasificado en los clados DOXA, DOXB, DOXC y JMJ. Las proteínas DOXA son homólogas de la dioxigenasa dependiente de α-cetoglutarato AlkB (por Alkylation B) de *Escherichia coli*, una enzima de reparación del ADN que revierte las metilaciones de los átomos N^1 de la adenina y N^3 de la citosina causadas por agentes alquilantes. Las proteínas DOXC constituyen la clase más amplia y diversa de las 2OGD, actuando en facetas del metabolismo vegetal como la biosíntesis y/o el catabolismo de la auxina y los lignanos, isoprenoides, flavonoides, glucosinolatos, alcaloides, estrigolactonas y cumarinas, y tienen importantes papeles en la homeostasis del etileno, las giberelinas, la auxina y el ácido salicílico. Las proteínas JMJ contienen un dominio Jumonji C (JmjC) y catalizan la desmetilación por hidroxilación de lisinas en las histonas. Las proteínas DOXB animales juegan un papel crucial en la síntesis del colágeno, el componente estructural mayoritario del espacio extracelular de muchos tejidos. Algunas proteínas DOXB de las plantas modifican postraduccionalmente determinadas O-glicoproteínas ricas en hidroxiprolina, como las extensinas, que son similares al colágeno. La familia CUPULIFORMIS (CP) incluye cinco proteínas DOXB: INCURVATA11 (ICU11), CP2, CP3, CP4 y CP5. A diferencia de todas las DOXB estudiadas hasta ahora, ICU11 y CP2 son nucleoplásmicas y tienen funciones epigenéticas.

Antes del comienzo de esta tesis se habían descrito dos mutantes *incurvata11* (*icu11*), que manifiestan hiponastia foliar y floración temprana. Estos rasgos morfológicos también los causan las mutaciones en genes que codifican algunos componentes de la maquinaria epigenética, como *CURLY LEAF* (*CLF*), que pertenece al grupo Polycomb (PcG). Las proteínas del PcG forman parte de dos Polycomb Repressive Complexes (PRC) heteromultiméricos con distintas actividades epigenéticas: el PRC1 es una ligasa de ubiquitina de la histona H2A, y el PRC2, una metiltransferasa de la lisina 27 de la histona H3 (H3K27). El PRC1 de Arabidopsis tiene cinco componentes principales, y el PRC2, ocho, uno de los cuales es EMBRYONIC FLOWER 2 (EMF2). Estos PRC también cuentan con proteínas

accesorias, que facilitan la incorporación del complejo a determinadas regiones de la cromatina. Un ejemplo de ello es EMBRYONIC FLOWER 1 (EMF1), que contribuye al depósito de la marca epigenética H3K27me3 en un subgrupo de los genes diana del PRC2 y también participa en la monoubiquitinación de la H2A por el PRC1.

El fenotipo morfológico de los mutantes *icu11* es relativamente débil, y los *cp2* son indistinguibles del tipo silvestre. Sin embargo, los dobles mutantes *icu11 cp2* muestran un fenotipo letal postembrionario muy similar al de los mutantes simples *emf1* y *emf2* más extremos: no manifiestan desarrollo vegetativo y forman órganos parecidos a flores inmediatamente después de la germinación, a los que se denomina flores embrionarias. También forma flores embrionarias el triple mutante *telomere repeat binding1-2* (*trb1-2*) *trb2-1 trb3-2*. Las proteínas TRB1, TRB2 y TRB3 se unen a las secuencias repetitivas teloméricas para el mantenimiento de los telómeros y además son proteínas accesorias del PRC2, al que reclutan a determinados genes para el depósito de la marca H3K27me3.

Col-0 es la estirpe silvestre de referencia y la de uso experimental más común en Arabidopsis. La redundancia funcional entre *ICU11* y *CP2* se infirió del estudio de los fenotipos sinérgicos de las combinaciones dobles mutantes y sesquimutantes de las mutaciones *icu11* y *cp2*, cuyos fondos genéticos eran S96 (*icu11-1*), Ws-2 (*icu11-2*) y Col-0 (*cp2-1, cp2-2* y *cp2-3*). En consecuencia, todas sus combinaciones genéticas tenían fondos genéticos híbridos S96/Col-0 o Ws-2/Col-0. Para evitar los eventuales efectos de los modificadores presentes en los fondos S-96 y Ws-2, la segunda parte de esta Tesis ha consistido en la obtención y caracterización de cuatro nuevos alelos de *ICU11*, mutagenizando las estirpes silvestres S96 (*icu11-4* e *icu11-7*) y Col-0 (*icu11-5* e *icu11-6*) mediante la tecnología CRISPR/Cas9. Los alelos *icu11-5* e *icu11-6* son aparentemente nulos, ya que presentan pequeñas deleciones que desfasan la pauta de lectura del primer exón del gen *ICU11* y originan un codón de terminación prematura, y no parecen haber sufrido mutaciones adicionales indeseadas. También manifiestan menor hiponastia foliar que *icu11-1*, aunque similares floración temprana e interacciones genéticas con los alelos mutantes de *CP2*. Hemos usado las mutaciones *icu11-5* e *icu11-6* para confirmar que la ausencia simultánea de las proteínas ICU11 y CP2 es letal y que los fenotipos de los dobles mutantes y sesquimutantes *icu11 cp2* son independientes de su fondo genético y no manifiestan especificidad de alelo.

En nuestro estudio de los mutantes *icu11-5 cp2-1* y *emf2-3* hemos establecido que su letalidad puede ser paliada si se cultivan en medio suplementado con un 3% en sacarosa, en lugar del 1% habitual, lo que a su vez permite estudiar su fenotipo morfológico a lo largo de todo su ciclo de vida. En esta condición de cultivo, las plantas *icu11-5 cp2-1* y *emf2-3* desarrollan tallos, hojas caulinares pequeñas, flores que manifiestan transformaciones

homeóticas de sépalos y pétalos en carpelos, y silicuas que rinden semillas que solo en algunos casos resultan viables. Estas observaciones indican que la letalidad de las flores embrionarias *icu11 cp2* y *emf2-3* se debe a su escasa capacidad fotosintética, derivada de su carencia de hojas vegetativas, y que ICU11 y/o CP2 se requieren para la especificación de la identidad de los órganos florales.

En la tercera parte de esta Tesis se ha intentado dilucidar la función de ICU11 y CP2 mediante análisis interactómicos y transcriptómicos. Durante el transcurso de esta Tesis, otros autores publicaron un artículo en el que se describía un tercer alelo de *ICU11* (*icu11-3*) y se demostraba, mediante un ensayo de coinmunoprecipitación, que la proteína ICU11 interacciona con varios componentes principales del PRC2. Hemos realizado escrutinios de interactores de las proteínas ICU11 y CP2 mediante purificación por afinidad en tándem. Hemos confirmado así que ICU11 interacciona con los componentes principales del PRC2 EMF2, FERTILIZATION INDEPENDENT ENDOSPERM (FIE), SWINGER (SWN) y MULTICOPY SUPPRESSOR OF IRA1 (MSI1) y con las proteínas accesorias de este complejo EMF1, TRB1, TRB2 y TRB3, y demostrado que también lo hace con otras proteínas nucleares. CP2 no presentó interacciones con componentes principales o proteínas accesorias del PRC2, aunque sí lo hizo con TRB4 y TRB5, miembros poco caracterizados de la familia TRB, y otras proteínas nucleares.

También hemos realizado ensayos de complementación de fluorescencia bimolecular mediante transformación transitoria de hojas de *Nicotiana benthamiana*, en los que tanto ICU11 como CP2 interaccionaron con los componentes principales del PRC2 SWN y CLF, y con sus proteínas accesorias TRB1 y TRB3. No hemos encontrado interacción alguna entre ICU11 y CP2, lo que indica que no forman heteromultímeros.

Hemos llevado a cabo mediante secuenciación masiva de ARN un análisis comparativo de los perfiles transcriptómicos de plántulas de Col-0, *cp2-1* e *icu11-5,* flores embrionarias de *icu11-5 cp2-1* y *emf2-3*, e inflorescencias de Col-0. Este análisis ha revelado la gran semejanza entre los perfiles del doble mutante *icu11-5 cp2-1* y el mutante simple *emf2-3*, así como con los de otros mutantes portadores de alelos de genes que codifican componentes principales del PRC2. Muchos de los genes desregulados en las flores embrionarias *icu11-5 cp2-1* son portadores de la marca represora H3K27me3 en Col-0.

Considerados en conjunto, nuestros resultados confirman que ICU11 es una proteína accesoria del PRC2, revelan que muy probablemente CP2 también lo sea, y aportan nuevos indicios de su relación funcional y de sus funciones epigenéticas parcialmente solapantes.

III.- SUMMARY

III.- SUMMARY

As a first part of this Thesis, we reviewed the current knowledge on the 2-oxoglutarate (also known as 2-ketoglutarate or α-ketoglutarate) and Fe^{2+}-dependent dioxygenase (2OGD) superfamily, which includes oxidative enzymes with an active site containing two histidines and, in most cases, one aspartic or glutamic acid residue. This conserved motif allows 2OGDs to catalyze demethylation, demethylenation, hydroxylation, halogenation, desaturation, ring cleavage, ring closure and epimerization reactions. The Arabidopsis genome contains more than 150 genes encoding 2OGD proteins, which have been classified into the DOXA, DOXB, DOXC and JMJ clades. DOXA proteins are homologs of the *Escherichia coli* α-ketoglutarate-dependent dioxygenase AlkB (for Alkylation B), a DNA repair enzyme that reverses the N^1-methyladenine and N^3-methylcytosine lesions caused by alkylating agents. DOXCs are the largest and most functionally diverse class of 2OGDs, acting in plant metabolism, including biosynthesis and/or catabolism of lignans, isoprenoids, flavonoids, glucosinolates, alkaloids, auxin, strigolactones, and coumarins, and playing important roles in ethylene, gibberellin, auxin, and salicylic acid homeostasis. The Jumonji C (JmjC) domain-containing (JMJ) proteins function in the demethylation by hydroxylation of lysine residues in histones. Animal DOXBs play a key role in the biosynthesis of collagen, the main structural component of the extracellular space in many tissues. Some plant DOXBs catalyze post-translational modifications of cell wall hydroxyproline-rich O-glycoproteins, such as extensins, which are similar to collagen. The CUPULIFORMIS (CP) family includes five DOXBs: INCURVATA11 (ICU11), CP2, CP3, CP4 and CP5. Unlike all other studied DOXBs, ICU11 and CP2 are nucleoplasmic and have epigenetic functions.

The two *icu11* mutants described before the beginning of this Thesis have hyponastic leaves and early flowering, traits that they share with mutants affected in genes encoding some components of the epigenetic machinery, such as *CURLY LEAF* (*CLF*), a Polycomb-group (PcG) gene. PcG proteins form part of two heteromultimeric Polycomb Repressive Complexes (PRCs) with different epigenetic activities: PRC1 is a H2A ubiquitin ligase, and PRC2 a lysine 27 of histone H3 (H3K27) methyl transferase. PRCs have core components; for example, EMBRYONIC FLOWER 2 (EMF2) is one of the eight known core components of Arabidopsis PRC2. PRCs also have accessory proteins, which facilitate their recruitment to specific chromatin regions; for example, EMBRYONIC FLOWER1 (EMF1) contributes to H3K27me3 deposition in a subgroup of PRC2 target genes, and is also required for H2A monoubiquitination by PRC1.

The *icu11* mutants have the mild morphological phenotype mentioned above, and the *cp2* mutants are indistinguishable from wild type. However, the *icu11 cp2* double mutants exhibit a severe, post-embryonic lethal phenotype reminiscent of *emf1* and *emf2* single mutants: lack of vegetative development and formation of flower-like organs immediately after germination, the so-called embryonic flowers. Embryonic flowers are also developed by the *telomere repeat binding1-2* (*trb1-2*) *trb2-1 trb3-2* triple mutant. Arabidopsis TRB1, TRB2 and TRB3 bind to the telomeric repeat DNA sequences to maintain chromosome ends and are assumed to be PRC2 accessory proteins, given that they recruit this complex to certain genes for H3K27me3 deposition.

Col-0 is the reference wild-type Arabidopsis accession and the most commonly used. The unequal functional redundancy between *ICU11* and *CP2* was inferred from the study of the synergistic phenotypes of the double mutant and sesquimutant combinations of *icu11* and *cp2* mutations, which had been isolated in the S96 and Col-0 genetic backgrounds, respectively. Therefore, all their genetic combinations had S96/Col-0 or Ws-2/Col-0 hybrid genetic backgrounds. In the second part of this Thesis and to avoid potential confounding effects arising from different genetic backgrounds, we generated via CRISPR/Cas9 genome editing the *icu11-4* and *icu11-7* mutants in the S96 background, and *icu11-5* and *icu11-6* in Col-0. The latter mutants carry apparently null alleles of *ICU11*, since they carry small deletions that cause frameshifts in the first exon of this gene, which in turn originate premature stop codons, and lack undesired offtarget mutations. The *icu11-5* and *icu11-6* mutants also show leaf hyponasty to a lesser extent than Col-0, but equivalent early flowering and synergistic genetic interactions with *cp2* alleles. We used the *icu11-5* e *icu11-6* mutants to confirm that the simultaneous absence of ICU11 and CP2 is lethal and to demonstrate that the unequal functional redundancy of *ICU11* and *CP2* and demonstrated that it is not allele or genetic background specific.

In our study of the *icu11 cp2* and *emf2-3* mutants, we found that an increase from 1% to 3% in sucrose content in the culture medium partially rescues their post-germinative lethality, allowing the study of their morphological phenotypes throughout the entire life cycle. In such culture condition, *icu11 cp2* and *emf2-3* developed shoots, small cauline leaves, flowers exhibiting homeotic transformations of sepals and petals into carpels, and siliques that rendered seeds that in only a few cases were viable. These observations indicate that the lethality of the *icu11 cp2* and *emf2-3* embryonic flowers is caused by their poor photosynthetic capacity, as a consequence of their lack of rosette leaves. We thus established that ICU11 and/or CP2 are required for proper floral organ identity specification.

In the third part of this Thesis, we attempted to assess the function of ICU11 and CP2 through interactomic and transcriptomic analyses. During the course of the current Thesis, other authors described a third allele of *ICU11* (*icu11-3*), found using co-immunoprecipitation that ICU11 interacts with several PRC2 core components, and thus proposed that it is a PRC2 acessory protein. We performed a Tandem Affinity Purification (TAP)-based screen for interactors of ICU11 and of CP2. In our TAP assays, ICU11 interacted with the PRC2 core components EMF2, FERTILIZATION INDEPENDENT ENDOSPERM (FIE), SWINGER (SWN) and MULTICOPY SUPPRESSOR OF IRA1 (MSI1) and with the PCR2 accessory proteins EMF1, TRB1, TRB2 and TRB3, as well as with other nuclear proteins. CP2 did not interact with PRC2 core components, neither with TRB1, TRB2 or TRB3, but it did with TRB4 and TRB5, poorly characterized members of the TRB family, and other nuclear proteins.

Through Bimolecular Fuorescence Complementation (BiFC) assays by transient transformation of *Nicotiana benthamiana* leaves, we found both ICU11 and CP2 to interact with the PRC2 core components SWN y CLF, as well as with the PRC2 accessory proteins TRB1 y TRB3. No interaction between ICU11 and CP2 was detected by TAP or BiFC, indicating that these proteins do not heteromultimerize.

We also conducted RNA-seq analyses of the Col-0, *cp2-1* and *icu11-5* seedlings, *icu11-5 cp2-1* and *emf2-3* embryonic flowers and Col-0 inflorescences, which revealed strong similarities in the transcriptomic profiles of *icu11-5 cp2-1* with *emf2-3* and with other single mutants affected in genes encoding PRC2 core components. A significant proportion of the genes misregulated in *icu11-5 cp2-1* are known to harbor H3K27me3 repressive marks in Col-0.

Taken together, our results confirm that ICU11 is a PRC2 accessory protein, reveal that CP2 is also a likely PRC2 accessory protein, and provide further genetic and molecular evidence of the functional relationship of ICU11 and CP2, and of their partially overlapping epigenetic functions.

IV.- INTRODUCCIÓN

IV.- INTRODUCCIÓN

IV.1.- Componentes y funciones de la maquinaria epigenética de las plantas

IV.1.1.- La epigenética de las plantas

Las acepciones modernas de la palabra epigenética son diversas: algunos autores consideran epigenético cualquier cambio en la cromatina (Springer y Schmitz, 2017), mientras que otros definen la epigenética como "el estudio de las variaciones en la función de los genes que son heredables mitótica o meióticamente y que no implican cambios en la secuencia del ADN" (Wu y Morris, 2001).

Un ejemplo clásico de fenómeno epigenético de las plantas es la paramutación, que se manifiesta en algunos heterocigotos para dos alelos de un gen cuyos niveles de expresión son distintos; en tales heterocigotos, uno de los dos alelos experimenta un cambio heredable de su nivel de expresión como consecuencia de la presencia del otro (Pilu, 2015; Hollick, 2017; Bente *et al.*, 2021). También son ejemplos de este tipo de fenómenos la impronta génica (la expresión de uno de los dos alelos de un gen en función de su origen paterno o materno; Gehring y Satyaki, 2017; Satyaki y Gehring, 2017; Batista y Köhler, 2020), el silenciamiento de ciertos transgenes y la inactivación de algunos transposones (Holoch y Moazed, 2015; Choi y Lee, 2020; Almeida *et al.*, 2022; Liu y Zhao, 2023). La gametogénesis masculina y femenina y el desarrollo temprano de la semilla (Wang y Köhler, 2017; Gehring, 2019; Han *et al.*, 2019) y la vernalización (Bloomer y Dean, 2017; Whittaker y Dean, 2017; He y Li, 2018; Xi *et al.*, 2020) tienen también una base epigenética demostrada, así como la aclimatación y la adquisición de resistencia sistémica (Pikaard y Mittelsten Scheid, 2014). Otros aspectos del desarrollo y la fisiología de las plantas están controlados epigenéticamente, al menos parcialmente, como su plasticidad morfológica, las respuestas a la luz y al estrés y el momento de la floración (He *et al.*, 2020; Ueda y Seki, 2020).

La epigenética ha desempeñado un papel cuya importancia está aún por establecer en la evolución de las angiospermas y la domesticación de las plantas cultivadas (Ding y Chen, 2018), participa en la memoria inmune (Ramirez-Prado *et al.*, 2018) y parece contribuir a la heterosis (Groszmann *et al.*, 2011; Groszmann *et al.*, 2013; Fujimoto *et al.*, 2018), a diferentes eventos del ciclo celular y al control del reloj circadiano (Barneche *et al.*, 2014). Una mejor comprensión de la variación epigenética natural y de sus causas permitiría la ingeniería epigenética, a nivel genómico, de las plantas cultivadas (Springer y Schmitz, 2017).

En los animales, la especificación y el mantenimiento de los destinos celulares están determinados epigenéticamente en gran medida. De hecho, se piensa que la diferenciación durante el desarrollo animal es un proceso fundamentalmente epigenético. Determinados

factores epigenéticos regulan las transiciones más importantes entre las fases del desarrollo embrionario de los mamíferos, como las que ocurren durante la gastrulación y en los blastocistos, así como en la especificación de los destinos celulares del cuerpo adulto. La concepción moderna de los papeles que juegan los componentes de la maquinaria epigenética en el desarrollo de los metazoos se debe en parte a estudios realizados con células madre pluripotentes, así como del desarrollo embrionario normal y de enfermedades humanas asociadas a la represión o activación erróneas de determinadas rutas reguladoras (Lee y Young, 2013; Chen y Dent, 2014; Feinberg *et al.*, 2016; Lee *et al.*, 2019; Mistry *et al.*, 2019; Li *et al.*, 2020; Park *et al.*, 2020; Chen *et al.*, 2022). Dado que el número de procesos regulados epigenéticamente parece netamente mayor en los animales que en las plantas, podría concluirse que la evolución ha concedido a la epigenética un protagonismo menor en el reino vegetal que en el animal. Una manera alternativa de interpretar esta observación es que es mucho lo que nos queda por aprender sobre la epigenética de las plantas.

La maquinaria epigenética vegetal está integrada por decenas de factores reguladores, que incluyen a moléculas de ARN no codificantes y proteínas implicadas en la metilación del ADN, la modificación química de las histonas, y su posicionamiento en los nucleosomas. Este amplio repertorio de componentes de la maquinaria epigenética está codificado por miembros de familias génicas que a menudo incluyen grupos de genes parálogos con funciones parcialmente redundantes, lo que hace a las plantas particularmente adecuadas para la disección genética de los fenómenos epigenéticos. En efecto, como consecuencia de la redundancia entre parálogos, los alelos nulos de no pocos genes que codifican proteínas con funciones epigenéticas son viables en las plantas y por tanto pueden ser estudiados, mientras que mutaciones similares en sus ortólogos animales son frecuentemente letales (Pikaard y Mittelsten Scheid, 2014; Provart *et al.*, 2016; Wu *et al.*, 2021).

Se conocen unos 130 genes que codifican componentes de la maquinaria epigenética de las plantas, que pueden clasificarse en cinco grupos, en función de la actividad de sus productos: (a) enzimas que catalizan modificaciones químicas del ADN (como la metilación de la citosina) o de las histonas (como la metilación, la acetilación, la fosforilación y la ubiquitinación), (b) proteínas del grupo Polycomb y sus interactores, (c) proteínas organizadoras del nucleosoma (también conocidas como remodeladoras de la cromatina, que controlan la accesibilidad de los factores de transcripción al ADN), y (d) proteínas y moléculas de ARN que participan en la metilación de ADN dirigida por ARN (RdDM, por RNA-directed DNA methylation; Chen y Dent, 2014; Pikaard y Mittelsten Scheid, 2014).

Se denomina marcas epigenéticas a las modificaciones covalentes del ADN y las histonas que realiza la maquinaria epigenética. En los eucariotas, la metilación del ADN suele

darse en la citosina, formándose 5-metilcitosina (m^5C), una marca represora asociada al silenciamiento transcripcional. En *Arabidopsis thaliana* (en adelante, Arabidopsis) y otras plantas superiores, la m^5C aparece en los contextos CG, CHG (en donde H es A, C o T) y CHH, como consecuencia de la actividad de enzimas que catalizan la metilación *de novo*, la de mantenimiento y la desmetilación (Seymour y Becker, 2017; Bartels *et al.*, 2018; Zhang *et al.*, 2018; Alagia y Gullerova, 2022; Fang *et al.*, 2022; He *et al.*, 2022).

La modificación postraduccional de las histonas es particularmente importante en la regulación epigenética de la expresión génica. Son ejemplos de marcas represoras la H3K9me2 (el producto de la dimetilación de la lisina 9 de la histona H3) y las H3K9me3, H3K27me2 y H3K27me3. Son ejemplos de marcas activadoras las H3K4me2, H3K4me3 y H3K9me1. Las proteínas y los complejos proteicos que actúan en la regulación epigenética interaccionando directa o indirectamente con las histonas pueden agruparse en tres clases: las que añaden (escritoras), eliminan (borradoras), o reconocen (lectoras) las marcas epigenéticas; son ejemplos de estas actividades enzimáticas las acetiltransferasas y metiltransferasas de las histonas, las desacetilasas y desmetilasas de las histonas, y las remodeladoras de la cromatina, respectivamente (Rothbart y Strahl, 2014; Liang *et al.*, 2020).

IV.1.2.- Los complejos represores Polycomb y sus interactores

En la regulación epigenética de la expresión génica durante el desarrollo o las respuestas al ambiente de *Drosophila melanogaster* juegan un papel importante dos tipos de proteínas con actividades opuestas: las activadoras de la transcripción, del grupo Trithorax (TrxG), y las represoras, del grupo Polycomb (PcG) (Hennig y Derkacheva, 2009; Butenko y Ohad, 2011). Las proteínas del PcG forman parte de los Polycomb Repressive Complex 1 (PRC1) y PRC2, cuyas funciones conservadas se han demostrado tanto en los animales como en las plantas (Holec y Berger, 2012; Sowpati *et al.*, 2015).

No pocas de las proteínas que integran la maquinaria epigenética se han descubierto en escrutinios genéticos realizados en distintas especies modelo. El gen *Polycomb*, miembro fundador del PcG de genes represores, fue identificado merced al aislamiento de un mutante de *Drosophila melanogaster* (Lewis, 1947). El primer gen del PcG descrito en Arabidopsis, *CURLY LEAF* (*CLF*), fue identificado cincuenta años después (Goodrich *et al.*, 1997). CLF es un componente principal del PRC2 y contiene un dominio SET, cuyo nombre deriva de los de las proteínas Suppresor of variegation 3-9 [Su(var)3-9], Enhancer of zeste [E(z)] y Trithorax (Trx) de *Drosophila melanogaster*. El dominio SET de CLF es responsable de su actividad metiltransferasa y presenta una gran homología con el de la proteína E(z) de *Drosophila melanogaster* (Tabla 1, en la página 11; Jones y Gelbart, 1990; Goodrich *et al.*, 1997).

Tabla 1.- Componentes principales y proteínas accesorias del PRC2 de Arabidopsis

	Proteína	Función	Dominio*	Ortólogas*
Componentes principales	CURLY LEAF (CLF)[a]	Metiltransferasa de histonas	SET	E(z)
	MEDEA (MEA)[b]	Metiltransferasa de histonas	SET	E(z)
	FERTILIZATION INDEPENDENT SEED2 (FIS2)[c]	Estabilidad del complejo	Zinc finger	Su(z)12
	FERTILIZATION INDEPENDENT ENDOSPERM (FIE)[d]	Unión a la marca H3K27me3	WD40	ESC
	EMBRYONIC FLOWER2 (EMF2)[e]	Estabilidad del complejo	Zinc finger	Su(z)12
	VERNALIZATION2 (VRN2)[f]	Estabilidad del complejo	Zinc finger	Su(z)12
	SWINGER (SWN)[g]	Metiltransferasa de histonas	SET	E(z)
	MULTICOPY SUPPRESSOR OF IRA1† (MSI1)[h]	Unión al nucleosoma	WD40	P55
Proteínas accesorias	TELOMERE REPEAT BINDING FACTOR1 (TRB1), TRB2 y TRB3[i]	Unión a ADN en regiones teloméricas	Myb; H1/H5	-
	PWWP-DOMAIN INTERACTOR OF POLYCOMBS1 (PWWP1)j	Unión a histonas	PWWP	-
	DAMAGED DNA-BINDING PROTEIN1A (DDB1A)[k]	Unión al nucleosoma	WD40	PIC
	ANTAGONIST OF LHP1‡ (ALP1)[l]	Inhibición de la represión que ejercen los PRC	Homeodomain	-
	CULLIN4 (CUL4)[m]	Unión a la cromatina; represión de *FLC*	Cullin Homology	CUL4
	VERNALIZATION5 (VRN5)[n]	Unión a la marca H3K9me2	PHD	-
	VERNALIZATION INSENSITIVE3 (VIN3)[o]	Unión a la marca H3K9me2	PHD	-
	VRN5/VERNALIZATION INSENSITIVE3-LIKE1 (VEL1)[o]	Unión a la marca H3K9me2	PHD	-
	ASYMMETRIC LEAVES1 (AS1) y AS2[p]	Factores de transcripción	SANT-MYB; AS2	-
	ARABIDOPSIS HOMOLOG OF TRITHORAX1 (ATX1)[q]	Unión a histonas y actividad metiltransferasa	SET	TRX
	BLISTER (BLI)[r]	Modulación de la actividad metiltransferasa	Coloid-coil	-
	UPWARD CURLY LEAF1 (UCL1)[s]	Ligasa E3 de ubiquitina; degradación de CLF	F-Box	-
	RETINOBLASTOMA-RELATED1 (RBR1)[t]	Unión a ADN	Pocket	RBF2
	TATA-BOX BINDING PROTEIN ASSOCIATED FACTOR 13 (TAF13)[u]	Unión a promotores	TFIID	TAF13
	ENHANCER OF LHP1 (EOL1)[v]	Mantenimiento de la marca H3K27me3	WD40	CTF4

†IRA1: INHIBITORY REGULATOR OF THE RAS-CAMP PATHWAY1. ‡LHP1: LIKE HETEROCHROMATIN PROTEIN1. *Dominio que caracteriza a cada proteína: SET, secuencia conservada entre Suppressor of variegation 3-9 [Su(var)3-9], E(z) y Trx; WD40, motivo de unos 40 aminoácidos con un dipéptido final WD (Trp-Asp); PHD, Plant Homeodomain; Myb, Myeloblastosis domain; H1/H5, Linker histone H1/H5 domain; PWWP, Pro-Trp-Trp-Pro; SANT-MYB, Switching-defective protein 3 (Swi3), Adaptor 2 (Ada2), Nuclear receptor co-repressor (N-CoR) y Transcription factor (TF)IIIB; F-Box, cyclin F-box motif, y

TFIID, Transcription Factor IID. *Nombres abreviados de las ortólogas en *Drosophila melanogaster* de las proteínas de Arabidopsis mencionadas en esta tabla. [a]Goodrich *et al.* (1997). [b]Grossniklaus *et al.* (1998). [c]Luo *et al.* (1999). [d]Ohad *et al.* (1999). [e]Yoshida *et al.* (2001). [f]Gendall *et al.* (2001). [g]Chanvivattana *et al.* (2004). [h]Köhler *et al.* (2003). [i]Zhou *et al.* (2018). [j]Hohenstatt *et al.* (2018). [k]Dumbliauskas *et al.* (2011). [l]Liang *et al.* (2015). [m]Pazhouhandeh *et al.* (2011). [n]De Lucia *et al.* (2008). [o]Sung y Amasino (2004). [p]Lodha *et al.* (2013). [q]Saleh *et al.* (2007). [r]Schatlowski *et al.* (2010). [s]Jeong *et al.* (2011). [t]Mosquna *et al.* (2004). [u]Lindner *et al.* (2013). [v]Zhou *et al.* (2017b).

Tabla 2.- Componentes principales y proteínas accesorias del PRC1 de Arabidopsis

	Proteína	Función	Dominio*	Homología*
Componentes principales	REALLY INTERESTING NEW GENE1a (RING1a)[a]	Ligasa E3 de ubiquitina	RING	SCE
	RING1b[a]	Ligasa E3 de ubiquitina	RING	SCE
	B LYMPHOMA MO-MLV INSERTION REGION 1A (BMI1A)[b]	Ligasa E3 de ubiquitina	RING	Psc-Su(z)2
	BMI1B[b]	Ligasa E3 de ubiquitina	RING	Psc-Su(z)2
	BMI1C[b]	Ligasa E3 de ubiquitina	RING	Psc-Su(z)2
Proteínas accesorias	EMBRYONIC FLOWER1 (EMF1)[c†]	Unión a ADN	LXXLL	-
	LIKE HETEROCROMATIN PROTEIN1 (LHP1)[d†]	Unión a H3K27me3	Chromodomain	-
	VERNALIZATION1 (VRN1)[e]	Unión a ADN	B3	
	VP1/ABI3-LIKE1-3 (VAL1-3)[f†]	Unión a ADN de *FLC*, reclutamiento de complejos PcG	B3	-
	ALFIN PROTEIN1 (AL1) a AL7[g†]	Factores de transcripción	PHD	-
	INHIBITOR OF GROWTH1 (ING1) a ING3[h]	Unión a H3K4me2 y H3K4me3	PHD	ING1-3
	JUMONJI 14 (JMJ14)[i]	Desmetilasa de histonas	JMJ	JARID2
	EARLY BOLTING IN SHORT DAYS (EBS)[j]	Unión a H3K27me3 y H3K4me3	BAH	-
	SHORT LIFE (SHL)[j]	Unión a H3K27me3 y H3K4me3		-

[†]Proteínas accesorias tanto del PRC1 como del PRC2, que se incluyen en esta tabla pero no en la anterior.*Dominio que caracteriza a cada proteína: RING, Really Interesting New Gene motif; LXXLL (L indica leucina y X, cualquier aminoácido); B3, dominio conservado en la región aminoterminal de las proteínas VIVIPAROUS1(VP1)/ABSCISIC ACID INSENSITIVE3 (ABI3); PHD, Plant Homeodomain; JMJ, JUMONJI; BAH, Bromo Adjacent Homology. *Nombres abreviados de sus ortólogas en *Drosophila melanogaster*: Sce, Sex Combs Extra; Psc-Su(z)2, Posterior sex combs-Suppressor of zeste 2; ING1-3, Inhibitor of Growth 1-3; JARID2, Jumonji and AT-Rich Interaction Domain containing 2. [a]Xu y Shen (2008). [b]Bratzel *et al.* (2010). [c]Aubert *et al.* (2001). [d]Chen *et al.* (2010) y Bratzel *et al.* (2010). [e]Huang *et al.* (2019). [f]Yang *et al.* (2013). [g]Molitor *et al.* (2014). [h]Lee *et al.* (2009). [i]Wang *et al.* (2014). [j]López-González *et al.* (2014).

El mutante *clf-1* fue aislado tras una mutagénesis con transposones *AC*/*Ds* y presenta hojas hiponásticas y floración temprana (Goodrich *et al.*, 1997; Kim *et al.*, 1998; Serrano-Cartagena *et al.*, 2000). *MEDEA* (*MEA*) y *SWINGER* (*SWN*) también son coortólogos del gen *E(z)* de *Drosophila melanogaster* en Arabidopsis (Tabla 1, en la página 11). El mutante *mea-1* fue aislado tras una mutagénesis mediante transposones *AC*/*Ds* y sufre letalidad embrionaria causada por una proliferación celular excesiva en la fase de corazón, probablemente como consecuencia de la desrepresión de genes que codifican factores de transcripción de la familia MADS-Box (Grossniklaus *et al.*, 1998; Köhler *et al.*, 2003). Aunque los mutantes *swn* son fenotípicamente silvestres, los dobles mutantes *swn clf* son enanos y de floración temprana. Este fenotipo sinérgico revela la redundancia funcional de *SWN* y *CLF* (Chanvivattana *et al.*, 2004). FERTILIZATION-INDEPENDENT ENDOSPERM (FIE) es otro componente principal del PRC2, presenta un dominio WD40 (de unos 40 aminoácidos; suele terminar en un dipéptido triptófano-ácido aspártico [WD]) y es la única ortóloga en Arabidopsis de la proteína Extra sex combs (Esc) de *Drosophila melanogaster* (Tabla 1; Ohad *et al.*, 1999; Mozgova y Hennig, 2015). El mutante *fie* fue aislado tras una mutagénesis de segundos sitios con metanosulfonato de etilo (EMS) en la que se perseguía suprimir la infertilidad del mutante *pollen-pistil incompatibility 1* (*pop1*; Preuss *et al.*, 1993; Ohad *et al.*, 1996). El silenciamiento parcial de *FIE* causa hiponastia foliar, floración temprana y la transformación homeótica de las hojas caulinares en estructuras semejantes a los carpelos (Katz *et al.*, 2004). El mutante *fertilization independent seed2* (*fis2*) también fue aislado tras una mutagénesis de segundos sitios, en este caso del mutante *pistilata* (*pi*), realizada con EMS (Bowman *et al.*, 1989; Chaudhury *et al.*, 1997). FIS2 es un componente principal del PRC2 y presenta un dominio de dedos de cinc del tipo Cys2His2, como sus parálogas EMBRYONIC FLOWER2 (EMF2) y VERNALIZATION 2 (VRN2; Tabla 1). FIS2, EMF2 y VRN2 son coortólogas de la proteína Su(z)12 de *Drosophila melanogaster* (Figura 1, en la página 14; Birve *et al.*, 2001; Kassis *et al.*, 2017).

La proteína p55 de *Drosophila melanogaster* tiene cinco ortólogas en Arabidopsis, denominadas MULTICOPY SUPPRESSOR OF IRA1 (MSI1) a MSI5 (Tabla 1; Hennig *et al.*, 2003; Köhler *et al.*, 2003). En una estirpe transgénica en la que se pretendía expresar constitutivamente el gen *MSI1* se produjo la cosupresión del transgén y el gen endógeno. Esta insuficiencia de función de *MSI1* causó una morfología foliar irregular, reducción de la dominancia apical y ausencia de pétalos y anteras en las flores, así como la transformación de los sépalos en estructuras carpelares como los estigmas, como resultado de la desrepresión ectópica de varios genes responsables del desarrollo floral (Hennig *et al.*, 2003).

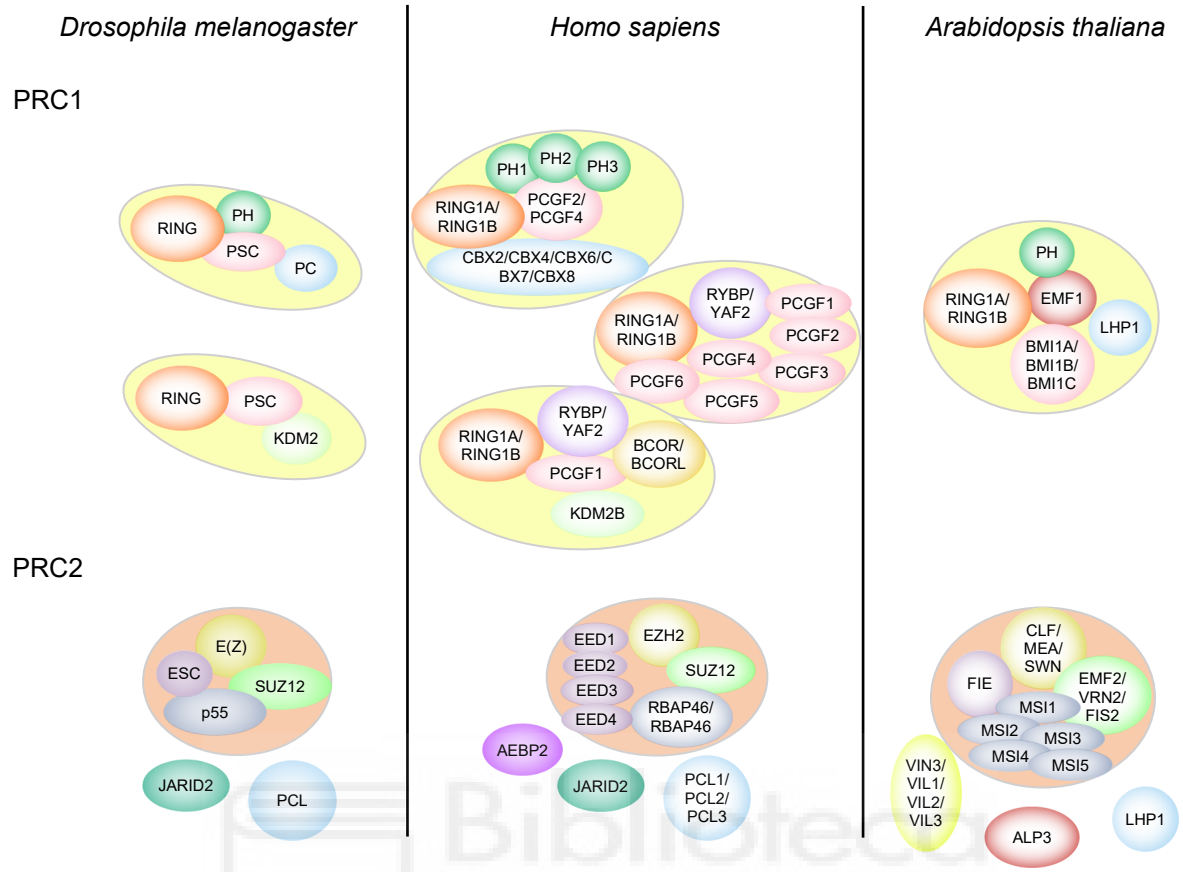

Figura 1.- Proteínas del PcG conservadas en *Drosophila melanogaster*, *Homo sapiens* y *Arabidopsis thaliana*. Los óvalos amarillos y naranjas agrupan a los componentes principales del PRC1 y el PRC2, respectivamente. Se representan separadas algunas proteínas accesorias del PRC2. Las subunidades homólogas se representan con el mismo color en las tres especies. Los nombres de las proteínas redundantes que se han identificado en conformaciones alternativas de cada PRC se separan con una barra (/). Las posiciones relativas de los componentes principales de cada complejo en esta figura no necesariamente se corresponden con sus interacciones físicas. Las abreviaturas que no se han definido previamente en esta memoria son las siguientes: AEBP2, AE binding protein 2; EED, enhanced ectoderm development; EZH2, enhancer of zeste homolog 2; JARID2, Jumonji and AT-rich interaction domain containing 2; KDM2B, lysine demethylase 2B; PCGF1, polycomb group ring finger 1; P55, protein 55; SUZ12, suppressor of zeste-12; VIL1-3, VERNALIZATION INSENSITIVE 3-LIKE 1-3; YAF2, YY1-associated factor 2. Modificado a partir de Lewis (2017).

Varios componentes principales del PRC1 de Arabidopsis fueron identificados por su homología con sus ortólogos de *Drosophila melanogaster*, demostrándose posteriormente sus interacciones: las proteínas RING1A y RING1B, con un dominio RING-finger aminoterminal, y BMI1A, BMI1B y BMI1C, con un dominio RING-finger And WD40 associated Ubiquitin-Like (RAWUL) carboxiterminal (Tabla 1; Sanchez-Pulido *et al.*, 2008; Bratzel *et al.*, 2010; Chen *et al.*, 2010).

El PRC2 ejerce su actividad represora en las plantas depositando la marca H3K27me3 en sus genes diana. Por su parte, el PRC1 actúa como una ligasa E3 de ubiquitina de la H2A (Figura 2). En los animales, el depósito de la marca H3K27me3 por el PRC2 precede y propicia la monoubiquitinación de la H2A por el PRC1 (Wang *et al.*, 2004). En las plantas, sin embargo, el reclutamiento del PRC1 a una diana especifica puede ocurrir por mecanismos tanto dependientes como independientes de la marca H3K27me3 (Blackledge *et al.*, 2015), e incluso en algunos casos el PRC1 recluta al PRC2 (Yang *et al.*, 2013; Blackledge *et al.*, 2014; Cooper *et al.*, 2014; Kalb *et al.*, 2014). Además, en la mayoría de los genes de las plantas, la trimetilación de la H3K27 por el PRC2 no ocurre salvo cuando es precedida por la monoubiquitinacion de la H2A (Zhou *et al.*, 2017a).

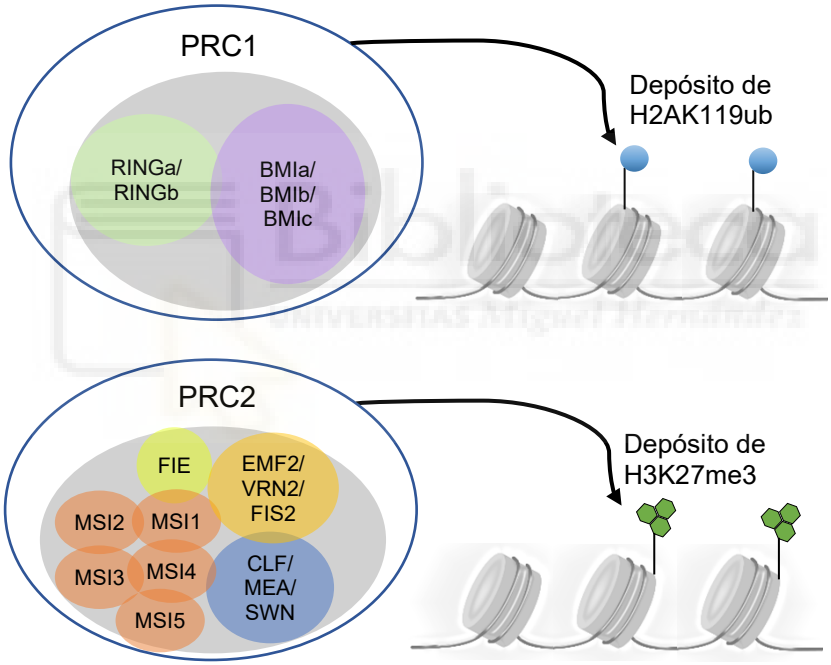

Figura 2.- Modificación de la cromatina por el PRC1 y el PRC2. Se representan los componentes principales del PRC1, que intervienen en su actividad ligasa E3 de ubiquitina, que ejerce sobre la lisina 119 de la histona H2A, y los del PRC2, que trimetila la lisina 27 de la histona H3. Los nombres de las distintas proteínas redundantes que se han identificado en conformaciones alternativas de cada PRC se separan con una barra (/). Modificado a partir de Blackledge *et al.* (2015) y Kim (2020).

El papel de las proteínas del PcG en el desarrollo esporofítico y gametofítico parece conservado desde los musgos hasta las plantas vasculares (Mosquna *et al.*, 2009; Okano *et al.*, 2009). Por ejemplo, el complejo FERTILIZATION-INDEPENDENT SEED (FIS; Wang *et al.*, 2006) es necesario para la gametogénesis y el desarrollo temprano de la semilla (Luo *et*

al., 1999; Chanvivattana *et al.*, 2004), y las proteínas EMBRYONIC FLOWER 1 (EMF1) y EMF2, para el desarrollo esporofítico (Sung *et al.*, 1992; Chen *et al.*, 1997). EMF1 es una proteína accesoria del PRC1 y el PRC2, y EMF2, un componente principal del PRC2; EMF1 es necesaria para el depósito de la marca H3K27me3 (Kim *et al.*, 2012; Yang *et al.*, 2013; Merini y Calonje, 2015). Los alelos de insuficiencia de función de *EMF1* y *EMF2* causan la desrepresión ectópica y heterocrónica de numerosos genes, incluidos los que son fundamentales para el desarrollo floral; esta desrepresión causa a su vez la pérdida de la identidad vegetativa de la planta. De hecho, los alelos *emf* de mayor insuficiencia de función son letales postembrionarios e impiden en homocigosis que se manifieste la fase vegetativa en las plantas portadoras. Estos mutantes no generan hojas y forman inmediatamente después de la germinación estructuras denominadas flores embrionarias, similares a los capullos florales, que contienen carpelos y óvulos (Sung *et al.*, 1992; Chen *et al.*, 1997).

IV.2.- Funciones epigenéticas de las dioxigenasas dependientes de 2-oxoglutarato y Fe^{2+}

Se conocen 18 clases funcionales de cupinas, un amplio grupo de proteínas que no solo incluye enzimas sino también proteínas de almacenamiento de las semillas, sin actividad enzimática (Dunwell *et al.*, 2004; Herr y Hausinger, 2018; Islam *et al.*, 2018). Existe un cierto grado de confusionismo en la literatura, ya que la tendencia mayoritaria es la de denominar superfamilia a las dioxigenasas dependientes de 2-oxoglutarato y Fe^{2+} (2OGD), sin tener en cuenta su relación filogenética con las restantes cupinas. Las 2OGD constituyen la clase más numerosa de las cupinas, y están presentes en las bacterias, los hongos, las plantas y los metazoos (Aravind y Koonin, 2001). Las 2OGD requieren 2-oxoglutarato (también llamado α-cetoglutarato) y oxígeno molecular como cosustratos, y Fe^{2+} como cofactor, para catalizar una reacción oxidativa, rindiendo usualmente el sustrato oxidado, succinato y CO_2 (Islam *et al.*, 2018). Las reacciones oxidativas catalizadas por las 2OGD son de varios tipos, tal como se describe en las páginas 42-44 (Farrow y Facchini, 2014).

Kawai *et al.* (2014) clasificaron a las 2OGD en tres clases en base a su filogenia. Se han descrito algunas 2OGD con funciones epigenéticas, como la modificación covalente de los ácidos nucleicos y las histonas. Las 2OGD de la clase DOXA están conservadas desde las bacterias hasta la especie humana y desmetilan ADN y ARN (Falnes *et al.*, 2002; Trewick *et al.*, 2002; Korvald *et al.*, 2011; Mielecki *et al.*, 2012). En los mamíferos, la desmetilación del ARNm por miembros de esta familia está bien caracterizada, particularmente en el caso de la marca epitranscriptómica más frecuentemente observada en la metilación del ARN, la N^6-metiladenosina (m^6A; Ougland *et al.*, 2015). En Arabidopsis, la proteína ALKBH9B desmetila

la m^6A del ARN del virus del mosaico de la alfalfa (Martínez-Pérez *et al.*, 2017). Pertenecen a la clase DOXB de las 2OGD 14 proteínas de Arabidopsis, algunas de las cuales presentan un subtipo del dominio 2OGD, denominado prolil 4-hidroxilasa (P4Hc), que participa en la modificación postraduccional de residuos de prolina en algunas proteínas de la pared celular y hormonas peptídicas (Hieta y Myllyharju, 2002; Matsubayashi, 2011; Velasquez *et al.*, 2015). La clase DOXC es la más numerosa y funcionalmente diversa de las 2OGD vegetales. Estas proteínas participan en el metabolismo general, lo que incluye la biosíntesis y/o el catabolismo de lignanos, isoprenoides, flavonoides, glucosinolatos, alcaloides y cumarinas. Las reacciones oxidativas catalizadas por las DOXC contribuyen a la homeostasis del etileno, las giberelinas y el ácido salicílico (Kawai *et al.*, 2014).

También son proteínas 2OGD las JMJ (JmjC; Cloos *et al.*, 2008; Dong *et al.*, 2014), que actúan como desmetilasas de histonas desde las levaduras a la especie humana (Accari y Fisher, 2015). Esta familia cuenta con 21 miembros en Arabidopsis (Chen *et al.*, 2011b). Las mutaciones en los genes JMJ alteran la transición floral, el desarrollo gametofítico y la inmunidad. Por ejemplo, el momento de la floración está regulado, entre otras muchas proteínas, por JMJ11, JMJ12, JMJ15 y JMJ27, que desmetilan las marcas H3K27me3, H3K4me3 y H3K9me1/2 en el gen *FLOWERING LOCUS C* (*FLC*; Noh *et al.*, 2004; Yang *et al.*, 2012; Dutta *et al.*, 2017; Crevillén, 2020). JMJ11 y JMJ12 también regulan la floración en otras especies como *Brassica rapa* (Poza-Viejo *et al.*, 2022).

IV.3.- Antecedentes y objetivos

IV.3.1.- Una disección genética del desarrollo foliar

Arabidopsis ha tenido durante décadas un impacto creciente en la literatura sobre el desarrollo vegetal, sobre la biología de las plantas en conjunto y sobre la biología del desarrollo de todos los seres vivos: se publicaron en 2022 más de 12000 artículos que incluyen la palabra Arabidopsis (según la base de datos Web of Science de Clarivate Analytics). El número de publicaciones sobre Arabidopsis sobrepasó en 2005 al de *Drosophila melanogaster*, y la diferencia no ha dejado de incrementarse desde entonces. Arabidopsis fue la planta con el mayor número anual de artículos publicados hasta 2016, año en que fue superada por el arroz (*Oryza sativa*).

Las hojas de las plantas capturan luz solar y CO_2, producen una parte importante del oxígeno que respiramos, y son la fuente indirecta o directa de prácticamente todos nuestros alimentos (Micol, 2009). Una comprensión completa de los mecanismos que regulan la determinación del número de hojas de una planta, así como de su forma, tamaño y estructura

interna, facilitaría la manipulación genética de las especies cultivadas para ayudar a satisfacer mejor las necesidades de la humanidad y del planeta en su conjunto.

El análisis del desarrollo de las hojas de las plantas se ha fundamentado en abordajes genéticos, que han permitido el aislamiento de mutantes con anomalías en la morfología foliar. La identificación y el estudio de los genes causantes de estos fenotipos mutantes han contribuido a la disección genética de los procesos en los que participan (Berná *et al.*, 1999; Horiguchi *et al.*, 2006; Micol, 2009). Entender cómo se construye una hoja es importante por diversas razones, que incluyen incrementar el conocimiento de la biología y la evolución de un órgano multicelular sin equivalentes en el reino animal, así como identificar —y eventualmente manipular— las claves genéticas, ambientales y hormonales que determinan su arquitectura y función final (Micol, 2009). La hoja es el órgano más visible y fácil de manipular de Arabidopsis, que puede ser usada como modelo para analizar dos de los procesos responsables del tamaño y la masa de la planta en su conjunto: la división y la expansión celulares. Por lo tanto, tal como afirma J.L. Micol, la hoja de Arabidopsis es el órgano modelo de una especie modelo, que facilita la identificación de genes responsables de procesos básicos que contribuyen a la organogénesis y el crecimiento de toda la planta: la proliferación, la expansión, la organización espacial y la diferenciación de las células.

Para arrojar luz sobre la formación de las hojas de las plantas, se inició en 1991 en el laboratorio de J.L. Micol un intento de saturar el genoma de Arabidopsis de mutaciones viables que causaran una morfología anormal de la hoja. Se han identificado y caracterizado funcionalmente así más de 70 genes, cuyos productos participan en varios procesos del desarrollo, tales como la expansión celular polar, la transducción de señales hormonales, la regulación de la expresión génica, la biogénesis de los plástidos y la señalización retrógrada, y el control epigenético del desarrollo. El amplio espectro de alteraciones morfológicas de la hoja de los mutantes estudiados en el laboratorio de J.L. Micol está facilitando el análisis de mecanismos específicos del desarrollo de la hoja, así como procesos celulares y tisulares básicos que contribuyen a otras facetas de la arquitectura corporal de Arabidopsis.

IV.3.2.- Componentes de la maquinaria epigenetica de Arabidopsis estudiados en el laboratorio de J.L. Micol

El grupo de J.L. Micol ha contribuido a la caracterización funcional de siete genes cuyos productos son componentes de la maquinaria epigenética de Arabidopsis; el punto de partida de todos estos estudios fue un mutante portador de un alelo del gen *CURLY LEAF* (Goodrich *et al.*, 1997; *CLF*, al que se denominó inicialmente *INCURVATA1* [*ICU1*] en el laboratorio de J.L. Micol; Serrano-Cartagena *et al.*, 2000); los genes *ELONGATA1* (*ELO1*) a

ELO4, que codifican acetiltransferasas de histonas (Nelissen *et al.*, 2005; Woloszynska *et al.*, 2016); *HISTONE MONOUBIQUITINATION1* (*HUB1*, al que inicialmente se denominó *ANGUSTA4* [*ANG4*] en el laboratorio de J.L. Micol), que codifica una ligasa E3 que monoubiquitina la histona H2B (Crevillén, 2020), e *INCURVATA2* (*ICU2*), que codifica la subunidad catalítica de la polimerasa α del ADN, que interacciona con complejos remodeladores de la cromatina y cuya insuficiencia de función altera el mantenimiento de la represión de la cromatina en los genes diana del PRC2 (Serrano-Cartagena *et al.*, 2000; Barrero *et al.*, 2007; Poza-Viejo *et al.*, 2022). *ELO2*, *ELO3*, *ELO4*, *HUB1* e *ICU2* fueron clonados posicionalmente en el laboratorio de J.L. Micol tras el correspondiente aislamiento de mutantes y análisis iterativo del ligamiento a marcadores moleculares; *CLF* fue identificado por J. Goodrich en el laboratorio de E. Meyerowitz (Goodrich *et al.*, 1997), y *ELO1* en el de M. Van Lijsebettens (Nelissen *et al.*, 2005; Van Lijsebettens y Grasser, 2014).

IV.3.3.- Estudios previos de las proteínas de la familia CUPULIFORMIS

IV.3.3.1.- INCURVATA11 y CUPULIFORMIS2 son componentes de la maquinaria epigenética

El mutante *cupuliformis* (*cp*; Nottingham Arabidopsis stock Center [NASC] N242) fue aislado por Jiřina Relichová en la Universidad Masaryk de Brno (República Checa) tras una mutagénesis con metilnitrosourea de semillas del acceso S96 de Arabidopsis, y donado a la colección pública del Arabidopsis Information Service (AIS) en 1976. En la década de los noventa se recopilaron en el laboratorio de J.L. Micol centenares de mutantes foliares, algunos de los cuales procedían de colecciones preexistentes. Para facilitar su análisis genético, estos mutantes fueron categorizados en clases fenotípicas. Se llamó Incurvata (Icu) a una de estas clases, dado que incluía mutantes que exhibían hojas vegetativas que se recurvan hacia el haz (hiponastia); uno de estos mutantes *icu* fue N242, al que se denominó entonces *icu11* (Serrano-Cartagena *et al.*, 1999) e *icu11-1* en esta Tesis.

El gen *ICU11* fue clonado posicionalmente mediante una combinación de análisis de ligamiento y secuenciación masiva de ADN del mutante *icu11-1* (Esteve-Bruna, 2013). Se estableció que *ICU11* pertenece a una familia génica de solo cinco miembros (*ICU11*, *CP2*, *CP3*, *CP4* y *CP5*) de la superfamilia de las 2OGD, a la que se llamó CUPULIFORMIS (CP) en homenaje a la Prof.ª Relichová. Kawai *et al.* (2014) no incluyeron en su estudio las proteínas CP2, CP3, CP4 ni CP5, y consideraron que ICU11 no se podía clasificar como DOXA, DOXB o DOXC. Sin embargo, la presencia de un dominio P4Hc claramente reconocible (y anotado como tal en la mayoría de las bases de datos de proteínas) en estas cinco proteínas indica claramente que pertenecen al clado DOXB.

También se identificó en el laboratorio de J.L. Micol el mutante *icu11-2*, portador de un alelo insercional de *ICU11*. Tanto *icu11-1* como *icu11-2* exhiben floración temprana, y análisis de retrotranscripción seguida de PCR cuantitativa (RT-qPCR; Mateo-Bonmatí *et al.*, 2018) demostraron que varios genes de identidad floral de la familia MADS-box estaban desreprimidos en las hojas de *icu11-1*: *AGAMOUS* (*AG* ;Yanofsky *et al.*, 1990), *AGAMOUS-LIKE42* (*AGL42*; Chen *et al.*, 2011a), *SHATTERPROOF2* (*SHP2*, también conocido como *AGL5*; Savidge *et al.*, 1995), *SEEDSTICK* (*STK*, también denominado *AGL11*; Rounsley *et al.*, 1995), *APETALA3* (*AP3*; Jack *et al.*, 1992), *SEPALLATA1* (*SEP1*), SEP2 y SEP3 (Pelaz *et al.*, 2000) y *MADS AFFECTING FLOWERING5* (*MAF5*; Kim y Sung, 2010). Estos rasgos eran similares a los de otros mutantes *icu* previamente estudiados en el laboratorio de J.L. Micol, portadores de alelos de genes que codifican componentes de la maquinaria epigenética, como *CLF* (*ICU1*; Goodrich *et al.*, 1997; Serrano-Cartagena *et al.*, 2000) e *ICU2* (Barrero *et al.*, 2007). Sin embargo, los mutantes simples *cp* eran indistinguibles del tipo silvestre. Por su parte, los dobles mutantes y sesquimutantes *icu11 cp2* manifestaron un fenotipo extremo (Figura 3) y letal postembrionario, generando inmediatamente después de la germinación flores embrionarias muy similares a los mutantes simples *emf1* y *emf2*, observaciones que reforzaron la hipótesis de que *ICU11* codificaba un componente de la maquinaria epigenética.

Figura 3.- Evidencias genéticas de la redundancia funcional de *ICU11* y *CP2*. (A-D) Hojas del primer nudo de la roseta de los tipos silvestres (A) S96 y (B) Col-0, y de los mutantes (C) *icu11-1/icu11-1* y (D) *cp2-3/cp2-3*, cuyos fondos genéticos son S96 y Col-0, respectivamente. (E) Flor madura de S96. (F) Flor embrionaria del sesquimutante *icu11-1/icu11-1;CP2/cp2-3*. La imagen F muestra la totalidad de la parte aérea de la planta. Barras de escala: 1 mm. Las fotografías se tomaron (A-D y F) 21 y (E) 42 días después de la estratificación (dde). Tomado de https://plantae.org/a-new-epigenetic-switch/, que a su vez se inspiró en Mateo-Bonmatí *et al.* (2018).

También se secuenció masivamente el ADN de *icu11-1* tratado con bisulfito sódico, así como su ARN. Se concluyó que este mutante sufre la desrepresión ectópica y heterocrónica de cientos de genes, y que la metilación de su ADN es indistinguible de la del tipo silvestre. Se realizaron ensayos de inmunoprecipitación de la cromatina de *icu11-1 cp2-1*

e *icu11-1* para seis de los genes que se encuentran más desreprimidos en este último, que revelaron que la presencia de la marca represora H3K27me3 estaba reducida, y la de la activadora H3K9/K14ac, incrementada. Se concluyó que ICU11 y CP2 actúan redundantemente como represores epigenéticos mediante un mecanismo desconocido, que conlleva la modificación química de las histonas, pero no la metilación del ADN. También se determinó que ICU11 y CP2 son proteínas nucleoplásmicas, que exhiben exclusión nucleolar, a diferencia de otras DOXB anteriormente estudiadas en Arabidopsis, como las P4H2, P4H5 y P4H13, que se localizan en el aparato de Golgi y el retículo endoplasmico (Velasquez *et al.*, 2015; Marzol *et al.*, 2018).

Los resultados más importantes de esta primera etapa del estudio de la familia CP fueron el descubrimiento de una nueva familia de proteínas de la superfamilia de las 2OGD y la demostración de que dos de sus miembros, ICU11 y CP2, eran nuevos componentes de la maquinaria epigenética, que actúan mediante un mecanismo aparentemente sin precedentes en todos los eucariotas. De hecho, no se ha descrito ninguna otra proteína DOXB con función epigenética (Mateo-Bonmatí *et al*., 2018).

IV.3.3.2.- ICU11 es muy probablemente una proteína accesoria del PRC2

Los grupos de Caroline Dean y Justin Goodrich publicaron durante la realización de esta Tesis (Bloomer *et al.*, 2020), un estudio del mutante *icu11-3*, hasta entonces no descrito y portador de una inserción del transposón Ds en el gen *ICU11*. Estos autores demostraron la desrepresión en este mutante de los genes *FLOWERING LOCUS T* (*FT*), *FLC, AGAMOUS* (*AG*), *APETALA1* (*AP1*), *APETALA3* (*AP3*) *y SHOOT MERISTEMLESS* (*STM*). También demostraron que el doble mutante *icu11-3 clf-2* era letal y producía flores embrionarias, y que este fenotipo morfológico estaba asociado a la desregulación de la transcripción de numerosos genes, de modo similar al previamente observado en las combinaciones dobles de los alelos de *CLF* y de genes que codifican proteínas accesorias del PRC2, como LIKE HETEROCROMATIN PROTEIN 1 (LHP1; Liang *et al.*, 2015). También demostraron mediante coinmunoprecipitación que ICU11 interacciona físicamente con proteínas principales (CLF, SWN, FIE, MSI y EMF2) y accesorias (EMF1 y LHP1) del PRC2, así como con TRB1, TRB2 y TRB3, que son factores de transcripción que también interaccionan con CLF y SWN (Zhou *et al.*, 2018). En base a estos resultados, se ha sugerido que ICU11 es una proteína accesoria del PRC2 (Godwin y Farrona, 2022).

IV.3.4.- Objetivos de esta Tesis

Uno de los objetivos genéricos que se pretendía alcanzar inicialmente con esta Tesis era demostrar que las interacciones genéticas previamente descritas entre los genes *ICU11* y *CP2* no eran específicas de alelo ni dependían del fondo genético de los mutantes con los que se habían obtenido combinaciones genéticas múltiples. Era necesario, en consecuencia, el aislamiento de nuevos alelos mutantes del gen *ICU11*, tras una mutagénesis del acceso Col-0. La razón de ello era que los fondos genéticos de los dos alelos disponibles antes del comienzo de esta Tesis (Mateo-Bonmatí *et al.*, 2018), así como el obtenido más tarde por otros autores (Bloomer *et al.*, 2020), eran distintos (S96, Ws-2 y L*er* para *icu11-1*, *icu11-2* e *icu11-3*, respectivamente) y de uso experimental menos común que Col-0. Este último es además el acceso que se usó para obtener la secuencia genómica de referencia (The Arabidopsis Genome Initiative, 2000) y la colección SALK de mutantes insercionales (Alonso *et al.*, 2003), la más numerosa de las disponibles. Col-0 es, en consecuencia, la estirpe más recomendable tanto para el estudio de perfiles transcriptómicos como para la obtención de dobles mutantes y la realización de análisis comparativos de sus fenotipos morfológicos y moleculares con los de otros mutantes simples y múltiples. De hecho, la presencia de modificadores de naturaleza desconocida en diferentes accesos hace desaconsejable la comparación de los fenotipos de los alelos de un mismo gen en diferentes fondos genéticos (Fernando *et al.*, 2018). En nuestro caso, resultaba de particular interés poder descartar cualquier efecto del fondo genético sobre los fenotipos morfológico y transcriptómico de los mutantes *icu11*, tanto individualmente como en sus combinaciones dobles mutantes. Se optó por la tecnología CRISPR/Cas9 para la la mutagénesis dirigida del gen *ICU11*.

La obtención de nuevos alelos mutantes *icu11* en el fondo genético Col-0 resultaba también de interés para confirmar las interacciones genéticas previamente estudiadas en dobles mutantes de fondos híbridos, concretamente S96/Col-0 y Ws-2/Col-0. Así mismo, al menos uno de dichos nuevos alelos *icu11* permitiría alcanzar un objetivo que excede los propósitos de esta Tesis: identificar nuevos interactores genéticos de *ICU11* tras una mutagénesis de segundos sitios con EMS, seguida de una selección de modificadores extragénicos. Los dobles mutantes así seleccionados que exhibieran supresión o incremento del fenotipo mutante de la línea *icu11* mutagenizada serían presuntos portadores de mutaciones en interactores genéticos de *ICU11*. La naturaleza molecular de estos genes modificadores probablemente proporcionaría información sobre el proceso molecular en el que actúa la proteína ICU11. El objetivo de este abordaje experimental era doble: (a) obtener información adicional sobre la función de *ICU11*, en base a sus interacciones genéticas con

nuevos alelos de genes previamente conocidos, que codifican componentes de la maquinaria genética, y (b) identificar nuevos genes de la maquinaria epigenética.

Para sentar las bases de la mutagénesis mencionada en el párrafo anterior se requerían dos logros previos: la obtención de al menos un alelo *icu11* en el fondo genético Col-0 y el desarrollo de herramientas bioinformáticas que facilitasen la cartografía mediante secuenciación masiva de los modificadores extragénicos del fenotipo morfológico de un mutante *icu11*. El primero de estos dos hitos se ha alcanzado en esta Tesis, y el segundo, en otra de las recientemente finalizadas en el laboratorio de José Luis Micol (Lup *et al.*, 2021; Lup *et al.*, 2022; Lup *et al.*, 2023).

El segundo y el tercero de los objetivos genéricos iniciales de esta Tesis fueron la obtención de información acerca de las funciones de las proteínas ICU11 y CP2 mediante la identificación de sus interactores físicos y el análisis transcriptómico de un mutante simple *cp2* y otro *icu11*, ambos con un fondo genético Col-0, así como del correspondiente doble mutante *icu11 cp2*. Se pretendía obtener por esta vía información molecular sobre las funciones de *ICU11* y *CP2* en base a los transcriptomas asociados a sus alelos mutantes. Este objetivo se completaría con análisis comparativos con los perfiles transcriptómicos de otros mutantes, portadores de alelos de genes cuya pertenencia a la maquinaria epigenética de Arabidopsis se hubiese demostrado previamente. Se optó por la purificación por afinidad en tándem (Tandem Affinity Purification; TAP; García-Leon *et al.*, 2018) para identificar interactores de las proteínas ICU11 y CP2.

En síntesis, nos propusimos: (1) la identificación de nuevos mutantes *icu11* mutagenizando el acceso Col-0 mediante la tecnología CRISPR/Cas9, (2) la caracterización de su fenotipo morfológico y (3) su combinación con los alelos nulos e hipomorfos de *CP2* disponibles, a fin de confirmar la redundancia funcional desigual previamente demostrada para *icu11-1*. Se elegió para este y otros propósitos el alelo *icu11-5*, aislado en esta Tesis. También nos propusimos la obtención de información sobre la función de los genes *ICU11* y *CP2*, mediante (4) la búsqueda de interactores genéticos de *icu11-5* y *cp2-1* en sus combinaciones dobles con alelos previamente descritos de genes cuya pertenencia a la maquinaria epigenética de Arabidopsis se hubiese demostrado o se sospechase; (5) la identificación de interactores físicos de las proteínas ICU11 y CP2 mediante purificación por afinidad en tándem y (6) su eventual validación mediante complementacion de fluorescencia bimolecular; (7) el análisis comparativo de los perfiles transcriptómicos, obtenidos mediante secuenciación masiva de ARN, de plántulas de los mutantes simples *icu11-5* y *cp2-1,* de las flores embrionarias del doble mutante *icu11-5 cp2-1* y el mutante simple *emf2-3*, y de la inflorescencia de Col-0. Por último, nos propusimos también (8) encontrar alguna condición

ambiental que paliase la letalidad del fenotipo de los mutantes *icu11-5 cp2-1* y *emf2-3*, a fin de poder estudiar sus fenotipos morfológico y molecular en etapas de su desarrollo posteriores a la de la aparición temprana de sus flores embrionarias letales.

V.- MATERIALES Y MÉTODOS

V.- MATERIALES Y MÉTODOS

Para la redacción de la introducción de esta memoria se han seguido las mismas pautas que en Tesis anteriores de los laboratorios de M.R. Ponce y J.L. Micol. Se ha preferido usar los acrónimos castellanizados ADN y ARN —de uso común en los medios de comunicación españoles—, en lugar de los recomendados por la International Union of Pure and Applied Chemistry, DNA y RNA, para los ácidos desoxirribonucleico y ribonucleico, respectivamente. Esta elección no está basada en ningún argumento que se considere incontestable; ambas opciones son aceptadas por el Diccionario de la Lengua Española (vigesimotercera edición, 2015) de la Real Academia Española (RAE). Tal como recomienda la RAE en su Ortografía de la lengua española (2010), en esta memoria no se realiza el plural de las siglas añadiendo al final una s minúscula: se escribe “el ARN” y también “los ARN”.

La nomenclatura que se aplica en esta memoria a genes, mutaciones y fenotipos nuevos se atiene a las pautas propuestas para Arabidopsis por Meinke y Koornneef (1997) . No hemos traducido al español muchos de los nombres de genes y proteínas que se mencionan en esta memoria; en estos casos solo hemos usado la cursiva para los genes. Los genotipos completos, como *icu11-1*/*icu11-1*, en los que los alelos en cromosomas homólogos se separan con una barra, se han utilizado únicamente cuando fue imprescindible. Salvo que se indique lo contrario, los individuos que se describen en este trabajo son homocigóticos para la mutación que se menciona en cada caso. Hemos utilizado en algunos casos un punto y coma como separador entre cromosomas no homólogos. Por ejemplo, el genotipo *icu11-5*/*icu11-5*;*CP2*/*cp2-3* es el de una planta sesquimutante, homocigótica para el alelo mutante *icu11-5* del gen *ICU11* (en el cromosoma 1) y heterocigótica para un alelo silvestre (*CP2*) y otro mutante (*cp2-3*) del gen *CP2* (en el cromosoma 2).

Las estirpes de Arabidopsis y las condiciones de cultivo empleadas en esta Tesis, así como sus cruzamientos y genotipado se describen en las páginas 46, 47 y 88. Hemos aislado ARN para su secuenciación masiva y su retrotranscripción seguida de PCR cuantitativa (páginas 89 y 90). Hemos secuenciado masivamente ARN y realizado el análisis bioinformático de los perfiles transcriptómicos así obtenidos (páginas 89 y 90). Hemos determinado el momento de la floración de los mutantes estudiados (página 47) y realizado diferentes observaciones mediante microscopía confocal (página 89). Hemos llevado a cabo una mutagénesis dirigida mediante CRISPR/Cas9 (página 47), ensayos de complementación de fluorescencia bimolecular (página 89) y búsquedas de interactores de ICU11 y CP2 mediante purificación por afinidad en tándem (página 88). En el ámbito de la bioinformática, hemos realizado alineamientos múltiples de secuencias proteicas (página 59), y análisis *in*

silico de nuestros resultados de secuenciación masiva de ARN, para lo que hemos mejorado protocolos previamente existentes (páginas 89 y 90).

VI.- RESULTADOS Y DISCUSIÓN

VI.- RESULTADOS Y DISCUSIÓN

En esta Tesis se han estudiado los genes parálogos *INCURVATA11* (*ICU11*) y *CUPULIFORMIS2* (*CP2*) de Arabidopsis, que pertenecen a la familia CUPULIFORMIS. Las proteínas ICU11 y CP2 son dioxigenasas dependientes de 2-oxoglutarato y Fe^{2+} (2OGD). Antes del comienzo de esta Tesis, se estableció en el laboratorio de J.L. Micol que *icu11-1* es un alelo de insuficiencia de función de un gen de la maquinaria epigenética de Arabidopsis, ya que su fenotipo morfológico comparte algunos rasgos con los causados por mutaciones hipomorfas y nulas previamente descritas en genes con funciones epigenéticas, como *clf-2*, *icu2-1, gigantea suppressor5* (*gis5*)*, early bolting in short days-1* (*ebs-1*)*, fasciata1* (*fas1*) y *terminal flower2-2* (*tfl2-2*). Las combinaciones dobles mutantes de estas mutaciones con *icu11-1* rinden fenotipos sinérgicos. Se constató además en el mutante *icu11-1* la desrepresión ectópica y heterocrónica de varios genes de identidad de órgano floral cuya regulación epigenética se había establecido o se sospechaba (apartado IV.3.3.1, en la página 19).

Hemos obtenido cuatro nuevos alelos del gen *ICU11* mediante la tecnología CRISPR/Cas9. Se mutagenizó el acceso Col-0 para obtener *icu11-5* e *icu11-6* y se hizo otro tanto en paralelo con S96, como control, para obtener *icu11-4* e *icu11-7*. Los cuatro nuevos mutantes presentaron los rasgos fenotípicos característicos de *icu11-1*, cuyo fondo genético es S96: hojas hiponásticas y floración temprana. Aunque estos cinco mutantes son aparentemente nulos, la hiponastia foliar de *icu11-5* y *icu11-6* es menor que la de los otros tres (página 48). Hemos comprobado que los mutantes *icu11-4*, *icu11-5*, *icu11-6* e *icu11-7* no son portadores de mutaciones no deseadas en las regiones extragénicas a *ICU11* cuyas secuencias son similares a la del ARN guía que hemos diseñado para la mutagénesis (página 60).

También hemos obtenido dobles mutantes cuyo fondo genético es Col-0, combinando *icu11-5* y *icu11-6* con el alelo nulo *cp2-3* y los hipomorfos *cp2-1* y *cp2-2* del gen *CP2.* Tal como se había demostrado previamente para *icu11-1*, los dobles mutantes con *cp2-3* resultaron ser letales gaméticos o embrionarios tempranos, y los restantes rindieron flores embrionarias letales.

Así mismo, hemos obtenido dobles mutantes combinando *icu11-5* o *cp2-3* con mutaciones hipomorfas o nulas de 23 genes de la maquinaria epigenética de Arabidopis. Seis de los dobles mutantes portadores de *icu11-5* manifestaron fenotipos sinérgicos, que indican la relación funcional de *ICU11* con *CLF*, *LIKE HETEROCHROMATIN PROTEIN 1* (*LHP1*; también denominado *TFL2*), *FAS1*, *EBS*, *GIS5* e *ICU2*. Los dobles mutantes de *clf-2*, *gis5* e

icu2-1 con *icu11-5* fueron similares a los anteriormente obtenidos con *icu11-1*; sin embargo, el fenotipo de los de *tfl2-2*, *ebs-1* y *fas1-1* fue más débil. Todos los dobles mutantes obtenidos con *cp2-3* fueron indistinguibles de su estirpe parental fenotípicamente mutante (página 51).

No hemos observado diferencias netas entre los dobles mutantes de *icu11-1* o *icu11-5* con *cp2-1* o *cp2-2*, ni entre sus sesquimutantes con *cp2-3*, todos los cuales son letales. Considerados en conjunto, estos resultados y los comentados en los tres párrafos anteriores sugieren que el fondo genético no solo modula el fenotipo foliar de alelos de *ICU11* igualmente nulos, sino también sus interacciones genéticas con alelos hipomorfos o nulos de otros genes de la maquinaria epigenética. La redundancia funcional desigual de los genes *ICU11* y *CP2*, sin embargo, no parece depender del fondo genético.

Hemos constatado que incrementando el contenido en sacarosa del medio de cultivo del 1% al 3% se rescata parcialmente la letalidad de las flores embrionarias de *icu11-5 cp2-1* y *emf2-3*, que en estas condiciones producen tallos, hojas caulinares, flores verdaderas que manifiestan transformaciones homeóticas de sépalos y pétalos en estructuras carpeloides (en *icu11-5 cp2-1*) o petaloides (en *emf2-3*), silicuas y solo algunas semillas viables (en *icu11-5 cp2-1*) o ninguna (en *emf2-3*) (página 52). Estos resultados indican que ICU11 y/o CP2 participan en la regulación de la expresión de algunos de los genes de identidad de órgano floral.

Hemos realizado escrutinios mediante purificación por afinidad en tándem, seguida de espectrometría de masas, para identificar interactores de las proteínas ICU11 y CP2. Hemos construido transgenes portadores de fusiones traduccionales de los genes *ICU11* y *CP2* con la secuencia que codifica la etiqueta GS^{Rhino} unida a su extremo 3′. La GS^{Rhino} incluye dos dominios de unión a IgG de la proteína G y un péptido de unión a la estreptavidina, separados por dos sitios de corte proteolítico del rinovirus 3C humano. Hemos transformado con estos transgenes suspensiones de células de la estirpe PSB-D de Arabidopsis. Hemos subcultivado iterativamente en medio líquido cinco presuntos transformantes para cada transgén, para extraer sus proteínas y someterlas a purificación por afinidad en tándem. Hemos identificado así presuntos interactores de ICU11: varios componentes principales del PCR2 (EMF2, SWN, FIE y MSI1) y varias de sus proteínas accesorias (EMF1, TRB1, TRB2 y TRB3), así como otras proteínas nucleares (NAC DOMAIN CONTAINING PROTEIN 50 [NAC050], NAC052 y CSN1). Los presuntos interactores de CP2 fueron TRB4, TRB5, NAC050, NAC052, CSN1, DRMY1 y DP1.

También hemos realizado ensayos de complementación de fluorescencia bimolecular mediante transformación transitoria en hojas de *Nicotiana benthamiana*, en los que tanto ICU11 como CP2 interaccionaron con CLF, SWN, LHP1, TRB1 y TRB3 (página 74), pero no

con FIE, TRB5 y DP1. No hemos encontrado indicio alguno de interacción entre ICU11 y CP2. A diferencia de nuestros resultados obtenidos *in vitro* mediante purificación por afinidad en tándem, los que también hemos obtenido *in vivo* mediante complementación de fluorescencia bimolecular sugieren que CP2 se une a los interactores de ICU11.

Hemos analizado el transcriptoma de plántulas de *icu11-5* y *cp2-1*, flores embrionarias de *icu11-5 cp2-1* y *emf2-3* e inflorescencias de Col-0, usando en todos los casos plántulas de Col-0 como referencia. Hemos comparado nuestros resultados entre sí y con los que obtuvieron autores anteriores con las flores embrionarias *trb1-2 trb2-1 trb3-2* y los callos *clf-29 swn-21.* Los transcriptomas de las plántulas Col-0 y *cp2-1* resultaron muy similares. En las plántulas *icu11-5*, las flores embrionarias *icu11-5 cp2-1, emf2-3* y *trb1-2 trb2-1 trb3-2*, y los callos *clf-29 swn-2,* el número de genes desreprimidos fue de 819, 3199, 2520, 3697 y 2852 respectivamente, y el de los reprimidos 78, 1770, 1774, 1945 y 2647, también respectivamente (páginas 78 y 110). Hemos encontrado muchas coincidencias entre los genes desregulados en *icu11-5, emf2-3* e *icu11-5 cp2-1* y los de expresión regulada epigenéticamente por las marcas H3K27me3 y H2AK121ub, así como con los que son dianas conocidas del PRC2 en Col-0 (página 82). Estas observaciones sugieren que la desregulación del transcriptoma de *icu11-5* e *icu11-5 cp2-1* está directa o indirectamente relacionada con cambios en las marcas activadoras o represoras de las dianas del complejo PRC2.

Los resultados de esta Tesis y su correspondiente discusión se recogen con todo detalle a partir de la página 45 de esta memoria.

VII.- CONCLUSIONES Y PERSPECTIVAS

VII.- CONCLUSIONES Y PERSPECTIVAS

En la primera parte de esta Tesis se realizó una revisión bibliográfica sobre el creciente número de proteínas de la superfamilia de las 2OGD con al menos una función demostrada experimentalmente. Algunos autores consideran que las 2OGD no constituyen una superfamilia, sino que son la clase más numerosa de la superfamilia de las cupinas, proteínas que comparten al menos uno de los motivos [$G(X)_5HXH-(X)_{3,4}E(X)_6G$] y [$G(X)_5PXG(X)_2H(X)_3N$] (en donde G, H, E, P, N y X denotan glicina, histidina, ácido glutámico, prolina, asparagina y cualquier aminoácido, respectivamente). Se han definido al menos 18 clases funcionales de cupinas, que no solo incluye enzimas sino también proteínas sin actividad enzimática, no pocas de las cuales han sido estudiadas fundamentalmente porque son alérgenas (Dunwell *et al.*, 2004; Herr y Hausinger, 2018; Islam *et al.*, 2018). Las cupinas sin actividad enzimática han perdido su capacidad de unirse al hierro y no pocas son proteínas de almacenamiento en semillas (Dunwell *et al.*, 2004; Galperin y Koonin, 2012).

Solo algunas 2OGD están implicadas en la regulación epigenética, en concreto, en la modificación covalente de los ácidos nucleicos y las histonas. Las de la clase DOXA, que están conservadas desde las bacterias hasta la especie humana, desmetilan ADN y ARN (Falnes *et al.*, 2002; Trewick *et al.*, 2002; Korvald *et al.*, 2011; Mielecki *et al.*, 2012). En los mamíferos, la desmetilación del ARNm por miembros de esta familia está bien caracterizada, particularmente en el caso de la marca epitranscriptómica más común, la N^6-metiladenosina (m^6A; Ougland *et al.*, 2015). En las plantas, ALKBH9B participa en el silenciamiento o la degradación de los ARNm (Martínez-Pérez *et al.*, 2017) y ALKBH10B en la regulación del desarrollo vegetativo y el tiempo de floración (Duan *et al.*, 2017).

La clase DOXC es la más numerosa y funcionalmente diversa de las 2OGD vegetales e incluye proteínas que participan en la biosíntesis y/o el catabolismo de lignanos, isoprenoides, flavonoides, glucosinolatos, alcaloides y cumarinas. Las reacciones oxidativas catalizadas por las DOXC contribuyen a la homeostasis del etileno, las giberelinas y el ácido salicílico (Kawai *et al.*, 2014).

También son proteínas 2OGD las JMJ (JmjC; Cloos *et al.*, 2008; Dong *et al.*, 2014), que actúan como desmetilasas de histonas, desde las levaduras a la especie humana (Accari y Fisher, 2015). Esta familia cuenta con 21 miembros en Arabidopsis (Chen *et al.*, 2011b). Las mutaciones en los genes JMJ alteran la transición floral, el desarrollo gametofítico y la inmunidad. Por ejemplo, el momento de la floración está regulado, entre otras muchas proteínas, por JMJ12, JMJ15, JMJ25 y JMJ27, que desmetilan las marcas H3K27me3,

H3K4me3 y H3K9me1/2 en el gen represor floral *FLOWERING LOCUS C* (*FLC*) (Serrano-Cartagena *et al.*, 2000; Nelissen *et al.*, 2005).

Pertenecen a la clase DOXB de las 2OGD 14 proteínas de Arabidopsis, algunas de las cuales presentan un subtipo del dominio 2OGD, el denominado prolil 4-hidroxilasa (P4Hc), que participa en la modificación postraduccional de residuos de prolina en proteínas de la pared celular y hormonas peptídicas (Hieta y Myllyharju, 2002; Matsubayashi, 2011; Velasquez *et al.*, 2015).

Tal como se ha indicado en el apartado VI, en la página 27, en esta Tesis hemos continuado el estudio de dos genes parálogos y desigualmente redundantes de la clase DOXB, previamente iniciado en el laboratorio de J.L. Micol: *ICU11* y *CP2*. Para evitar los eventuales efectos de los modificadores presentes en los fondos S-96 y Ws-2, hemos obtenido y caracterizado cuatro nuevos alelos de *ICU11*, mutagenizando las estirpes silvestres S96 (*icu11-4* e *icu11-7*) y Col-0 (*icu11-5* e *icu11-6*) mediante la tecnología CRISPR/Cas9. Hemos usado las mutaciones *icu11-5* e *icu11-6* para confirmar que la ausencia simultánea de las proteínas ICU11 y CP2 es letal y que los fenotipos de los dobles mutantes y sesquimutantes *icu11 cp2* son independientes de su fondo genético y no manifiestan especificidad de alelo.

En nuestro estudio de los mutantes *icu11-5 cp2-1* y *emf2-3* hemos establecido que su letalidad puede ser paliada si se cultivan en medio suplementado con un 3% en sacarosa, en lugar del 1% habitual, lo que a su vez permite estudiar su fenotipo morfológico a lo largo de todo su ciclo de vida. Nuestras observaciones indican que la letalidad de las flores embrionarias *icu11 cp2* y *emf2-3* se debe a su escasa capacidad fotosintética, derivada de su carencia de hojas vegetativas, y que ICU11 y/o CP2 se requieren para la especificación de la identidad de los órganos florales.

Hemos intentado dilucidar la función de ICU11 y CP2 mediante análisis interactómicos y transcriptómicos. Durante el transcurso de esta Tesis, otros autores publicaron un artículo en el que se describía un tercer alelo de *ICU11* (*icu11-3*) y se demostraba, mediante un ensayo de coinmunoprecipitación, que la proteína ICU11 interacciona con varios componentes principales del PRC2. Hemos realizado escrutinios de interactores de las proteínas ICU11 y CP2 mediante purificación por afinidad en tándem. Hemos confirmado así que ICU11 interacciona con los componentes principales del PRC2 EMF2, FIE, SWN y MSI1 y con las proteínas accesorias de este complejo EMF1, TRB1, TRB2 y TRB3 (Tabla 1, en la página 11). CP2 no presentó interacciones con componentes principales o proteínas accesorias del PRC2, aunque sí lo hizo con TRB4 y TRB5, miembros poco caracterizados de la familia TRB. Consideramos particularmente relevante que tanto ICU11 como CP2 interaccionen con las proteínas nucleares NAC050, NAC052 y CSN1.

También hemos realizado ensayos de complementación de fluorescencia bimolecular mediante transformación transitoria de hojas de *Nicotiana benthamiana*, en los que tanto ICU11 como CP2 interaccionaron con los componentes principales del PRC2 SWN y CLF, y con sus proteínas accesorias TRB1 y TRB3. No hemos encontrado interacción alguna entre ICU11 y CP2, lo que indica que no forman heteromultímeros.

Hemos llevado a cabo mediante secuenciación masiva de ARN un análisis comparativo de los perfiles transcriptómicos de plántulas de Col-0, *cp2-1* e *icu11-5,* flores embrionarias de *icu11-5 cp2-1* y *emf2-3*, e inflorescencias de Col-0. Este análisis ha revelado la gran semejanza entre los perfiles del doble mutante *icu11-5 cp2-1* y el mutante simple *emf2-3*, así como con los de otros mutantes portadores de alelos de genes que codifican componentes principales del PRC2. Muchos de los genes desregulados en las flores embrionarias *icu11-5 cp2-1* son portadores de la marca represora H3K27me3 en el tipo silvestre Col-0.

Considerados en conjunto, nuestros resultados confirman que ICU11 es una proteína accesoria del PRC2, revelan que muy probablemente CP2 también lo sea, y aportan nuevos indicios sobre la relación funcional entre ICU11 y CP2 y sobre sus funciones epigenéticas parcialmente solapantes. Esta conclusión se representa gráficamente en la página 102. El análisis de la función de CP2 requerirá investigaciones adicionales, que deberán superar las dificultades derivadas de su redundancia con ICU11.

Las conclusiones y perspectivas de esta Tesis se recogen con todo detalle a partir de la página 45 de esta memoria.

VIII.- BIBLIOGRAFÍA DE LOS APARTADOS IV-VII

VIII.- BIBLIOGRAFÍA DE LOS APARTADOS IV-VII

Accari, S.L., y Fisher, P.R. (2015). Emerging roles of JmjC domain-containing proteins. *International Review of Cell and Molecular Biology* **319,** 165-220.

Alagia, A., y Gullerova, M. (2022). The methylation game: epigenetic and epitranscriptomic dynamics of 5-methylcytosine. *Frontiers in Cell and Developmental Biology* **10,** 915685.

Almeida, M.V., Vernaz, G., Putman, A.L.K., y Miska, E.A. (2022). Taming transposable elements in vertebrates: from epigenetic silencing to domestication. *Trends in Genetics* **38,** 529-553.

Alonso, J.M., Stepanova, A.N., Leisse, T.J., Kim, C.J., Chen, H., Shinn, P., Stevenson, D.K., Zimmerman, J., Barajas, P., Cheuk, R., Gadrinab, C., Heller, C., Jeske, A., Koesema, E., Meyers, C.C., Parker, H., Prednis, L., Ansari, Y., Choy, N., Deen, H., Geralt, M., Hazari, N., Hom, E., Karnes, M., Mulholland, C., Ndubaku, R., Schmidt, I., Guzman, P., Aguilar-Henonin, L., Schmid, M., Weigel, D., Carter, D.E., Marchand, T., Risseeuw, E., Brogden, D., Zeko, A., Crosby, W.L., Berry, C.C., y Ecker, J.R. (2003). Genome-wide insertional mutagenesis of *Arabidopsis thaliana. Science* **301,** 653-657.

Aravind, L., y Koonin, E.V. (2001). The DNA-repair protein AlkB, EGL-9, and leprecan define new families of 2-oxoglutarate- and iron-dependent dioxygenases. *Genome Biology* **2,** 00071-00078.

Aubert, D., Chen, L., Moon, Y.H., Martin, D., Castle, L.A., Yang, C.H., y Sung, Z.R. (2001). EMF1, a novel protein involved in the control of shoot architecture and flowering in Arabidopsis. *Plant Cell* **13,** 1865-1875.

Barneche, F., Malapeira, J., y Mas, P. (2014). The impact of chromatin dynamics on plant light responses and circadian clock function. *Journal of Experimental Botany* **65,** 2895-2913.

Barrero, J.M., González-Bayón, R., del Pozo, J.C., Ponce, M.R., y Micol, J.L. (2007). *INCURVATA2* encodes the catalytic subunit of DNA polymerase alpha and interacts with genes involved in chromatin-mediated cellular memory in *Arabidopsis thaliana. Plant Cell* **19,** 2822-2838.

Bartels, A., Han, Q., Nair, P., Stacey, L., Gaynier, H., Mosley, M., Huang, Q.Q., Pearson, J.K., Hsieh, T.F., An, Y.C., y Xiao, W. (2018). Dynamic DNA methylation in plant growth and development. *International Journal of Molecular Sciences* **19,** 2144.

Batista, R.A., y Köhler, C. (2020). Genomic imprinting in plants-revisiting existing models. *Genes and Development* **34,** 24-36.

Bente, H., Foerster, A.M., Lettner, N., y Mittelsten Scheid, O. (2021). Polyploidy-associated paramutation in Arabidopsis is determined by small RNAs, temperature, and allele structure. *PLOS Genetics* **17,** e1009444.

Berná, G., Robles, P., y Micol, J.L. (1999). A mutational analysis of leaf morphogenesis in *Arabidopsis thaliana. Genetics* **152,** 729-742.

Birve, A., Sengupta, A.K., Beuchle, D., Larsson, J., Kennison, J.A., Rasmuson-Lestander, A., y Müller, J. (2001). *Su(z)12*, a novel *Drosophila* Polycomb group gene that is conserved in vertebrates and plants. *Development* **128,** 3371-3379.

Blackledge, N.P., Farcas, A.M., Kondo, T., King, H.W., McGouran, J.F., Hanssen, L.L., Ito, S., Cooper, S., Kondo, K., Koseki, Y., Ishikura, T., Long, H.K., Sheahan, T.W., Brockdorff, N., Kessler, B.M., Koseki, H., y Klose, R.J. (2014). Variant PRC1 complex-dependent H2A ubiquitylation drives PRC2 recruitment and polycomb domain formation. *Cell* **157,** 1445-1459.

Blackledge, N.P., Rose, N.R., y Klose, R.J. (2015). Targeting Polycomb systems to regulate gene expression: modifications to a complex story. *Nature Reviews Molecular Cell Biology* **16,** 643-649.

Bloomer, R.H., y Dean, C. (2017). Fine-tuning timing: natural variation informs the mechanistic basis of the switch to flowering in *Arabidopsis thaliana. Journal of Experimental Botany* **68,** 5439-5452.

Bloomer, R.H., Hutchison, C.E., Bäurle, I., Walker, J., Fang, X., Perera, P., Velanis, C.N., Gümüs, S., Spanos, C., Rappsilber, J., Feng, X., Goodrich, J., y Dean, C. (2020). The *Arabidopsis* epigenetic

regulator ICU11 as an accessory protein of Polycomb Repressive Complex 2. *Proceedings of the National Academy of Sciences of the USA* **117,** 16660-16666.

Bowman, J.L., Smyth, D.R., y Meyerowitz, E.M. (1989). Genes directing flower development in *Arabidopsis*. *Plant Cell* **1,** 37-52.

Bratzel, F., López-Torrejón, G., Koch, M., del Pozo, J.C., y Calonje, M. (2010). Keeping cell identity in *Arabidopsis* requires PRC1 RING-finger homologs that catalyze H2A monoubiquitination. *Current Biology* **20,** 1853-1859.

Butenko, Y., y Ohad, N. (2011). Polycomb-group mediated epigenetic mechanisms through plant evolution. *Biochimica and Biophysica Acta* **1809,** 395-406.

Cloos, P.A., Christensen, J., Agger, K., y Helin, K. (2008). Erasing the methyl mark: histone demethylases at the center of cellular differentiation and disease. *Genes and Development* **22,** 1115-1140.

Cooper, S., Dienstbier, M., Hassan, R., Schermelleh, L., Sharif, J., Blackledge, N.P., De Marco, V., Elderkin, S., Koseki, H., Klose, R., Heger, A., y Brockdorff, N. (2014). Targeting Polycomb to pericentric heterochromatin in embryonic stem cells reveals a role for H2AK119u1 in PRC2 recruitment. *Cell Reports* **7,** 1456-1470.

Crevillén, P. (2020). Histone demethylases as counterbalance to H3K27me3 silencing in plants. *iScience* **23,** 101715.

Chanvivattana, Y., Bishopp, A., Schubert, D., Stock, C., Moon, Y.H., Sung, Z.R., y Goodrich, J. (2004). Interaction of Polycomb-group proteins controlling flowering in *Arabidopsis*. *Development* **131,** 5263-5276.

Chaudhury, A.M., Ming, L., Miller, C., Craig, S., Dennis, E.S., y Peacock, W.J. (1997). Fertilization-independent seed development in *Arabidopsis thaliana*. *Proceedings of the National Academy of Sciences of the USA* **94,** 4223-4228.

Chen, C., Gao, Y., Liu, W., y Gao, S. (2022). Epigenetic regulation of cell fate transition: learning from early embryo development and somatic cell reprogramming. *Biology of Reproduction* **107,** 183-195.

Chen, D., Molitor, A., Liu, C., y Shen, W.H. (2010). The *Arabidopsis* PRC1-like ring-finger proteins are necessary for repression of embryonic traits during vegetative growth. *Cell Research* **20,** 1332-1344.

Chen, L., Cheng, J.C., Castle, L., y Sung, Z.R. (1997). *EMF* genes regulate Arabidopsis inflorescence development. *Plant Cell* **9,** 2011-2024.

Chen, M.K., Hsu, W.H., Lee, P.F., Thiruvengadam, M., Chen, H.I., y Yang, C.H. (2011a). The MADS box gene, *FOREVER YOUNG FLOWER*, acts as a repressor controlling floral organ senescence and abscission in Arabidopsis. *Plant Journal* **68,** 168-185.

Chen, T., y Dent, S.Y. (2014). Chromatin modifiers and remodellers: regulators of cellular differentiation. *Nature Reviews Genetics* **15,** 93-106.

Chen, X., Hu, Y., y Zhou, D.X. (2011b). Epigenetic gene regulation by plant Jumonji group of histone demethylase. *Biochimica and Biophysica Acta* **1809,** 421-426.

Choi, J.Y., y Lee, Y.C.G. (2020). Double-edged sword: The evolutionary consequences of the epigenetic silencing of transposable elements. *PLOS Genetics* **16,** e1008872.

De Lucia, F., Crevillen, P., Jones, A.M., Greb, T., y Dean, C. (2008). A PHD-polycomb repressive complex 2 triggers the epigenetic silencing of *FLC* during vernalization. *Proceedings of the National Academy of Sciences of the USA* **105,** 16831-16836.

Ding, M., y Chen, Z.J. (2018). Epigenetic perspectives on the evolution and domestication of polyploid plant and crops. *Current Opinion in Plant Biology* **42,** 37-48.

Dong, C., Zhang, H., Xu, C., Arrowsmith, C.H., y Min, J. (2014). Structure and function of dioxygenases in histone demethylation and DNA/RNA demethylation. *International Union of Crystallography Journal* **1,** 540-549.

Duan, H.C., Wei, L.H., Zhang, C., Wang, Y., Chen, L., Lu, Z., Chen, P.R., He, C., y Jia, G. (2017). ALKBH10B is an RNA N^6-methyladenosine demethylase affecting *Arabidopsis* floral transition. *Plant Cell* **29,** 2995-3011.

Dumbliauskas, E., Lechner, E., Jaciubek, M., Berr, A., Pazhouhandeh, M., Alioua, M., Cognat, V., Brukhin, V., Koncz, C., Grossniklaus, U., Molinier, J., y Genschik, P. (2011). The Arabidopsis CUL4-DDB1 complex interacts with MSI1 and is required to maintain *MEDEA* parental imprinting. *EMBO JOURNAL* **30,** 731-743.

Dunwell, J.M., Purvis, A., y Khuri, S. (2004). Cupins: the most functionally diverse protein superfamily? *Phytochemistry* **65,** 7-17.

Dutta, A., Choudhary, P., Caruana, J., y Raina, R. (2017). JMJ27, an Arabidopsis H3K9 histone demethylase, modulates defense against *Pseudomonas syringae* and flowering time. *Plant Journal* **91,** 1015-1028.

Esteve-Bruna, D. (2013). Caracterización de mutantes que manifiestan perturbaciones locales en el desarrollo de los tejidos internos de la hoja de Arabidopsis. Tesis Doctoral. Universidad Miguel Hernández de Elche.

Falnes, P.O., Johansen, R.F., y Seeberg, E. (2002). AlkB-mediated oxidative demethylation reverses DNA damage in *Escherichia coli*. *Nature* **419,** 178-182.

Fang, J., Jiang, J., Leichter, S.M., Liu, J., Biswal, M., Khudaverdyan, N., Zhong, X., y Song, J. (2022). Mechanistic basis for maintenance of CHG DNA methylation in plants. *Nature Communication* **13,** 3877.

Farrow, S.C., y Facchini, P.J. (2014). Functional diversity of 2-oxoglutarate/Fe(II)-dependent dioxygenases in plant metabolism. *Frontiers in Plant Science* **5,** 524.

Feinberg, A.P., Koldobskiy, M.A., y Göndör, A. (2016). Epigenetic modulators, modifiers and mediators in cancer aetiology and progression. *Nature Reviews Genetics* **17,** 284-299.

Fernando, V.C.D., Al Khateeb, W., Belmonte, M.F., y Schroeder, D.F. (2018). Role of Arabidopsis *ABF1*/*3*/*4* during *det1* germination in salt and osmotic stress conditions. *Plant Molecular Biology* **97,** 149-163.

Fujimoto, R., Uezono, K., Ishikura, S., Osabe, K., Peacock, W.J., y Dennis, E.S. (2018). Recent research on the mechanism of heterosis is important for crop and vegetable breeding systems. *Breeding Science* **68,** 145-158.

Galperin, M.Y., y Koonin, E.V. (2012). Divergence and convergence in enzyme evolution. *Journal of Biological Chemistry* **287,** 21-28.

García-Leon, M., Iniesto, E., y Rubio, V. (2018). Tandem affinity purification of protein complexes from Arabidopsis cell cultures. *Methods in Molecular Biology* **1794,** 297-309.

Gehring, M., y Satyaki, P.R. (2017). Endosperm and imprinting, inextricably linked. *Plant Physiology* **173,** 143-154.

Gehring, M. (2019). Epigenetic dynamics during flowering plant reproduction: evidence for reprogramming? *New Phytologist* **224,** 91-96.

Gendall, A.R., Levy, Y.Y., Wilson, A., y Dean, C. (2001). The *VERNALIZATION 2* gene mediates the epigenetic regulation of vernalization in *Arabidopsis*. *Cell* **107,** 525-535.

Godwin, J., y Farrona, S. (2022). The importance of networking: plant Polycomb Repressive Complex 2 and its interactors. *Epigenomes* **6**.

Goodrich, J., Puangsomlee, P., Martin, M., Long, D., Meyerowitz, E.M., y Coupland, G. (1997). A Polycomb-group gene regulates homeotic gene expression in *Arabidopsis*. *Nature* **386,** 44-51.

Grossniklaus, U., Vielle-Calzada, J.P., Hoeppner, M.A., y Gagliano, W.B. (1998). Maternal control of embryogenesis by *MEDEA*, a *Polycomb* group gene in *Arabidopsis*. *Science* **280,** 446-450.

Groszmann, M., Greaves, I.K., Albert, N., Fujimoto, R., Helliwell, C.A., Dennis, E.S., y Peacock, W.J. (2011). Epigenetics in plants—vernalisation and hybrid vigour. *Biochimica and Biophysica Acta* **1809,** 427-437.

Groszmann, M., Greaves, I.K., Fujimoto, R., Peacock, W.J., y Dennis, E.S. (2013). The role of epigenetics in hybrid vigour. *Trends in Genetics* **29,** 684-690.

Han, Q., Bartels, A., Cheng, X., Meyer, A., An, Y.C., Hsieh, T.F., y Xiao, W. (2019). Epigenetics regulates reproductive development in plants. *Plants (Basel)* **8,** 564-585.

He, L., Huang, H., Bradai, M., Zhao, C., You, Y., Ma, J., Zhao, L., Lozano-Durán, R., y Zhu, J.K. (2022). DNA methylation-free *Arabidopsis* reveals crucial roles of DNA methylation in regulating gene expression and development. *Nature Communication* **13,** 1335.

He, Y., y Li, Z. (2018). Epigenetic environmental memories in plants: establishment, maintenance, and reprogramming. *Trends in Genetics* **34,** 856-866.

He, Y., Chen, T., y Zeng, X. (2020). Genetic and epigenetic understanding of the seasonal timing of flowering. *Plant Communications* **1,** 100008.

Hennig, L., Taranto, P., Walser, M., Schönrock, N., y Gruissem, W. (2003). *Arabidopsis* MSI1 is required for epigenetic maintenance of reproductive development. *Development* **130,** 2555-2565.

Hennig, L., y Derkacheva, M. (2009). Diversity of Polycomb group complexes in plants: same rules, different players? *Trends in Genetics* **25,** 414-423.

Herr, C.Q., y Hausinger, R.P. (2018). Amazing diversity in biochemical roles of Fe(II)/2-oxoglutarate oxygenases. *Trends Biochemical Sciences* **43,** 517-532.

Hieta, R., y Myllyharju, J. (2002). Cloning and characterization of a low molecular weight prolyl 4-hydroxylase from *Arabidopsis thaliana*. Effective hydroxylation of proline-rich, collagen-like, and hypoxia-inducible transcription factor α-like peptides. *Journal of Biological Chemistry* **277,** 23965-23971.

Hohenstatt, M.L., Mikulski, P., Komarynets, O., Klose, C., Kycia, I., Jeltsch, A., Farrona, S., y Schubert, D. (2018). PWWP-DOMAIN INTERACTOR OF POLYCOMBS1 interacts with Polycomb-group proteins and histones and regulates Arabidopsis flowering and development. *Plant Cell* **30,** 117-133.

Holec, S., y Berger, F. (2012). Polycomb group complexes mediate developmental transitions in plants. *Plant Physiology* **158,** 35-43.

Holoch, D., y Moazed, D. (2015). RNA-mediated epigenetic regulation of gene expression. *Nature Reviews Genetics* **16,** 71-84.

Hollick, J.B. (2017). Paramutation and related phenomena in diverse species. *Nature Reviews Genetics* **18,** 5-23.

Horiguchi, G., Fujikura, U., Ferjani, A., Ishikawa, N., y Tsukaya, H. (2006). Large-scale histological analysis of leaf mutants using two simple leaf observation methods: identification of novel genetic pathways governing the size and shape of leaves. *Plant Journal* **48,** 638-644.

Huang, Y., Jiang, L., Liu, B.Y., Tan, C.F., Chen, D.H., Shen, W.H., y Ruan, Y. (2019). Evolution and conservation of polycomb repressive complex 1 core components and putative associated factors in the green lineage. *BMC Genomics* **20,** 533.

Islam, M.S., Leissing, T.M., Chowdhury, R., Hopkinson, R.J., y Schofield, C.J. (2018). 2-Oxoglutarate-dependent oxygenases. *Annual Review of Biochemistry* **87,** 585-620.

Jack, T., Brockman, L.L., y Meyerowitz, E.M. (1992). The homeotic gene *APETALA3* of *Arabidopsis thaliana* encodes a MADS box and is expressed in petals and stamens. *Cell* **68,** 683-697.

Jeong, C.W., Roh, H., Dang, T.V., Choi, Y.D., Fischer, R.L., Lee, J.S., y Choi, Y. (2011). An E3 ligase complex regulates SET-domain polycomb group protein activity in *Arabidopsis thaliana. Proceedings of the National Academy of Sciences of the USA* **108,** 8036-8041.

Jones, R.S., y Gelbart, W.M. (1990). Genetic analysis of the *Enhancer of zeste* locus and its role in gene regulation in *Drosophila melanogaster. Genetics* **126,** 185-199.

Kalb, R., Latwiel, S., Baymaz, H.I., Jansen, P.W., Müller, C.W., Vermeulen, M., y Müller, J. (2014). Histone H2A monoubiquitination promotes histone H3 methylation in Polycomb repression. *Nature Structural and Molecular Biology* **21,** 569-571.

Kassis, J.A., Kennison, J.A., y Tamkun, J.W. (2017). Polycomb and Trithorax Group genes in *Drosophila. Genetics* **206,** 1699-1725.

Katz, A., Oliva, M., Mosquna, A., Hakim, O., y Ohad, N. (2004). FIE and CURLY LEAF polycomb proteins interact in the regulation of homeobox gene expression during sporophyte development. *Plant Journal* **37,** 707-719.

Kawai, Y., Ono, E., y Mizutani, M. (2014). Evolution and diversity of the 2-oxoglutarate-dependent dioxygenase superfamily in plants. *Plant Journal* **78,** 328-343.

Kim, D.H., y Sung, S. (2010). The Plant Homeo Domain finger protein, VIN3-LIKE 2, is necessary for photoperiod-mediated epigenetic regulation of the floral repressor, MAF5. *Proceedings of the National Academy of Sciences of the USA* **107,** 17029-17034.

Kim, D.H. (2020). Current understanding of flowering pathways in plants: focusing on the vernalization pathway in Arabidopsis and several vegetable crop plants. *Horticulture, Environment, and Biotechnology* **61,** 209–227.

Kim, G.T., Tsukaya, H., y Uchimiya, H. (1998). The *CURLY LEAF* gene controls both division and elongation of cells during the expansion of the leaf blade in *Arabidopsis thaliana. Planta* **206,** 175-183.

Kim, S.Y., Lee, J., Eshed-Williams, L., Zilberman, D., y Sung, Z.R. (2012). EMF1 and PRC2 cooperate to repress key regulators of Arabidopsis development. *PLOS Genetics* **8,** e1002512.

Köhler, C., Hennig, L., Bouveret, R., Gheyselinck, J., Grossniklaus, U., y Gruissem, W. (2003). *Arabidopsis* MSI1 is a component of the MEA/FIE *Polycomb* group complex and required for seed development. *EMBO JOURNAL* **22,** 4804-4814.

Korvald, H., Molstad Moe, A.M., Cederkvist, F.H., Thiede, B., Laerdahl, J.K., Bjørås, M., y Alseth, I. (2011). *Schizosaccharomyces pombe* Ofd2 is a nuclear 2-oxoglutarate and iron dependent dioxygenase interacting with histones. *PLOS One* **6,** e25188.

Lee, J.E., Schmidt, H., Lai, B., y Ge, K. (2019). Transcriptional and epigenomic regulation of adipogenesis. *Molecular and Cellular Biology* **39,** e00601-00618.

Lee, T.I., y Young, R.A. (2013). Transcriptional regulation and its misregulation in disease. *Cell* **152,** 1237-1251.

Lee, W.Y., Lee, D., Chung, W.I., y Kwon, C.S. (2009). Arabidopsis ING and Alfin1-like protein families localize to the nucleus and bind to H3K4me3/2 via plant homeodomain fingers. *Plant Journal* **58,** 511-524.

Lewis, P.H. (1947). Pc: Polycomb. *Drosophila Information Service* **21,** 69.

Lewis, Z.A. (2017). Polycomb group systems in fungi: new models for understanding Polycomb Repressive Complex 2. *Trends in Genetics* **33,** 220-231.

Li, X., Li, Y., Li, S., Li, H., Yang, C., y Lin, J. (2020). The role of Shh signalling pathway in central nervous system development and related diseases. *Cell Biochemistry and Function* **39,** 180-189.

Liang, S.C., Hartwig, B., Perera, P., Mora-García, S., de Leau, E., Thornton, H., de Lima Alves, F., Rappsilber, J., Yang, S., James, G.V., Schneeberger, K., Finnegan, E.J., Turck, F., y Goodrich, J. (2015). Kicking against the PRCs – a domesticated transposase antagonises silencing mediated by Polycomb Group proteins and is an accessory component of Polycomb Repressive Complex 2. *PLOS Genetics* **11,** e1005660.

Liang, Z., Riaz, A., Chachar, S., Ding, Y., Du, H., y Gu, X. (2020). Epigenetic modifications of mRNA and DNA in plants. *Molecular Plant* **13,** 14-30.

Lindner, M., Simonini, S., Kooiker, M., Gagliardini, V., Somssich, M., Hohenstatt, M., Simon, R., Grossniklaus, U., y Kater, M.M. (2013). TAF13 interacts with PRC2 members and is essential for *Arabidopsis* seed development. *Developmental Biology* **379,** 28-37.

Liu, B., y Zhao, M. (2023). How transposable elements are recognized and epigenetically silenced in plants? *Current Opinion in Plant Biology* **75,** 102428.

Lodha, M., Marco, C.F., y Timmermans, M.C. (2013). The ASYMMETRIC LEAVES complex maintains repression of KNOX homeobox genes via direct recruitment of Polycomb-repressive complex2. *Genes and Development* **27,** 596-601.

López-González, L., Mouriz, A., Narro-Diego, L., Bustos, R., Martínez-Zapater, J.M., Jarillo, J.A., y Piñeiro, M. (2014). Chromatin-dependent repression of the *Arabidopsis* floral integrator genes involves plant specific PHD-containing proteins. *Plant Cell* **26,** 3922-3938.

Luo, M., Bilodeau, P., Koltunow, A., Dennis, E.S., Peacock, W.J., y Chaudhury, A.M. (1999). Genes controlling fertilization-independent seed development in *Arabidopsis thaliana. Proceedings of the National Academy of Sciences of the USA* **96,** 296-301.

Lup, S.D., Wilson-Sánchez, D., Andreu-Sánchez, S., y Micol, J.L. (2021). Easymap: a user-friendly software package for rapid mapping-by-sequencing of point mutations and large insertions. *Frontiers in Plant Science* **12,** 655286.

Lup, S.D., Wilson-Sánchez, D., y Micol, J.L. (2022). Mapping-by-sequencing of point and insertional mutations with Easymap. *Methods in Molecular Biology* **2484,** 343-361.

Lup, S.D., Navarro-Quiles, C., y Micol, J.L. (2023). Versatile mapping-by-sequencing with Easymap v.2. *Frontiers in Plant Science* **14,** 1042913.

Martínez-Pérez, M., Aparicio, F., López-Gresa, M.P., Bellés, J.M., Sánchez-Navarro, J.A., y Pallás, V. (2017). *Arabidopsis* m^6A demethylase activity modulates viral infection of a plant virus and the m^6A abundance in its genomic RNAs. *Proceedings of the National Academy of Sciences of the USA* **114,** 10755-10760.

Marzol, E., Borassi, C., Bringas, M., Sede, A., Rodríguez Garcia, D.R., Capece, L., y Estevez, J.M. (2018). Filling the Gaps to Solve the Extensin Puzzle. *Molecular Plant* **11,** 645-658.

Mateo-Bonmatí, E., Esteve-Bruna, D., Juan-Vicente, L., Nadi, R., Candela, H., Lozano, F.M., Ponce, M.R., Pérez-Pérez, J.M., y Micol, J.L. (2018). *INCURVATA11* and *CUPULIFORMIS2* are redundant genes that encode epigenetic machinery components in Arabidopsis. *Plant Cell* **30,** 1596-1616.

Matsubayashi, Y. (2011). Post-translational modifications in secreted peptide hormones in plants. *Plant and Cell Physiology* **52,** 5-13.

Meinke, D., y Koornneef, M. (1997). Community standards for *Arabidopsis* genetics. *Plant Journal* **12,** 247-253.

Merini, W., y Calonje, M. (2015). PRC1 is taking the lead in PcG repression. *Plant Journal* **83,** 110-120.

Micol, J.L. (2009). Leaf development: time to turn over a new leaf? *Current Opinion in Plant Biology* **12,** 9-16.

Mielecki, D., Zugaj, D.Ł., Muszewska, A., Piwowarski, J., Chojnacka, A., Mielecki, M., Nieminuszczy, J., Grynberg, M., y Grzesiuk, E. (2012). Novel AlkB dioxygenases—alternative models for *in silico* and *in vivo* studies. *PLOS One* **7,** e30588.

Mistry, P., Nakabo, S., O'Neil, L., Goel, R.R., Jiang, K., Carmona-Rivera, C., Gupta, S., Chan, D.W., Carlucci, P.M., Wang, X., Naz, F., Manna, Z., Dey, A., Mehta, N.N., Hasni, S., Dell'Orso, S., Gutierrez-Cruz, G., Sun, H.W., y Kaplan, M.J. (2019). Transcriptomic, epigenetic, and functional analyses implicate neutrophil diversity in the pathogenesis of systemic lupus erythematosus. *Proceedings of the National Academy of Sciences of the USA* **116,** 25222-25228.

Molitor, A.M., Bu, Z., Yu, Y., y Shen, W.H. (2014). *Arabidopsis* AL PHD-PRC1 complexes promote seed germination through H3K4me3-to-H3K27me3 chromatin state switch in repression of seed developmental genes. *PLOS Genetics* **10,** e1004091.

Mosquna, A., Katz, A., Shochat, S., Grafi, G., y Ohad, N. (2004). Interaction of FIE, a polycomb protein, with pRb: a possible mechanism regulating endosperm development. *Molecular Genetics and Genomics* **271,** 651-657.

Mosquna, A., Katz, A., Decker, E.L., Rensing, S.A., Reski, R., y Ohad, N. (2009). Regulation of stem cell maintenance by the Polycomb protein FIE has been conserved during land plant evolution. *Development* **136,** 2433-2444.

Mozgova, I., y Hennig, L. (2015). The Polycomb group protein regulatory network. *Annual Review in Plant Biology* **66,** 269-296.

Nelissen, H., Fleury, D., Bruno, L., Robles, P., De Veylder, L., Traas, J., Micol, J.L., Van Montagu, M., Inzé, D., y Van Lijsebettens, M. (2005). The *elongata* mutants identify a functional Elongator complex in plants with a role in cell proliferation during organ growth. *Proceedings of the National Academy of Sciences of the USA* **102,** 7754-7759.

Noh, B., Lee, S.H., Kim, H.J., Yi, G., Shin, E.A., Lee, M., Jung, K.J., Doyle, M.R., Amasino, R.M., y Noh, Y.S. (2004). Divergent roles of a pair of homologous Jumonji/Zinc-Finger-Class transcription factor proteins in the regulation of Arabidopsis flowering time. *Plant Cell* **16,** 2601-2613.

Ohad, N., Margossian, L., Hsu, Y.C., Williams, C., Repetti, P., y Fischer, R.L. (1996). A mutation that allows endosperm development without fertilization. *Proceedings of the National Academy of Sciences of the USA* **93,** 5319-5324.

Ohad, N., Yadegari, R., Margossian, L., Hannon, M., Michaeli, D., Harada, J.J., Goldberg, R.B., y Fischer, R.L. (1999). Mutations in *FIE*, a WD polycomb group gene, allow endosperm development without fertilization. *Plant Cell* **11,** 407-416.

Okano, Y., Aono, N., Hiwatashi, Y., Murata, T., Nishiyama, T., Ishikawa, T., Kubo, M., y Hasebe, M. (2009). A polycomb repressive complex 2 gene regulates apogamy and gives evolutionary insights into early land plant evolution. *Proceedings of the National Academy of Sciences of the USA* **106,** 16321-16326.

Ougland, R., Rognes, T., Klungland, A., y Larsen, E. (2015). Non-homologous functions of the AlkB homologs. *Journal of Molecular Cell Biology* **7,** 494-504.

Park, S., Kim, G.W., Kwon, S.H., y Lee, J.S. (2020). Broad domains of histone H3 lysine 4 trimethylation in transcriptional regulation and disease. *FEBS Journal* **287,** 2891-2902.

Pazhouhandeh, M., Molinier, J., Berr, A., y Genschik, P. (2011). MSI4/FVE interacts with CUL4-DDB1 and a PRC2-like complex to control epigenetic regulation of flowering time in *Arabidopsis*. *Proceedings of the National Academy of Sciences of the USA* **108,** 3430-3435.

Pelaz, S., Ditta, G.S., Baumann, E., Wisman, E., y Yanofsky, M.F. (2000). B and C floral organ identity functions require *SEPALLATA* MADS-box genes. *Nature* **405,** 200-203.

Pikaard, C.S., y Mittelsten Scheid, O. (2014). Epigenetic regulation in plants. *Cold Spring Harbor Perspectives in Biolology* **6,** a019315.

Pilu, R. (2015). Paramutation phenomena in plants. *Seminars in Cell and Developmental Biology* **44,** 2-10.

Poza-Viejo, L., Payá-Milans, M., San Martín-Uriz, P., Castro-Labrador, L., Lara-Astiaso, D., Wilkinson, M.D., Piñeiro, M., Jarillo, J.A., y Crevillén, P. (2022). Conserved and distinct roles of H3K27me3 demethylases regulating flowering time in *Brassica rapa*. *Plant, Cell and Environment* **45,** 1428-1441.

Preuss, D., Lemieux, B., Yen, G., y Davis, R.W. (1993). A conditional sterile mutation eliminates surface components from *Arabidopsis* pollen and disrupts cell signaling during fertilization. *Genes and Developement* **7,** 974-985.

Provart, N.J., Alonso, J., Assmann, S.M., Bergmann, D., Brady, S.M., Brkljacic, J., Browse, J., Chapple, C., Colot, V., Cutler, S., Dangl, J., Ehrhardt, D., Friesner, J.D., Frommer, W.B., Grotewold, E., Meyerowitz, E., Nemhauser, J., Nordborg, M., Pikaard, C., Shanklin, J., Somerville, C., Stitt, M., Torii, K.U., Waese, J., Wagner, D., y McCourt, P. (2016). 50 years of Arabidopsis research: highlights and future directions. *New Phytologist* **209,** 921-944.

Ramirez-Prado, J.S., Abulfaraj, A.A., Rayapuram, N., Benhamed, M., y Hirt, H. (2018). Plant immunity: from signaling to epigenetic control of defense. *Trends in Plant Science* **23,** 833-844.

Rothbart, S.B., y Strahl, B.D. (2014). Interpreting the language of histone and DNA modifications. *Biochimica and Biophysica Acta* **1839,** 627-643.

Rounsley, S.D., Ditta, G.S., y Yanofsky, M.F. (1995). Diverse roles for MADS box genes in Arabidopsis development. *Plant Cell* **7,** 1259-1269.

Saleh, A., Al-Abdallat, A., Ndamukong, I., Alvarez-Venegas, R., y Avramova, Z. (2007). The *Arabidopsis* homologs of trithorax (ATX1) and enhancer of zeste (CLF) establish 'bivalent chromatin marks' at the silent *AGAMOUS* locus. *Nucleic Acids Research* **35,** 6290-6296.

Sanchez-Pulido, L., Devos, D., Sung, Z.R., y Calonje, M. (2008). RAWUL: a new ubiquitin-like domain in PRC1 ring finger proteins that unveils putative plant and worm PRC1 orthologs. *BMC Genomics* **9,** 308.

Satyaki, P.R., y Gehring, M. (2017). DNA methylation and imprinting in plants: machinery and mechanisms. *Critical Reviews in Biochemistry and Molecular Biology* **52,** 163-175.

Savidge, B., Rounsley, S.D., y Yanofsky, M.F. (1995). Temporal relationship between the transcription of two Arabidopsis MADS box genes and the floral organ identity genes. *Plant Cell* **7,** 721-733.

Schatlowski, N., Stahl, Y., Hohenstatt, M.L., Goodrich, J., y Schubert, D. (2010). The CURLY LEAF interacting protein BLISTER controls expression of polycomb-group target genes and cellular differentiation of *Arabidopsis thaliana. Plant Cell* **22,** 2291-2305.

Serrano-Cartagena, J., Robles, P., Ponce, M.R., y Micol, J.L. (1999). Genetic analysis of leaf form mutants from the *Arabidopsis* Information Service collection. *Molecular and General Genetics* **261,** 725-739.

Serrano-Cartagena, J., Candela, H., Robles, P., Ponce, M.R., Pérez-Pérez, J.M., Piqueras, P., y Micol, J.L. (2000). Genetic analysis of *incurvata* mutants reveals three independent genetic operations at work in Arabidopsis leaf morphogenesis. *Genetics* **156,** 1363-1377.

Seymour, D.K., y Becker, C. (2017). The causes and consequences of DNA methylome variation in plants. *Current Opinion in Plant Biology* **36,** 56-63.

Sowpati, D.T., Ramamoorthy, S., y Mishra, R.K. (2015). Expansion of the polycomb system and evolution of complexity. *Mechanisms of Developement* **138** 97-112.

Springer, N.M., y Schmitz, R.J. (2017). Exploiting induced and natural epigenetic variation for crop improvement. *Nature Reviews Genetics* **18,** 563-575.

Sung, S., y Amasino, R.M. (2004). Vernalization in *Arabidopsis thaliana* is mediated by the PHD finger protein VIN3. *Nature* **427,** 159-164.

Sung, Z.R., Belachew, A., Shunong, B., y Bertrand-Garcia, R. (1992). *EMF*, an *Arabidopsis* gene required for vegetative shoot development. *Science* **258,** 1645-1647.

The Arabidopsis Genome Initiative (2000). Analysis of the genome sequence of the flowering plant *Arabidopsis thaliana. Nature* **408,** 796-815.

Trewick, S.C., Henshaw, T.F., Hausinger, R.P., Lindahl, T., y Sedgwick, B. (2002). Oxidative demethylation by *Escherichia coli* AlkB directly reverts DNA base damage. *Nature* **419,** 174-178.

Ueda, M., y Seki, M. (2020). Histone modifications form epigenetic regulatory networks to regulate abiotic stress response. *Plant Physiology* **182,** 15-26.

Van Lijsebettens, M., y Grasser, K.D. (2014). Transcript elongation factors: shaping transcriptomes after transcript initiation. *Trends in Plant Science* **19,** 717-726.

Velasquez, S.M., Ricardi, M.M., Poulsen, C.P., Oikawa, A., Dilokpimol, A., Halim, A., Mangano, S., Denita Juarez, S.P., Marzol, E., Salgado Salter, J.D., Dorosz, J.G., Borassi, C., Möller, S.R., Buono, R., Ohsawa, Y., Matsuoka, K., Otegui, M.S., Scheller, H.V., Geshi, N., Petersen, B.L., Iusem, N.D., y Estevez, J.M. (2015). Complex regulation of prolyl-4-hydroxylases impacts root hair expansion. *Molecular Plant* **8,** 734-746.

Wang, D., Tyson, M.D., Jackson, S.S., y Yadegari, R. (2006). Partially redundant functions of two SET-domain Polycomb-group proteins in controlling initiation of seed development in *Arabidopsis. Proceedings of the National Academy of Sciences of the USA* **103,** 13244-13249.

Wang, G., y Köhler, C. (2017). Epigenetic processes in flowering plant reproduction. *Journal of Experimental Botany* **68,** 797-807.

Wang, H., Wang, L., Erdjument-Bromage, H., Vidal, M., Tempst, P., Jones, R.S., y Zhang, Y. (2004). Role of histone H2A ubiquitination in Polycomb silencing. *Nature* **431,** 873-878.

Wang, Y., Gu, X., Yuan, W., Schmitz, R.J., y He, Y. (2014). Photoperiodic control of the floral transition through a distinct Polycomb repressive complex. *Developmental Cell* **28,** 727-736.

Whittaker, C., y Dean, C. (2017). The *FLC* Locus: A Platform for Discoveries in Epigenetics and Adaptation. *Annual Reviews of Cell and Developmental Biology* **33,** 555-575.

Woloszynska, M., Le Gall, S., y Van Lijsebettens, M. (2016). Plant Elongator-mediated transcriptional control in a chromatin and epigenetic context. *Biochimica and Biophysica Acta* **1859,** 1025-1033.

Wu, C.-t., y Morris, J.R. (2001). Genes, genetics, and epigenetics: a correspondence. *Science* **293,** 1103-1105.

Wu, C.J., Liu, Z.Z., Wei, L., Zhou, J.X., Cai, X.W., Su, Y.N., Li, L., Chen, S., y He, X.J. (2021). Three functionally redundant plant-specific paralogs are core subunits of the SAGA histone acetyltransferase complex in *Arabidopsis*. *Molecular Plant* **14,** 1071-1087.

Xi, Y., Park, S.R., Kim, D.H., Kim, E.D., y Sung, S. (2020). Transcriptome and epigenome analyses of vernalization in *Arabidopsis thaliana. Plant Journal* **103,** 1490-1502.

Xu, L., y Shen, W.H. (2008). Polycomb silencing of *KNOX* genes confines shoot stem cell niches in *Arabidopsis*. *Current Biology* **18,** 1966-1971.

Yang, C., Bratzel, F., Hohmann, N., Koch, M., Turck, F., y Calonje, M. (2013). VAL- and AtBMI1-mediated H2Aub initiate the switch from embryonic to postgerminative growth in *Arabidopsis*. *Current Biology* **23,** 1324-1329.

Yang, H., Mo, H., Fan, D., Cao, Y., Cui, S., y Ma, L. (2012). Overexpression of a histone H3K4 demethylase, JMJ15, accelerates flowering time in *Arabidopsis*. *Plant Cell Reports* **31,** 1297-1308.

Yanofsky, M.F., Ma, H., Bowman, J.L., Drews, G.N., Feldmann, K.A., y Meyerowitz, E.M. (1990). The protein encoded by the *Arabidopsis* homeotic gene *agamous* resembles transcription factors. *Nature* **346,** 35-39.

Yoshida, N., Yanai, Y., Chen, L., Kato, Y., Hiratsuka, J., Miwa, T., Sung, Z.R., y Takahashi, S. (2001). EMBRYONIC FLOWER2, a novel polycomb group protein homolog, mediates shoot development and flowering in Arabidopsis. *Plant Cell* **13,** 2471-2481.

Zhang, H., Lang, Z., y Zhu, J.K. (2018). Dynamics and function of DNA methylation in plants. *Nature Reviews Molecular Cell Biology* **19,** 489-506.

Zhou, Y., Romero-Campero, F.J., Gómez-Zambrano, A., Turck, F., y Calonje, M. (2017a). H2A monoubiquitination in *Arabidopsis thaliana* is generally independent of LHP1 and PRC2 activity. *Genome Biology* **18,** 69.

Zhou, Y., Tergemina, E., Cui, H., Förderer, A., Hartwig, B., Velikkakam James, G., Schneeberger, K., y Turck, F. (2017b). Ctf4-related protein recruits LHP1-PRC2 to maintain H3K27me3 levels in dividing cells in *Arabidopsis thaliana*. *Proceedings of the National Academy of Sciences of the USA* **114,** 4833-4838.

Zhou, Y., Wang, Y., Krause, K., Yang, T., Dongus, J.A., Zhang, Y., y Turck, F. (2018). Telobox motifs recruit CLF/SWN-PRC2 for H3K27me3 deposition via TRB factors in *Arabidopsis*. *Nature Genetics* **50,** 638-644.

IX.- PUBLICACIONES

CellPress
PARTNER JOURNAL

Molecular Plant
Spotlight

The 2OGD Superfamily: Emerging Functions in Plant Epigenetics and Hormone Metabolism

The 2-oxoglutarate and Fe (II)-dependent dioxygenase (2OGD) superfamily includes oxidative enzymes with an active site containing two histidines and (in most cases) one aspartic or glutamic acid residue. This conserved motif is termed the 2-His-1-carboxylate facial triad, chelates iron, and is housed within a double-stranded β-helix fold, also known as the DSBH, jelly-roll, cupin, or Jumonji C fold (Martinez and Hausinger, 2015). The reactions catalyzed by 2OGDs (also called 2ODDs, 2ODOs, and 2OGXs) include but are not limited to demethylation, demethylenation, hydroxylation, halogenation, desaturation, ring cleavage, ring closure, and epimerization (Farrow and Facchini, 2014).

The list of plant 2OGDs is long and growing; for example, the *Arabidopsis thaliana* (hereafter, Arabidopsis) genome contains more than 150 genes encoding proteins containing a 2OGD domain. These Arabidopsis proteins can be classified into the DOXA, DOXB, DOXC (Kawai et al., 2014), and JMJ groups, which include 14, 14, 102, and 21 proteins, respectively. DOXA proteins are homologs of *Escherichia coli* alpha-ketoglutarate-dependent dioxygenase (AlkB), a DNA repair enzyme that reverses the N^1-methyladenine (m^1A) and N^3-methylcytosine (m^3C) lesions caused by alkylating agents. Nine AlkB homologs (ALKBHs) have been found in mammals, and their substrates include DNA (m^1A and m^3C), RNA (m^6A, the most abundant RNA methylation mark), and proteins (methylated lysine). Two Arabidopsis DOXAs, the close paralogs ALKBH9B and ALKBH10B, have been recently found to demethylate m^6A in RNA (Figure 1A). ALKBH9B is the first plant RNA demethylase described that demethylates m^6A marks of specific foreign RNAs. ALKBH9B physically interacts with the coat protein of *Alfalfa mosaic virus* (AMV), thereby regulating its capacity for infection. AMV-infected *alkbh9b* Arabidopsis mutants exhibit reduced systemic infection and lower levels of viral RNA, which was found to be hypermethylated. In addition, ALKBH9B demethylates single-stranded AMV RNA *in vitro* (Martínez-Pérez et al., 2017). ALKBH10B demethylates endogenous mRNAs in Arabidopsis. The *alkbh10b* mutant flowers late due to instability of mRNAs from genes regulating flowering time. ALKBH10B reduces the m^6A methylation of *FLOWERING LOCUS T*, *SQUAMOSA PROMOTER BINDING PROTEIN-LIKE 3* (*SPL3*), and *SPL9* mRNAs, increasing their stability and capacity to trigger the floral transition (Duan et al., 2017).

Proteins of the DOXB clade have a subtype of the 2OGD domain, the prolyl 4-hydroxylase (P4Hc) domain. Animal P4H proteins play a key role in the biosynthesis of collagen, the main structural component of the extracellular space in many tissues. Some plant P4Hs catalyze post-translational modifications of cell wall hydroxyproline-rich *O*-glycoproteins, such as extensins, which are structurally similar to collagen. Arabidopsis P4H2, P4H5, and P4H13 participate in extensin hydroxylation (Figure 1B), which is required for proper cell wall architecture and thus root hair tip growth (Velasquez et al., 2015). The recently discovered CUPULIFORMIS (CP) family includes five proteins already annotated as 2OGDs with a P4Hc: INCURVATA11 (ICU11), and CP2 to CP5. The *icu11* mutants have hyponastic leaves and early flowering, traits that they share with mutants affected in genes encoding some components of the epigenetic machinery, such as *CURLY LEAF* (*CLF*), a Polycomb-group (PcG) gene. The *cp2* mutants are indistinguishable from wild type, but the *icu11 cp2* double mutants exhibit a severe, post-embryonic lethal phenotype reminiscent of single mutants carrying alleles of the PcG genes *EMBRYONIC FLOWER 1* (*EMF1*) and *EMF2*. The *icu11* mutants have ectopic and heterochronic derepression of hundreds of genes, and in at least some of these genes, histone methylation and acetylation are altered, suggesting that ICU11 and CP2 act redundantly as epigenetic repressors through histone modification but not DNA methylation. Unlike P4H2, P4H5, and P4H13, which localize to the secretory pathway, ICU11 and CP2 are nucleoplasmic proteins (Mateo-Bonmatí et al., 2018).

The Jumonji C (JmjC) domain-containing (JMJ) proteins function in the demethylation by hydroxylation of lysine residues in histones (Figure 1C). Mutations in Arabidopsis *JMJ* genes affect reproductive development and plant immunity. For example, flowering time is modulated by JMJ27, which demethylates H3K9me1/2 *in vitro* and *in vivo*, and directly or indirectly removes H3K9me2 methyl marks from the promoters of major flowering time genes, including *FLOWERING LOCUS C*, which encodes a repressor of flowering (Dutta et al., 2017). Different to the direct histone demethylase activity of other JMJs, JMJ24 indirectly demethylates H3K9me2. JMJ24 has a 2OGD domain that has lost demethylating activity but is able to bind H3, and also a RING domain, which is shared by many ubiquitin ligases. JMJ24 prevents DNA methylation in the CHG context, destabilizing the DNA methyltransferase CHROMOMETHYLASE3 (CMT3). Through its RING motif, JMJ24 ubiquitinates CMT3, tagging it for degradation. Hence, CHG but not CG or CHH methylation increased in the *jmj24* mutant as a consequence of excess CMT3 function. Given the positive feedback loop between CHG methylation and H3K9me2, JMJ24 apparently regulates the presence of H3K9me2 by controlling CHG methylation (Deng et al., 2016; Kabelitz et al., 2016).

DOXCs are the largest and most functionally diverse class of 2OGDs. These enzymes act in plant metabolism, including biosynthesis and/or catabolism of lignans, isoprenoids, flavonoids, glucosinolates, alkaloids, and coumarins. DOXCs play important roles in ethylene, gibberellin, auxin, and salicylic acid homeostasis (Kawai et al., 2014). The terpenoid strigolactones,

Published by the Molecular Plant Shanghai Editorial Office in association with Cell Press, an imprint of Elsevier Inc., on behalf of CSPB and IPPE, SIBS, CAS.

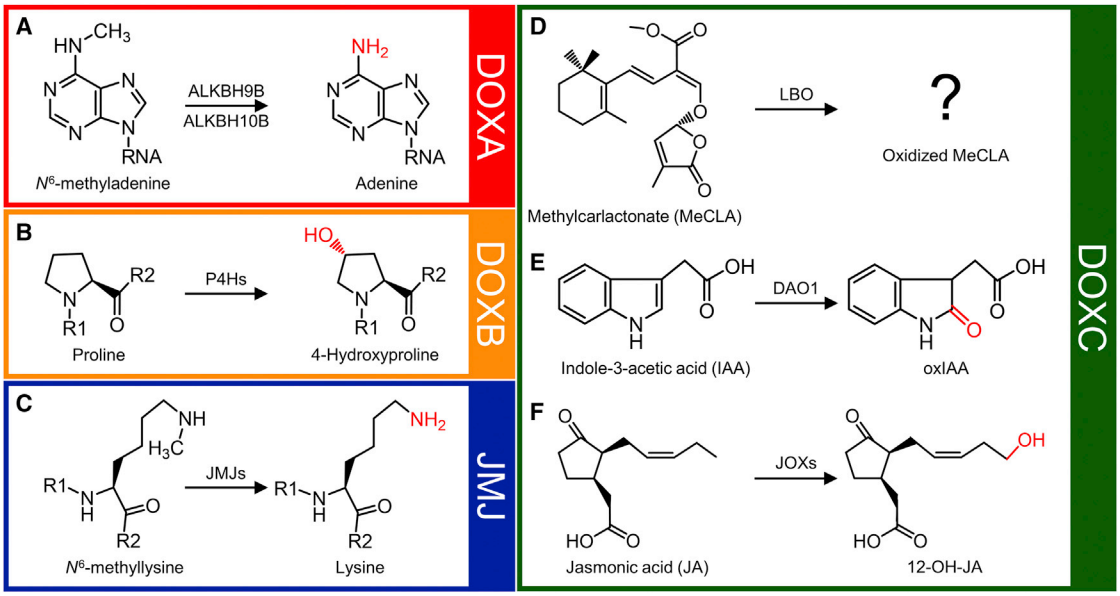

Figure 1. Chemical Reactions Catalyzed by the 2OGDs Mentioned in this Spotlight.
Examples of reactions catalyzed by some DOXA **(A)**, DOXB **(B)**, JMJ **(C)**, and DOXC **(D–F)** enzymes are represented. Only the main substrates and products of each reaction are shown.
(A) Oxidative demethylation of m^6A in RNA by ALKBH9B and ALKBH10B. **(B)** Proline hydroxylation by P4H DOXBs (the reaction involving CP proteins is not represented because is yet unknown). **(C)** Oxidative demethylation of Me-lysine by JMJs. **(D)** Oxidation of MeCLA by LBO. **(E)** Oxidation of IAA by DAO. **(F)** Hydroxylation of JA by the JAO/JOX proteins. R1 and R2 in **(B)** and **(C)**: neighboring amino acid residues. Only the methyl groups participating in a demethylation reaction are represented as CH_3 **(A and C)**.

which optimize plant growth and development and promote soil microbe interactions, were recently added to this list of hormones. Carlactone (CL) is a common precursor to all strigolactones. Treatments modifying auxin levels and mutations that alter strigolactone homeostasis change the expression levels of *MORE AXILLARY GROWTH 3* (*MAX3*) and *MAX4*, which encode enzymes required for CL biosynthesis. Wild-type plants treated with an auxin transport inhibitor, decapitated, or decapitated and treated with auxin were subjected to transcriptomic analysis, together with the *max* mutants. Some genes were found coexpressed with *MAX3*, and study of the mutant alleles of these genes identified LATERAL BRANCHING OXIDOREDUCTASE (LBO) as a DOXC protein that oxidizes methyl carlactonoate (MeCLA) to render an unidentified strigolactone-like compound (Figure 1D). The *lbo* mutants exhibit increased shoot branching, a phenotype associated with strigolactone depletion (Brewer et al., 2016).

Auxin controls many aspects of plant growth and development. The optimal concentration of indole-3-acetic acid (IAA), the major form of active auxin, is regulated by mechanisms including its degradation and reversible conjugation. Arabidopsis DIOXYGENASE FOR AUXIN OXIDATION 1 (DAO1) is a DOXC protein recently shown to be the major regulator of auxin degradation; DAO1 oxidizes IAA to the inactive 2-oxoindole-3-acetic acid (oxIAA) (Figure 1E). IAA levels in the *dao1* mutants were only mildly affected, in spite of the strong variations in the concentration of oxIAA and IAA conjugates shown by these mutants. DAO1 seems to act redundantly with GH3 IAA-conjugating enzymes to maintain optimal IAA concentrations (Porco et al., 2016; Zhang et al., 2016). The lipid-derived hormone jasmonic acid (JA) plays a key role activating defense responses to pathogen attack or wounding. Most JA responses require JA activation to form the conjugate jasmonoyl-isoleucine (JA-Ile). The DOXC paralogs JASMONATE-INDUCED OXYGENASE 1 (JOX1) to JOX4, also named JASMONIC ACID OXIDASES (JAOs), have been recently found to hydroxylate JA to 12-hydroxy-JA (12-OH-JA) (Figure 1F). The *jao2* mutants display permanent defense expression in the absence of stress, and strongly increased resistance against subsequent fungal infection. At least three of the JOX/JAO paralogs hydroxylate JA into 12-OH-JA *in vitro*. JAO2/JOX2 defines a metabolic diversion mechanism that contributes to maintain JA-Ile-dependent responses repressed in wild-type plants (Caarls et al., 2017; Smirnova et al., 2017).

Members of the large and ancient 2OGD superfamily participate in post-translational and epigenetic processes, as well as in metabolic pathways. In plants, the functions of most 2OGDs remain uncharacterized. Some enzymatic activities of the recently described plant 2OGDs mentioned above were somewhat predictable from their homologs across kingdoms, such as those of ALKBHs and JMJs in demethylating nucleic acids and histones, respectively. By contrast, the CP proteins play a role completely unexpected for the DOXB class, because they behave as components of the epigenetic machinery instead of participating in post-translational modification of cell wall proteins. In addition, the roles of the *LBO*, *DAO1*, and *JAO/JOX* DOXC genes in strigolactone biosynthesis, auxin and JA-Ile down-regulation, respectively, were also somewhat unexpected; identification of these genes has allowed the discovery of missing metabolic pathway steps.

Phylogenetic analyses have eased functional studies of gene families. The full-length sequences of the 2OGD superfamily

members, however, show low identities and similarities, which hinder their reliable clustering and the study of their evolutionary relationships. Combinations of phylogenetic, transcriptomic, and forward and reverse genetic analyses have proven to be useful for 2OGD functional studies, and have shown that in some cases, jointly clustered members of a clade may have divergent and/or additional roles, as seen for the CP family of DOXBs or JMJ24. Functional redundancy is a major limitation for the functional analysis of the members of large gene families, as shown by the *icu11* and *cp2* mutants—and to a lesser extent, the *jao/jox* mutants—mentioned here. Re-examination of some clades of the 2OGD superfamily using approaches to overcome the genetic redundancy may uncover novel functions, which may involve domains or motifs other than the 2OGD domain in these proteins. Although some JMJ proteins contain domains additional to the JmjC domain, such as JmjN, zinc finger, tudor, and PHD finger domains, this does not seem to be the case for the remaining 2OGDs. As already shown for some gene families, CRISPR-based technologies may be used to simultaneously inactivate groups of 2OGD paralogs, producing plants homozygous for multiple mutations. These technologies also provide ways to modify genes *in vivo* for the production of tagged but fully functional proteins, allowing fast purification of protein complexes and the identification of protein interactors on a large scale. These experimental approaches will speed up the unraveling of novel 2OGD catalytic activities in already known or yet unknown pathways.

Plant metabolism is estimated to produce hundreds of thousands of compounds. Kawai et al. (2014) noted that the number of DOXA and DOXB proteins is similar in all the plant taxa they studied, whereas 31 of the 57 DOXC-class clades they defined were found only in a single species. This indicates that 2OGDs are at least partially responsible for the diversification of plant metabolites. Thus, further searches for novel members of this superfamily probably will reveal novel biosynthetic pathways.

FUNDING

This work was supported by grants from the Ministerio de Economía, Industria y Competitividad of Spain (BIO2014-53063-P) and the Generalitat Valenciana (PROMETEOII/2014/006) to J.L.M.

ACKNOWLEDGMENTS

No conflict of interest declared. We apologize that, owing to space limitations, some original publications may have been omitted.

Received: July 10, 2018
Revised: September 11, 2018
Accepted: September 11, 2018
Published: September 18, 2018

*Riad Nadi, Eduardo Mateo-Bonmatí, Lucía Juan-Vicente and José Luis Micol**

Instituto de Bioingeniería, Universidad Miguel Hernández, Campus de Elche, 03202 Elche, Spain

***Correspondence: José Luis Micol (jlmicol@umh.es)**

https://doi.org/10.1016/j.molp.2018.09.002

REFERENCES

Brewer, P.B., Yoneyama, K., Filardo, F., Meyers, E., Scaffidi, A., Frickey, T., Akiyama, K., Seto, Y., Dun, E.A., Cremer, J.E., et al. (2016). *LATERAL BRANCHING OXIDOREDUCTASE* acts in the final stages of strigolactone biosynthesis in *Arabidopsis*. Proc. Natl. Acad. Sci. USA **113**:6301–6306.

Caarls, L., Elberse, J., Awwanah, M., Ludwig, N.R., de Vries, M., Zeilmaker, T., Van Wees, S.C.M., Schuurink, R.C., and Van den Ackerveken, G. (2017). *Arabidopsis* JASMONATE-INDUCED OXYGENASES down-regulate plant immunity by hydroxylation and inactivation of the hormone jasmonic acid. Proc. Natl. Acad. Sci. USA **114**:6388–6393.

Deng, S., Jang, I.C., Su, L., Xu, J., and Chua, N.H. (2016). JMJ24 targets CHROMOMETHYLASE3 for proteasomal degradation in *Arabidopsis*. Genes Dev. **30**:251–256.

Duan, H.C., Wei, L.H., Zhang, C., Wang, Y., Chen, L., Lu, Z., Chen, P.R., He, C., and Jia, G. (2017). ALKBH10B is an RNA N^6-methyladenosine demethylase affecting Arabidopsis floral transition. Plant Cell **29**:2995–3011.

Dutta, A., Choudhary, P., Caruana, J., and Raina, R. (2017). JMJ27, an Arabidopsis H3K9 histone demethylase, modulates defense against *Pseudomonas syringae* and flowering time. Plant J. **91**:1015–1028.

Farrow, S.C., and Facchini, P.J. (2014). Functional diversity of 2-oxoglutarate/Fe(II)-dependent dioxygenases in plant metabolism. Front. Plant Sci. **5**:524.

Kabelitz, T., Brzezinka, K., Friedrich, T., Górka, M., Graf, A., Kappel, C., and Bäurle, I. (2016). A JUMONJI protein with E3 ligase and histone H3 binding activities affects transposon silencing in Arabidopsis. Plant Physiol. **171**:344–358.

Kawai, Y., Ono, E., and Mizutani, M. (2014). Evolution and diversity of the 2-oxoglutarate-dependent dioxygenase superfamily in plants. Plant J. **78**:328–343.

Martínez-Pérez, M., Aparicio, F., López-Gresa, M.P., Bellés, J.M., Sánchez-Navarro, J.A., and Pallás, V. (2017). *Arabidopsis* m^6A demethylase activity modulates viral infection of a plant virus and the m^6A abundance in its genomic RNAs. Proc. Natl. Acad. Sci. USA **114**:10755–10760.

Martinez, S., and Hausinger, R.P. (2015). Catalytic mechanisms of Fe(II)- and 2-oxoglutarate-dependent oxygenases. J. Biol. Chem. **290**:20702–20711.

Mateo-Bonmatí, E., Esteve-Bruna, D., Juan-Vicente, L., Nadi, R., Candela, H., Lozano, F.M., Ponce, M.R., Pérez-Pérez, J.M., and Micol, J.L. (2018). *INCURVATA11* and *CUPULIFORMIS2* are redundant genes that encode epigenetic machinery components in Arabidopsis. Plant Cell **30**:1596–1616.

Porco, S., Pěnčik, A., Rashed, A., Voß, U., Casanova-Sáez, R., Bishopp, A., Golebiowska, A., Bhosale, R., Swarup, R., Swarup, K., et al. (2016). Dioxygenase-encoding AtDAO1 gene controls IAA oxidation and homeostasis in *Arabidopsis*. Proc. Natl. Acad. Sci. USA **113**:11016–11021.

Smirnova, E., Marquis, V., Poirier, L., Aubert, Y., Zumsteg, J., Ménard, R., Miesch, L., and Heitz, T. (2017). Jasmonic acid oxidase 2 hydroxylates jasmonic acid and represses basal defense and resistance responses against *Botrytis cinerea* infection. Mol. Plant **10**:1159–1173.

Velasquez, S.M., Ricardi, M.M., Poulsen, C.P., Oikawa, A., Dilokpimol, A., Halim, A., Mangano, S., Denita Juarez, S.P., Marzol, E., Salgado Salter, J.D., et al. (2015). Complex regulation of prolyl-4-hydroxylases impacts root hair expansion. Mol. Plant **8**:734–746.

Zhang, J., Lin, J.E., Harris, C., Pereira, F.C.M., Wu, F., Blakeslee, J.J., and Peer, W.A. (2016). DAO1 catalyzes temporal and tissue-specific oxidative inactivation of auxin in *Arabidopsis thaliana*. Proc. Natl. Acad. Sci. USA **113**:11010–11015.

frontiers | Frontiers in Plant Science

TYPE Original Research
PUBLISHED 15 November 2023
DOI 10.3389/fpls.2023.1239093

OPEN ACCESS

EDITED BY
Baohua Wang,
Nantong University, China

REVIEWED BY
Sang-Tae Kim,
The Catholic University of Korea, Republic of Korea
Cécile Raynaud,
UMR9213 Institut des Sciences des Plantes de Paris Saclay (IPS2), France

*CORRESPONDENCE
José Luis Micol
jlmicol@umh.es

†PRESENT ADDRESS
Eduardo Mateo-Bonmatí,
Centro de Biotecnología y Genómica de Plantas (CBGP), Universidad Politécnica de Madrid (UPM) – Instituto Nacional de Investigación y Tecnología Agraria y Alimentaria (INIA)/CSIC, Pozuelo de Alarcón, Madrid, Spain

RECEIVED 12 June 2023
ACCEPTED 26 October 2023
PUBLISHED 15 November 2023

CITATION
Nadi R, Juan-Vicente L, Mateo-Bonmatí E and Micol JL (2023) The unequal functional redundancy of Arabidopsis *INCURVATA11* and *CUPULIFORMIS2* is not dependent on genetic background.
Front. Plant Sci. 14:1239093.
doi: 10.3389/fpls.2023.1239093

The unequal functional redundancy of Arabidopsis *INCURVATA11* and *CUPULIFORMIS2* is not dependent on genetic background

Riad Nadi, Lucía Juan-Vicente, Eduardo Mateo-Bonmatí† and José Luis Micol*

Instituto de Bioingeniería, Universidad Miguel Hernández, Elche, Spain

The paralogous genes *INCURVATA11* (*ICU11*) and *CUPULIFORMIS2* (*CP2*) encode components of the epigenetic machinery in Arabidopsis and belong to the 2-oxoglutarate and Fe (II)-dependent dioxygenase superfamily. We previously inferred unequal functional redundancy between *ICU11* and *CP2* from a study of the synergistic phenotypes of the double mutant and sesquimutant combinations of *icu11* and *cp2* mutations, although they represented mixed genetic backgrounds. To avoid potential confounding effects arising from different genetic backgrounds, we generated the *icu11-5* and *icu11-6* mutants via CRISPR/Cas genome editing in the Col-0 background and crossed them to *cp2* mutants in Col-0. The resulting mutants exhibited a postembryonic-lethal phenotype reminiscent of strong *embryonic flower* (*emf*) mutants. Double mutants involving *icu11-5* and mutations affecting epigenetic machinery components displayed synergistic phenotypes, whereas *cp2-3* did not besides *icu11-5*. Our results confirmed the unequal functional redundancy between *ICU11* and *CP2* and demonstrated that it is not allele or genetic background specific. An increase in sucrose content in the culture medium partially rescued the post-germinative lethality of *icu11 cp2* double mutants and sesquimutants, facilitating the study of their morphological phenotypes throughout their life cycle, which include floral organ homeotic transformations. We thus established that the *ICU11-CP2* module is required for proper flower organ identity.

KEYWORDS

epigenetic machinery, *Arabidopsis thaliana*, ICU11, 2OGD, *CUPULIFORMIS2*, CRISPR/Cas9

10.3389/fpls.2023.1239093

Introduction

In *Arabidopsis thaliana* (hereafter, *Arabidopsis*), as in many other model species, the genetic dissection of biological phenomena typically involves the isolation and genetic analysis of mutants (Nüsslein-Volhard and Wieschaus, 1980; Jürgens et al., 1991; Koornneef et al., 1991; Wilkins, 1992; Haffter et al., 1996; Berná et al., 1999). The choice of the wild-type strain to be mutagenized is a key step in this endeavor, as mutant phenotypes clearly distinguishable from the wild type will not be produced for some genes in some genetic backgrounds (Lee et al., 1994; Koornneef et al., 2004; Chandler et al., 2013; Leng et al., 2022).

In addition, comparative analysis of the morphological, physiological, and molecular phenotypes of double or higher-order mutant combinations obtained by crossing single mutants is not always straightforward, given that different genetic backgrounds sometimes need to be mixed because of mutation availability in distinct strains (Huq and Quail, 2002; Scortecci et al., 2003; Clerkx et al., 2004). Indeed, phenotypes may be strongly influenced by modifiers present in the genomes of wild-type strains subjected to mutagenesis (Fernando et al., 2018). One strategy to partially overcome this problem is to first introgress each mutation of interest into an adequate genetic background, but this approach is time consuming and often leaves traces of the donor background (Rustérucci et al., 2001; Mouchel et al., 2004; Yoo et al., 2007; Zikherman et al., 2009; Kradolfer et al., 2013). An alternative approach is now accessible via clustered regularly interspaced short palindromic repeats (CRISPR)/CRISPR-associated nuclease (Cas)-mediated genome editing, which allows the relatively rapid isolation of single or multiple mutants in the same genetic background. CRISPR/Cas9 is now the preferred choice for directed mutagenesis due to its high specificity, efficiency, and simplicity (Jinek et al., 2012; Cong et al., 2013; Gaj et al., 2013; Jia et al., 2016; Zhao et al., 2016; Wang et al., 2022).

The Arabidopsis paralogous epigenetic factors INCURVATA11 (ICU11) and CUPULIFORMIS2 (CP2; Mateo-Bonmatí et al., 2018) belong to one of the largest known protein superfamilies, the 2-oxoglutarate and Fe (II)-dependent dioxygenases (2OGDs), which is represented by about 150 members in plants (Kawai et al., 2014; Martinez and Hausinger, 2015; Nadi et al., 2018). These proteins catalyze oxidation reactions using 2-oxoglutarate (also called α-ketoglutarate) and molecular oxygen as cosubstrates, and ferrous iron (Fe^{2+}) as a cofactor (Islam et al., 2018). ICU11 is a POLYCOMB REPRESSIVE COMPLEX 2 (PRC2) accessory protein likely involved in removing the active histone mark H3K36me3 (trimethylation of lysine 36 of histone H3; Bloomer et al., 2020).

We previously described unequal functional redundancy between *ICU11* and *CP2* (Mateo-Bonmatí et al., 2018). The *icu11-1* and *icu11-2* mutant alleles in the S96 and Wassilewskija-2 (Ws-2) genetic backgrounds, respectively, showed mild but pleiotropic phenotypic defects, such as early flowering and curled (hyponastic) rosette leaves, while the *cp2-1*, *cp2-2*, and *cp2-3* alleles in Columbia-0 (Col-0) were indistinguishable from their wild type. Notably, double mutant combinations between the *icu11* null alleles and the hypomorphic *cp2* alleles *cp2-1* and *cp2-2* skipped the vegetative phase and flowered immediately after germination, producing aberrant and sterile embryonic flowers. Double mutants with the null *cp2-3* allele were not obtained. The reciprocal sesquimutants *ICU11/icu11-1*;*cp2-3/cp2-3* and *icu11-1/icu11-1*; *CP2/cp2-3*, each only harboring one functional gene copy out of four, were not equivalent: while one copy of *ICU11* was sufficient to obtain plants that were phenotypically wild type, a single copy of *CP2* was not, with this sesquimutant producing lethal embryonic flowers (Mateo-Bonmatí et al., 2018).

It is not clear whether genetic background may influence redundancy in general or unequal redundancy in particular. An example of background-specific unequal redundancy has been described for the brassinosteroid receptor BRASSINOSTEROID INSENSITIVE 1 (BRI1) and its paralog BRI-LIKE1 (BRL1): in the Col-0 background, while no mutant phenotype is caused by *brl1-2*, *bri1* mutants have altered vasculature and are dwarf, only the latter trait being enhanced in the *bri1 brl1* double mutants. In contrast, the *brl1-1* mutant in Ws-2 background is altered in vasculature development (Caño-Delgado et al., 2004; Briggs et al., 2006). An example of unequal redundancy not dependent on genetic background is provided by the *SULFATE TRANSPORTER 1;1* (*SULTR1;1*) and *SULTR1;2* paralogs, encoding high-affinity sulfate uptake transporters. Whereas the *sultr1;1* mutant is similar to the wild type in root length, shoot biomass and sulfate uptake, the phenotype of the *sultr1;1 sultr1;2* double mutant is extreme, and that of *sultr1;2* is intermediate. These single and double mutants were studied both in Col-0 and Ws-2 and no effect of the genetic background was observed (Yoshimoto et al., 2007; Barberon et al., 2008).

Here, we obtained by CRISPR/Cas9-mediated gene editing alleles of *ICU11* in the Col-0 and S96 backgrounds. They had differing phenotypes as single mutants but apparently identical genetic interactions with *cp2* alleles in double mutant combinations. We therefore provide evidence that the lethal postembryonic phenotype of the *icu11 cp2* double mutants and sesquimutants is not specific to the allele or the genetic background. We also discovered that this seedling lethality can be circumvented by increasing the sucrose content of the growth medium, which in turn allowed us to obtain evidence of the requirement of the *ICU11-CP2* module for proper flower organ identity.

Materials and methods

Plant material, culture conditions, and crosses

Unless otherwise stated, all *Arabidopsis thaliana* (L.) Heynh. plants studied in this work were homozygous for the mutations indicated. The Nottingham Arabidopsis Stock Centre (NASC) provided seeds for the wild-type accessions Columbia-0 (Col-0; N1092), S96 (N914), and Wassilewskija-2 (Ws-2; N1601), as well as the following mutants: *icu11-1* (N242) in the S96 background; *curly leaf-2* (*clf-2*; N8853) in the Landsberg *erecta* (*Ler*) background;

arabidopsis trithorax1-2 (*atx1-2*; N649002), *arabidopsis trithorax-related protein 5* (*atxr5*; N630607), *atxr6* (N866134), *atxr7-1* (N667600), *cp2-1* (N861581), *cp2-2* (N828642), *cp2-3* (N826626), *demeter-like 2-3* (*dml2-3*; N631712), *dml3-1* (N556440), *dna methyltransferase-2-2* (*dnmt2-2*; N836854), *domains rearranged methylase 1-2* (*drm1-2*; N521316), *drm2-2* (N650863), *histone acetyltransferase of the cbp family 1-3* (*hac1-3*; N580380), *histone acetyltransferase of the myst family 1-1* (*ham1-1*; N655396), *methyltransferase 1-4* (*met1-4*; N836155), *repressor of silencing 1-4* (*ros1-4*; N682295), *ros3-2* (N522363), *terminal flower2-2* (*tfl2-2*; N3797), and *embryonic flower2-3* (*emf2-3*; N16240) in the Col-0 background; *icu2-1* (N329) and *fasciata1-1* (*fas1-1*; N265) in the Enkheim2 (En-2) background; *methyl-cpg-binding domain10-1* (*mbd10-1*; N872244) and *variant in methylation 3-2* (*vim3-2*; N804664) in the Col-3 background; and *histone deacetylase 6-6* (*hda6-6*; N66153) and *hda6-7* (N66154) in the Col background. Seeds for *early bolting in short days-1* (*ebs-1*, in the L*er* background; Piñeiro et al., 2003) were provided by Manuel Piñeiro (CBGP, UPM-INIA-CSIC, Madrid, Spain), those of *gigantea supressor5* (*gis5*, in the Col-0 background; Iglesias et al., 2015) by Pablo D. Cerdán (Fundación Instituto Leloir, IIBBA-CONICET, Buenos Aires, Argentina), and those of *icu11-2* (in the Ws-2 background) by the Versailles Arabidopsis Stock Center (Brunaud et al., 2002). The presence and positions of all T-DNA insertions were confirmed by PCR amplification using gene-specific primers, with the LbB1.3 and LB1 primers used for the SALK and SAIL T-DNA insertions, respectively (Supplementary Table S1).

Unless otherwise stated, all seeds were surface sterilized, plated onto 140-mm (diameter) Petri dishes containing 100 ml half-strength Murashige and Skoog (MS) plant agar medium with 1% (w/v) sucrose at 20 ± 1°C, 60-70% relative humidity, and continuous illumination at ~75 µmol m^{-2} s^{-1}, as previously described (Ponce et al., 1998). Crosses were performed as previously described (Quesada et al., 2000).

Plant morphology and pollen staining

Photographs showing morphology were taken with a Nikon SMZ1500 stereomicroscope equipped with a Nikon DXM1200F digital camera and the ACT-1 software (Nikon). Pollen grains were stained with Alexander red solution for 5–10 min before observation and photographed using a Leica DMRB microscope equipped with a Nikon DXM1200 digital camera.

Gene constructs and plant transformation

The pKI1.1R-ICU11_sgRNA1 plasmid was constructed as described by Tsutsui and Higashiyama (2017). In brief, the pKI1.1R plasmid (85808; Addgene) was linearized by restriction digest with *Aar*I (Thermo Fisher Scientific), and treated with FastAP alkaline phosphatase (Thermo Fisher Scientific). The ICU11_sgRNA1_F/R oligonucleotides were phosphorylated using T4 polynucleotide kinase (New England Biolabs) and hybridized in a thermal cycler (Bio-Rad Laboratories T100). The ligation reaction was performed with T4 DNA ligase (Thermo Fisher Scientific), and the ligation product was transformed into chemically competent *Escherichia coli* DH5α cells using the heat-shock method. Plasmid and insert integrity were verified by Sanger sequencing using an Applied Biosystems 3500 Genetic Analyzer (Thermo Fisher Scientific). Putative off-targets were identified using the default parameters of the ChopChop tool (Labun et al., 2019). The pKI1.1R-ICU11_sgRNA1 plasmid was mobilized into *Agrobacterium tumefaciens* GV3101 (C58C1 Rif^R) cells, which were used to transform Arabidopsis S96 and Col-0 plants via the floral dip method (Clough and Bent, 1998). T_1 Arabidopsis transgenic plants were selected on plates with half-strength MS medium containing 15 mg l^{-1} hygromycin B (Thermo Fisher Scientific). Absence of the transgene in T_2 plants was verified by selecting DsRED negative seeds and confirmed by negative PCR amplifications using Cas9 specific primers (Supplementary Table S1).

Flowering time analysis

Flowering time was determined based on the total number of rosette leaves (counted when internode elongation was visible) and the number of days to bolting (Bouveret et al., 2006). To determine flowering time, all plants were grown on half-strength MS medium for five days and transferred to soil (a 2:2:1 mixture of perlite, vermiculite and sphagnum peat moss) in individual pots in a TC30 growth chamber (Conviron).

Accession numbers

Sequence data from this article can be found at The Arabidopsis Information Resource (http://www.arabidopsis.org) under the following accession numbers: *ICU11* (At1g22950), *CP2* (At3g18210), *EBS* (At4g22140), *FAS1* (At1g65470), *GIS5* (At5g63960), *ICU2* (At5g67100), *CLF* (At2g23380), *TFL2* (At5g17690), *EMF2* (At5g51230), *DML2* (At3g10010), *DML3* (At4g34060), *DNMT2* (At5g25480), *DRM1* (At5g15380), *DRM2* (At5g14620), *MBD10* (At1g15340), *MET1* (At5g49160), *ROS1* (At2g36490), *ROS3* (At5g58130), *VIM3* (At5g39550), *ATX1* (At2g31650), *ATXR5* (At5g09790), *ATXR6* (At5g24330), *ATXR7* (At5g42400), *HAC1* (At1g79000), *HDA6* (At5g63110), and *HAM1* (At5g64610).

Results

Isolation of novel *icu11* mutants in a Col-0 background after CRISPR/Cas9 mutagenesis

We previously characterized two loss-of-function *icu11* alleles: *icu11-1* and *icu11-2* (Mateo-Bonmatí et al., 2018). A third allele, *icu11-3*, was identified in an Ac/Ds transposon-tagging mutagenesis screen (Bancroft et al., 1993; Bloomer et al., 2020). Although these three mutants appear to carry null alleles (Figure 1), the hyponasty of

10.3389/fpls.2023.1239093

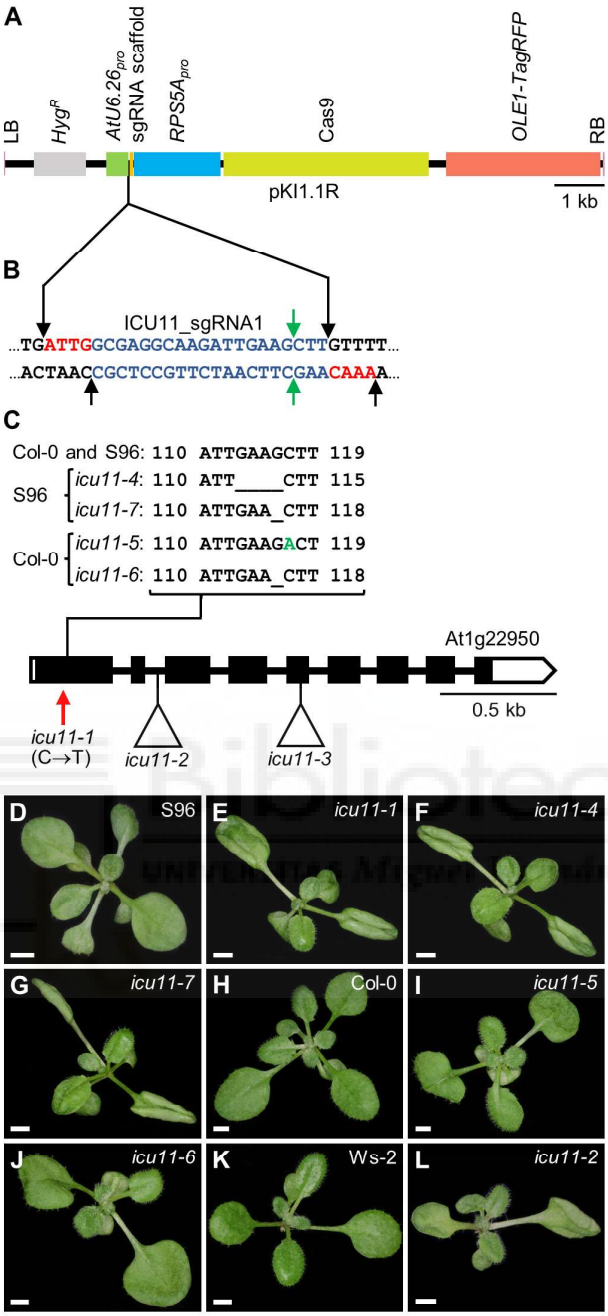

FIGURE 1
Molecular nature and morphological phenotypes of the *icu11* mutations obtained in this work. **(A)** Diagram of the T-DNA fragment of the pKIR1.1R vector that is integrated into the plant genome. Structural features are represented as boxes: LB and RB, left and right T-DNA borders (pink); *Hyg*^{R}, hygromycin resistance gene (gray); *AtU6.26*$_{pro}$, promoter of *U6 SMALL NUCLEOLAR RNA26* (green); sgRNA scaffold, the sequence that serves as a binding site for *Streptococcus pyogenes* Cas9 protein (orange); *RPS5A*$_{pro}$, promoter of *RIBOSOMAL PROTEIN 5A* (blue); Cas9, CRISPR-associated protein 9 (pale green); *OLE1-TagRFP*, a translational fusion of the gene encoding OLEOSIN 1, the most abundant oleosin in Arabidopsis seeds, and that of the red fluorescent protein (RFP; red). Between the *AtU6.26* promoter and the sgRNA scaffold, there are two restriction sites for the type IIS *Aar*I restriction enzyme. **(B)** Nucleotide sequence of the sgRNA scaffold (black) and the *ICU11* sgRNA1 (blue) with four-nucleotide overhangs used for cloning (red). Black and green arrows indicate the *Aar*I restriction sites and predicted Cas9 cleavage sites, respectively. **(C)** Schematic representation of the structure of the *ICU11* gene with indication of the nature and positions of *icu11* mutations. White and black boxes represent untranslated and coding regions of exons, respectively; lines represent introns. A red vertical arrow indicates the *icu11-1* point mutation, and triangles indicate the *icu11-2* T-DNA and *icu11-3* Ds insertions (not studied in this work). The sequences of the *icu11-4*, *icu11-6*, and *icu11-7* deletions and the *icu11-5* insertion (+1 bp, in green) are also shown. **(D–L)** Rosettes of the **(D)** S96, **(H)** Col-0, and **(K)** Ws-2 wild-type accessions, and the **(E)** *icu11-1*, **(F)** *icu11-4*, **(G)** *icu11-7*, **(I)** *icu11-5*, **(J)** *icu11-6*, and **(L)** *icu11-2* single mutants. Photographs were taken 15 days after stratification (das). Scale bars, 2 mm.

icu11-1 leaves is stronger than that caused by the *icu11-2* and *icu11-3* alleles, which is likely due to their different genetic backgrounds (S96, Ws-2, and L*er*, respectively). Different or hybrid genetic backgrounds may not facilitate proper comparisons of the morphological and molecular phenotypes of single and multiple mutants (Page and Grossniklaus, 2002; Chandler et al., 2013; Taylor and Ehrenreich, 2015). Therefore, as all *cp2* alleles were in the Col-0 background but there were no available *icu11* alleles in this background, we subjected Col-0 plants to CRISPR/Cas9 mutagenesis targeting *ICU11*. We also mutagenized S96 plants as a control. Accordingly, we designed a 20-nt single guide RNA (sgRNA) that targets the first exon of the *ICU11* gene, with a predicted targeting efficiency of 49.7% (Figures 1A, B; Supplementary Figure S1A). We obtained seven chimeric T_1 plants, from which we isolated four T_2 independent homozygous lines: the *icu11-4* and *icu11-7* mutants in the S96 background, carrying deletions of 4 bp and 1 bp, respectively, and *icu11-5* and *icu11-6* in the Col-0 background, carrying a 1-bp insertion and a 1-bp deletion, respectively (Figure 1C; Supplementary Figure S1B). All these mutations are predicted to cause frameshifts that introduce premature stop codons, producing truncated proteins of only 86 (*icu11-4*), 44 (*icu11-5*), or 87 (*icu11-6* and *icu11-7*) amino acids, instead of the 397 amino acids of wild-type ICU11 (Supplementary Figure S1C). We sequenced Cas9-free lines by Sanger sequencing to examine the two most likely off-targets, both of which presented four mismatches with at least one mismatch located in the 5 bp adjacent to the protospacer adjacent motif (PAM) of our sgRNA (Supplementary Figure S2A); neither off-target was mutated in subsequent generations of our mutant lines (Supplementary Figure S2B).

The seedling lethal phenotype of the *icu11 cp2* double mutants is independent of genetic background

As expected from their S96 background, the *icu11-4* and *icu11-7* mutants exhibited a morphological phenotype indistinguishable from that of *icu11-1* (Figures 1D–G). The *icu11-5* and *icu11-6* mutants showed wavy leaves that did not reach hyponasty (Figures 1H–J), different to that of *icu11-2* (Figures 1K, L) and *icu11-3* (Bloomer et al., 2020). In addition, *icu11-5* and *icu11-6* shared other phenotypic traits with the other *icu11* mutants, such as cotyledon epinasty (Figures 1D–L) and early flowering (Figures 2A, B). We observed significantly more unfertilized ovules per half silique in the *icu11-4*, *icu11-5*, *icu11-6* and *icu11-7* mutants compared to their respective wild types (Figures 2C–L). Taken together, these observations indicate that our new *icu11* mutants are phenotypically similar to previously reported mutants, with only minor differences caused by their genetic background, which are particularly visible in their rosette leaf morphology.

Although the morphological phenotypes caused by the *icu11* alleles are relatively mild, and the *cp2* null mutants are indistinguishable from wild type, the phenotypes of *icu11 cp2* double mutants are synergistic: they are seedling lethal, as might be expected for the genetic combination of mutations in two close paralogs with a high degree of functional redundancy (Ohno, 1970; Nowak et al., 1997; Cusack et al., 2021). Our previously obtained *icu11 cp2* double mutants had hybrid genetic backgrounds, which prevented a clear conclusion as to the seedling lethality presented by these double mutants. Here, we thus crossed *icu11-5* and *icu11-6* with the *cp2-1* and *cp2-2* hypomorphic alleles of *CP2*, and with the *cp2-3* null allele, all of which are in the Col-0 genetic background. The double homozygous mutant combinations between *icu11-5* or *icu11-6* and *cp2-1* or *cp2-2* exhibited an embryonic-flowering seedling-lethal phenotype, as did the *icu11*/*icu11*;*CP2*/*cp2-3* sesquimutants (Figure 3). We obtained no *icu11-5 cp2-3* or *icu11-6 cp2-3* double mutants, as was previously published for *icu11-1 cp2-3* (Mateo-Bonmatí et al., 2018). The *ICU11*/*icu11*;*cp2-3*/*cp2-3* sesquimutants were indistinguishable from the wild type (Figures 3I, N), as were those we previously published in hybrid genetic backgrounds.

icu11-5, but not *cp2-3*, genetically interacts with loss-of-function alleles of genes encoding PRC2 core components and accessory proteins

Synergistic phenotypes visualized in double mutants shed light on functional relationships between genes (Pérez-Pérez et al., 2009), including those encoding components of the epigenetic machinery of Arabidopsis. For example, PWWP-DOMAIN INTERACTOR OF POLYCOMB1 (PWO1) is a histone reader that recruits PcG proteins (Hohenstatt et al., 2018), and BLISTER (BLI) is a PRC2 interactor and a regulator of stress-responsive genes (Kleinmanns et al., 2017). Both *pwo1* and *bli* loss-of-function mutations display synergistic phenotypes when combined with strong mutant alleles of *CURLY LEAF* (*CLF*), which encodes a PRC2 core component responsible for the deposition of H3K27me3 repressive marks (Goodrich et al., 1997; Schatlowski et al., 2010).

With the aim to expand the spectrum of genes demonstrated to genetically interact with *ICU11*, we crossed *icu11-1* to loss-of-function mutants of 17 genes encoding components of the epigenetic machinery that include proteins involved in DNA or histone methylation, acetylation, or deacetylation (Pikaard and Mittelsten Scheid, 2014). We identified 18 double mutants with additive phenotypes (Supplementary Table S2). Also we obtained double mutant combinations of *icu11-5* with loss-of-function alleles of *CLF*, *LIKE HETEROCHROMATIN PROTEIN 1* (*LHP1*; also named *TFL2*), *FASCIATA1* (*FAS1*), *EARLY BOLTING IN SHORT DAYS* (*EBS*), *GIGANTEA SUPRESSOR5* (*GIS5*), and *ICU2*, previously found to genetically interact with *icu11-1* (Mateo-Bonmatí et al., 2018). FAS1 is a component of the Chromatin Assembly Factor 1 (CAF-1) complex that promotes the deposition of histone H3 and H4 at newly synthesized DNA during replication (Schönrock et al., 2006). EBS is an H3K27me3 and H3K4me3 reader that regulates the floral phase transition (Piñeiro et al., 2003; López-González et al., 2014; Yang et al., 2018). GIS5 and ICU2 are the catalytic subunits of DNA polymerase δ and α, respectively (Barrero et al., 2007; Iglesias et al., 2015). The double mutant combinations of *icu11-5* with *clf-2*, *ebs-1*, *gis5*, *icu2-1*, *tfl2-2*, or *fas1-1* exhibited strong synergistic phenotypes consisting of dwarf rosettes; extreme leaf hyponasty in the cases of *gis5*, *icu2-1*, and *fas1-1*; and some degree of anthocyanin accumulation in the *icu11-5 tfl2-2* rosette center

10.3389/fpls.2023.1239093

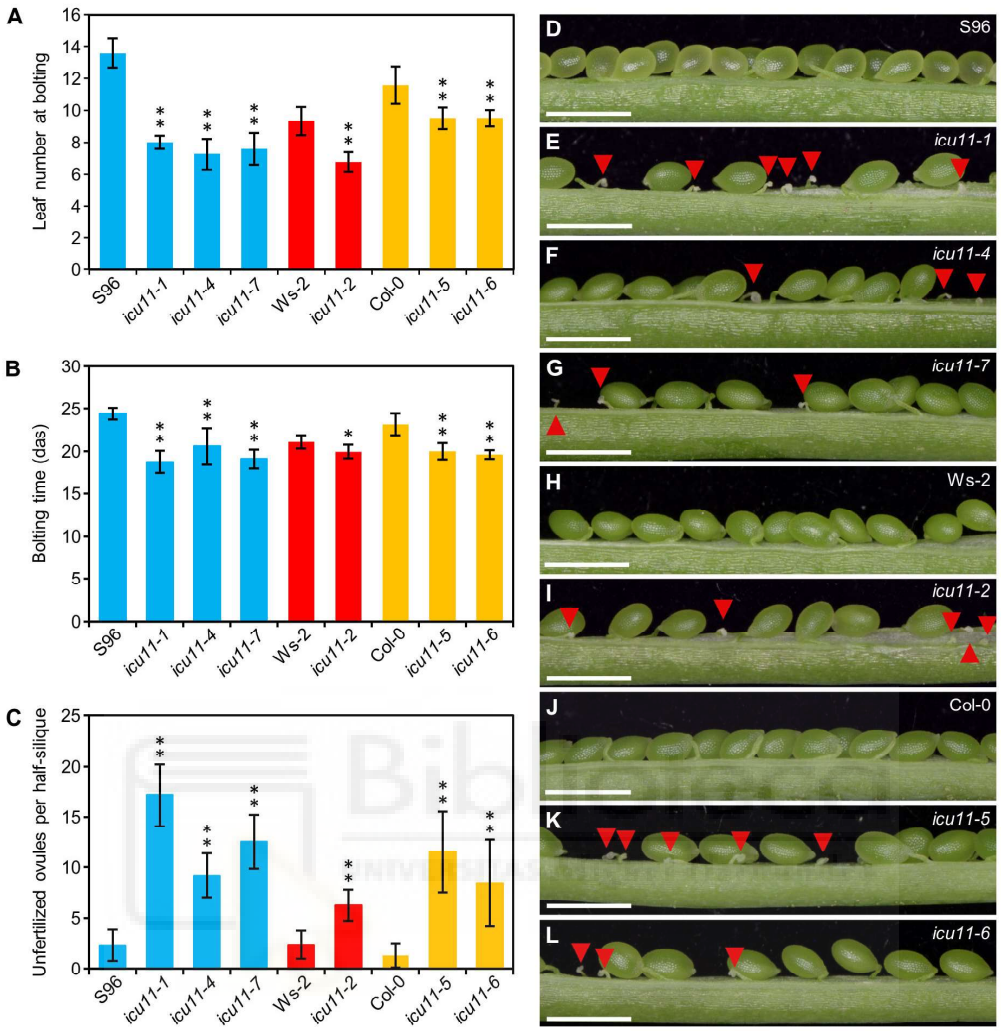

FIGURE 2
Flowering and reproductive phenotypes of the *icu11-5* and *icu11-6* mutants. **(A, B)** Flowering time of S96, *icu11-1*, *icu11-4*, *icu11-7*, Ws-2, *icu11-2*, Col-0, *icu11-5*, and *icu11-6* plants, expressed as **(A)** leaf number at bolting and **(B)** number of days to bolting. **(C)** Number of unfertilized ovules per half silique for the indicated genotypes. Data are means ± standard deviation. Asterisks indicate values significantly different from the corresponding wild type in a Mann-Whitney *U* test (*$P < 0.01$ and **$P < 0.001$). Blue, red, and yellow bars indicate that the plants of the genotypes shown are in the S96, Ws-2, and Col-0 backgrounds, respectively. **(D–L)** Dissected fully elongated siliques with the indicated genotypes. Red arrowheads indicate unfertilized ovules. Photographs were taken 45 das. Scale bars, 1 mm. All siliques in **(C–L)** were collected from plants grown simultaneously within the same growth chamber. Pictures in **(D, E, H, I, J)** are similar to those that we published in the Supplemental Figure 2 **(A–D, G)** of Mateo-Bonmatí et al. (2018), respectively. Siliques of S96, *icu11-1*, Ws-2, *icu11-2* and Col-0 are included here to allow comparison with *icu11-4*, *icu11-7*, *icu11-5* and *icu11-6*. The numbers shown in **(C)** for S96, *icu11-1*, Ws-2, *icu11-2* and Col-0 have been obtained independently of those of Supplemental Figure 2L of Mateo-Bonmatí et al. (2018).

(Figure 4). The phenotypes of the double mutant combinations of *icu11-5* with *clf-2*, *gis5*, and *icu2-1* were similar to those previously reported using *icu11-1*; however, those involving *tfl2-2*, *ebs-1*, and *fas1-1* were milder in combination with *icu11-5* (Figures 4L–N) than with *icu11-1* (Mateo-Bonmatí et al., 2018).

We also combined the mutations mentioned above with the *cp2-3* mutation, which lacks a distinctive phenotype; the resulting F_2 progeny showed rosette phenotypes that were indistinguishable from those of their corresponding phenotypically mutant parent (Figures 4P–U). We conclude that, unlike *ICU11*, the loss of *CP2* function is not sufficient to modify the phenotypes caused by mutations in other genes involved in epigenetic modifications, confirming the previously proposed unequal functional redundancy between *ICU11* and *CP2* (Mateo-Bonmatí et al., 2018).

Sucrose partially rescues the lethality of the *icu11 cp2* double mutants

There is an expanding list of Arabidopsis mutants exhibiting morphological phenotypes that are partially or fully rescued by the exogenous supplementation of sucrose, such as *phosphatidylglycerol*

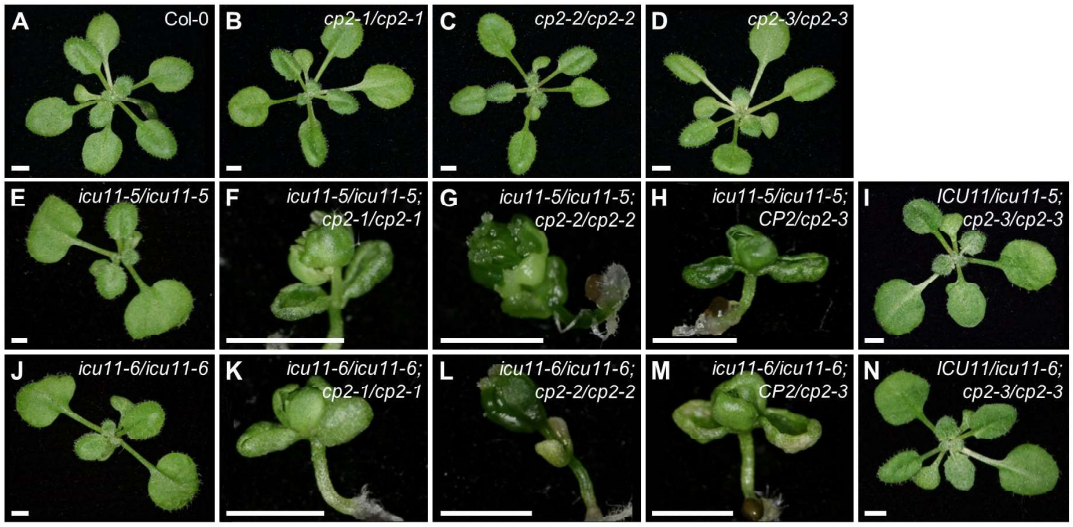

FIGURE 3
Genetic interactions between the loss-of-function *icu11* and *cp2* alleles in the Col-0 genetic background. *icu11-5*, *icu11-6*, and *cp2-3* are null alleles, while *cp2-1* and *cp2-2* are hypomorphic. Rosettes of **(A)** the wild-type Col-0; the homozygous single mutants **(B)** *cp2-1*, **(C)** *cp2-2*, **(D)** *cp2-3*, **(E)** *icu11-5*, and **(J)** *icu11-6*; the double mutants **(F)** *icu11-5 cp2-1*, **(G)** *icu11-5 cp2-2*, **(K)** *icu11-6 cp2-1*, and **(L)** *icu11-6 cp2-2*; and the sesquimutants **(H)** *icu11-5/icu11-5;CP2/cp2-3*, **(I)** *ICU11/icu11-5;cp2-3/cp2-3*, **(M)** *icu11-6/icu11-6;CP2/cp2-3* and **(N)** *ICU11/icu11-6;cp2-3/cp2-3*. Photographs were taken 16 das. Scale bars, 2 mm.

phosphate synthase 1 (*pgp1*) and *cyclophilin 38* (*cyp38*), which are defective in the assembly and proper function of photosystem II protein complexes, respectively (Fu et al., 2007; Kobayashi et al., 2016; Duan et al., 2021). This phenomenon is true for other Arabidopsis genes that are functionally unrelated, but whose mutations directly or indirectly impair or abolish photosynthesis. We observed the same effect in *icu11 cp2-1* and *icu11 cp2-2* double mutant seedlings, in which photosynthesis is diminished because they do not form true leaves, instead developing embryonic flowers immediately after germination. These mutants had a very slow growth rate, did not develop further, and died 20–40 days after stratification (das; Figures 5A–C). When we raised the

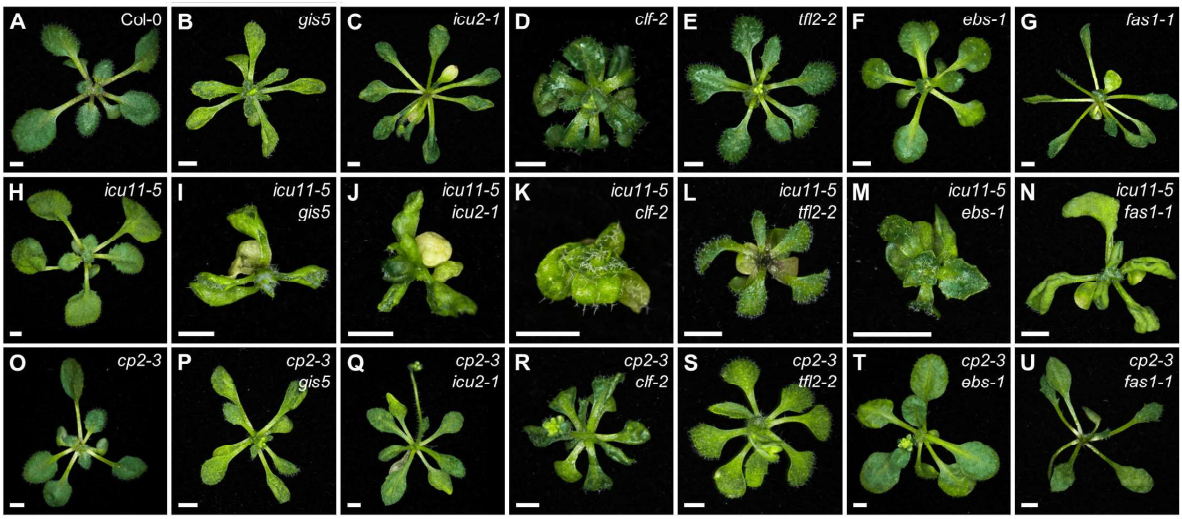

FIGURE 4
Phenotypes of double mutants involving *icu11-5* and *cp2-3* with *gis5*, *icu2-1*, *clf-2*, *tfl2-2*, *ebs-1*, and *fas1-1*. Rosettes of **(A)** the wild-type Col-0; the single mutants **(B)** *gis5*, **(C)** *icu2-1*, **(D)** *clf-2*, **(E)** *tfl2-2*, **(F)** *ebs-1*, **(G)** *fas1-1*, **(H)** *icu11-5*, and **(O)** *cp2-3*; and the double mutants **(I)** *icu11-5 gis5*, **(J)** *icu11-5 icu2-1*, **(K)** *icu11-5 clf-2*, **(L)** *icu11-5 tfl2-2*, **(M)** *icu11-5 ebs-1*, **(N)** *icu11-5 fas1-1*, **(P)** *cp2-3 gis5*, **(Q)** *cp2-3 icu2-1*, **(R)** *cp2-3 clf-2*, **(S)** *cp2-3 tfl2-2*, **(T)** *cp2-3 ebs-1*, and **(U)** *cp2-3 fas1-1*. Photographs were taken 15 das. Scale bars, 2 mm.

10.3389/fpls.2023.1239093

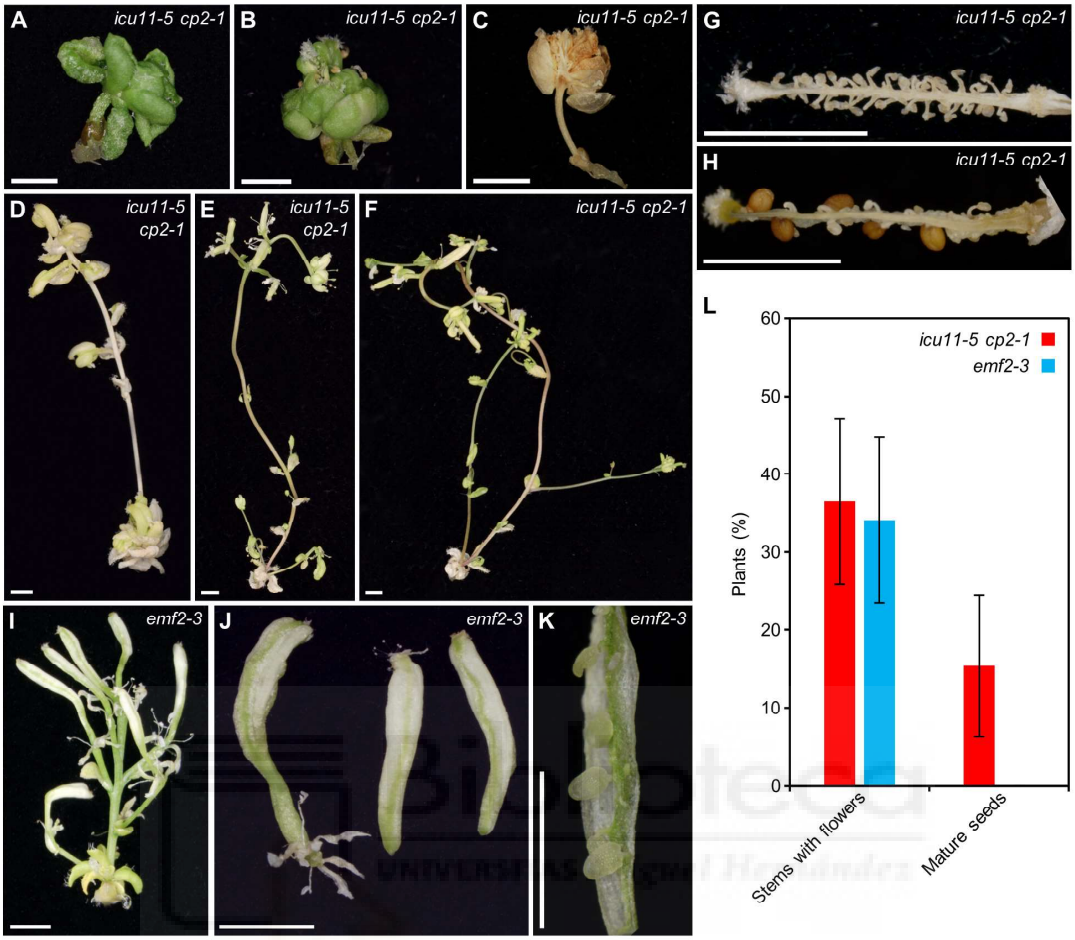

FIGURE 5
Partial rescue of the post-germinative lethality phenotype of *icu11-5 cp2-1* and *emf2-3* plants grown on culture medium supplemented with 3% sucrose. **(A–K)** Pictures of **(A–H)** the *icu11-5 cp2-1* double mutant or **(I–K)** the *emf2-3* single mutant, showing **(A–C)** embryonic flowers; seedlings developing **(D–F)** stems, **(I)** flowers, **(J)** siliques, and **(G, H, K)** dissected siliques. **(L)** Percentage of *icu11-5 cp2-1* and *emf2-3* plants with different phenotypes grown on culture medium supplemented with 3% sucrose. Error bars indicate standard deviation. A total of 136 *icu11-5 cp2-1* and 110 *emf2-3* plants were classified. Photographs were taken **(A, B)** 26, **(D–F, I–K)** 36, **(G, H)** 60, and **(C)** 84 das. Scale bars, 2 mm.

concentration of sucrose in the growth medium from 1% (w/v) to 3%, *icu11-5 cp2-1* double mutant plants developed main and axillary shoots with long internodes, small cauline leaves, disorganized flowers, and short siliques. Most of the disorganized flowers showed homeotic transformations of sepals and petals into carpels and had few stamens (Figures 5D–H).

The *emf2-3* single mutant (Yoshida et al., 2001), whose morphological phenotype is similar to that of *icu11 cp2* double mutant plants, also exhibited a partial rescue under increased sucrose supplementation. These plants growing on 3% sucrose medium produced main and axillary shoots lacking apical dominance, as well as flowers with an altered structure that developed into short siliques with extended white sectors reminiscent of petal tissue (Figures 5I–K). When grown on growth medium supplemented with 3% sucrose, 36.5% of *icu11-5 cp2-1* (n = 136) and 34.1% of *emf2-3* (n = 110) plants developed stems with flowers, although even with hand pollination only 15.3% of *icu11-5 cp2-1* plants and no *emf2-3* plants produced mature seeds (Figure 5L). Only one out of the 23 seeds obtained in this manner from *icu11-5 cp2-1* plants germinated on medium supplemented with 3% sucrose, and still developed embryonic flowers.

An alteration in pollen viability may explain why only some *icu11-5 cp2-1* double mutant plants produced seeds. To assess pollen grain viability in the *icu11-5*, *cp2-1*, and *icu11-5 cp2-1* mutants, we stained their anthers with Alexander solution. We detected no aberrations in anther shape or size or in pollen grain viability for the *cp2-1* and *icu11-5* anthers when compared to Col-0 (Figures 6A–F). However, 66% of the observed *icu11-5 cp2-1* anthers were smaller and carried fewer but viable pollen grains (Figures 6G, H, K). The remaining 34% of anthers were also small and contained only non-viable pollen that turned blue/gray upon staining (Figures 6G–K).

10.3389/fpls.2023.1239093

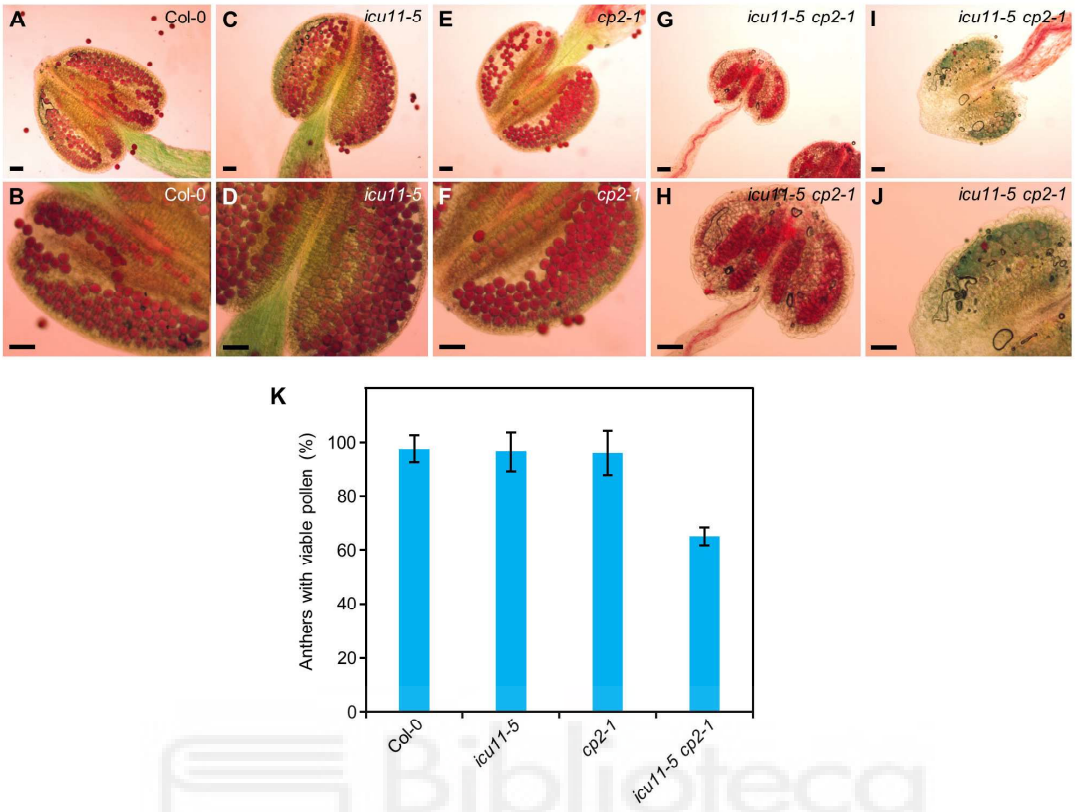

FIGURE 6
Pollen grain viability in *icu11-5*, *cp2-1*, and *icu11-5 cp2-1*. **(A–J)** Anthers of **(A, B)** Col-0, **(C, D)** *icu11-5*, **(E, F)** *cp2-1*, and **(G–J)** *icu11-5 cp2-1* plants. Col-0, *icu11-5*, and *cp2-1* plants were grown on standard culture medium (supplemented with 1% sucrose), while *icu11-5 cp2-1* plants were grown on medium supplemented with 3% sucrose. Purple/red and blue/gray grains are viable and non-viable pollen, respectively. All samples were treated for 5 min with Alexander solution. Scale bars, 50 µm. **(K)** Percentage of anthers containing viable pollen after collecting and studying 28 anthers (three or four per plant). Error bars indicate standard deviation.

Discussion

The severity of leaf aberrations in the *icu11* single mutants is dependent on genetic background

A common task in developmental genetics is the analysis of phenotypic differences between mutants carrying different alleles of a given gene, as well as the comparison of their corresponding double mutants. Many studies have shown that morphological phenotypes can vary depending on the genetic background; for example, the *gibberellin biosynthesis* (*ga5*) mutant in L*er* displays a much more pronounced drop in shoot fresh weight than the *ga20ox1-3* (another loss-of-function allele of the *GA5* gene) mutant, in the Col-0 background (Barboza-Barquero et al., 2015). Such phenotypic difference can be due to allele specifity, the *erecta* mutation carried by L*er*, or to any other of the many differences between the genetic backgrounds of L*er* and Col-0. Another example is the transfer of transgenes carrying either the functional L*er* allele or the loss-of-function allele from the Japanese accession Fuk of the MADS box transcription factor gene *SHORT VEGETATIVE PHASE* (*SVP*), which regulates flowering time, into five Arabidopsis accessions. In some of these accessions, the presence of *SVP*-Fuk accelerated flowering, whereas *SVP*-L*er* delayed it; however, in other accessions, no noticeable differences were observed (Méndez-Vigo et al., 2013). The genetic modifiers partially or fully responsible for genetic background effects have been identified in a few cases. For example, the *short stem and midrib* (*ssm*) mutant in Col-0 is semi-dwarf and has wavy leaves; in the progeny of crosses of L*er* to *ssm*, such phenotype was rescued by a gene apparently present in L*er* but absent from Col-0. *ssm* was found to be a null allele of *SYNTAXIN OF PLANTS 22* (*SYP22*), which encodes a syntaxin-related protein required for vacuolar assembly. The L*er* allele of *SYP23*, a close paralog of *SYP22*, is functional and complements *ssm*, whereas the Col-0 allele of *SYP23* is mutated (Ohtomo et al., 2005).

The *icu11-1* mutant exhibits a developmental phenotype previously observed in other mutants that carry alleles of genes encoding components of the epigenetic machinery (Mateo-Bonmatí et al., 2018). These characteristic aberrations, such as leaf hyponasty

and early flowering, are in some cases associated with a reduced deposition of the epigenetic mark H3K27me3 across a large number of genes (Förderer et al., 2016). The gene-edited *icu11-5* and *icu11-6* null alleles of *ICU11* that we obtained in the Col-0 genetic background in this study exhibited a leaf incurvature milder than that of *icu11-1* in the S96 background. These differences are most likely due to differences in the genetic backgrounds, as we also obtained two CRISPR/Cas9 mutants in the S96 background, *icu11-4* and *icu11-7*, which displayed identical leaf curvature as *icu11-1*. Furthermore, it is worth mentioning here that *icu11-6* and *icu11-7* carry independently obtained but identical mutations: a deletion of one nucleotide immediately downstream of the PAM; therefore, their differences in leaf phenotype can only be due to their different genetic backgrounds.

The unequal functional redundancy between the *ICU11* and *CP2* paralogs is not dependent on genetic background

CP2 and *ICU11* are unequally redundant paralogs, as we inferred from the phenotype of the *icu11-1*/*icu11-1*;*CP2*/*cp2-3* sesquimutant, which develops lethal embryonic flowers, while the reciprocal *ICU11*/*icu11-1*;*cp2-3*/*cp2-3* sesquimutant is phenotypically wild type (Mateo-Bonmatí et al., 2018). The *icu11-1 cp2-1* and *icu11-1 cp2-2* double mutants also developed embryonic flowers, whereas the *ICU11*/*icu11-1*;*cp2-1*/*cp2-1* and *ICU11*/*icu11-1*;*cp2-2*/*cp2-2* sesquimutants were indistinguishable from wild type plants, and the *icu11-1*/*icu11-1*;*CP2*/*cp2-1* and *icu11-1*/*icu11-1*;*CP2*/*cp2-2* sesquimutants were indistinguishable from *icu11-1* single mutant plants. While the genetic background of these double mutants and sesquimutants was hybrid (S96/Col-0), all combinations between the *icu11-5*, *icu11-6*, *cp2-1*, *cp2-2*, and *cp2-3* mutations that we obtained here were in a single genetic background (Col-0). Furthermore, as previously shown for *icu11-1*/*icu11-1*;*cp2-3*/*cp2-3*, no *icu11-5*/*icu11-5*;*cp2-3*/*cp2-3* or *icu11-6*/*icu11-6*;*cp2-3*/*cp2-3* double mutants were obtained likely because of their gametic or early embryonic mortality. The genetic combination of our new *icu11* alleles with *cp2* alleles, all in the Col-0 background, confirmed that *CP2* behaves as a haploinsufficient locus in a homozygous *icu11* background (Pérez-Pérez et al., 2009; Meinke, 2013; Navarro-Quiles et al., 2023), and in particular, that the embryonic flower phenotype of the double mutant and some sesquimutant combinations of their alleles are not influenced by the S96, Ws-2, or Col-0 genetic backgrounds.

We also provided further evidence for the unequal functional redundancy between *ICU11* and *CP2* through the analysis of their genetic interactions with loss-of-function alleles of other epigenetic machinery components. We established that *icu11-5* synergistically interacts with *clf-2*, *ebs-1*, *gis5*, *icu2-1*, *tfl2-2*, and *fas1-1* in the presence of two wild-type *CP2* copies, as previously reported for *icu11-1*. There were some minor differences between the synergistic phenotypes of the double mutant combinations of *ebs-1* (in the L*er* background), *tfl2-2* (Col-0), and *fas1-1* (En-2) with *icu11-1* (S96) or *icu11-5* (Col-0), which can be attributed to the genetic background. By contrast, the double mutant combinations of *ebs-1*, *tfl2-2*, or *fas1-1* with the *cp2-3* null allele, in the presence of two *ICU11* wild-type copies, resulted in phenotypes indistinguishable from those of the *ebs-1*, *tfl2-2*, or *fas1-1* single mutants. Apparently, the presence of a wild-type allele of *ICU11* impedes the identification of *CP2* genetic interactors, as they are redundant. Thus, the lethality of the *icu11 cp2* double mutants is an obstacle for an independent characterization of *CP2*.

The viability of the double mutant and sesquimutant combinations of alleles of *ICU11* and *CP2* is dependent on exogenous carbon

The phenotype of a large number of mutants in genes that are primarily associated with photosynthesis or processes closely linked to it can be partially or completely alleviated by supplementation with an exogenous carbon source. Indeed, photosynthesis, primarily occurring in plant leaves, serves as the ultimate source of sugars, which are the primary carriers of both sunlight energy and carbon required for metabolism. Sugar availability is crucial for Arabidopsis development, leading to early developmental arrest in mutants with impaired photosynthesis, such as *pgp1* (Kobayashi et al., 2016), and *fructokinase-like 2-4* (*fln2-4*; Huang et al., 2013) or *white cotyledons* (*wco*; Yamamoto et al., 2000). Since WCO is only required for chloroplast biogenesis in cotyledons but not in true leaves, *wco* mutants can be supplied with 3% sucrose for a few days to enable them to survive and produce true leaves, after which the plants develop normally. Other mutations of genes involved in photosynthesis are not seedling or plant lethal but delay growth; for example, CYP38 participates in the assembly and maintenance of photosystem II, and loss-of-function *cyp38* alleles show retarded growth and pale green leaves. A 1% sucrose supplementation was sufficient to rescue rosette growth, although *cyp38* still displayed hypersensitivity to light, while higher concentrations of sucrose increased the length of the primary root (Fu et al., 2007; Duan et al., 2021).

Although several genes repress flowering in Arabidopsis, the *emf* single mutants are unique because they completely skip the vegetative phase after seed germination without generating true leaves (Sung et al., 1992; Yang et al., 1995). The *icu11 cp2* double mutants resembled the *emf* single mutants, as they also lacked true leaves. Impaired carbon fixation results in the early-development arrest of these mutants, so they cannot produce reproductive structures beyond a disorganized embryonic flower. These mutants represent a class completely different from those mentioned above, as they are not mutated in genes primarily related to photosynthesis. Instead, they skip vegetative development and die because they cannot develop leaves, which does not allow them to photosynthesize properly.

ICU11 and CP2 appear to regulate flower organ identity genes

The increase from 1% to 3% sucrose in the growth medium was sufficient to allow the formation in our *icu11 cp2* double mutants of axillary shoots, cauline leaves, and disorganized inflorescences exhibiting flowers with homeotic transformations. Analysis of these structures revealed that *ICU11* and *CP2* are not only required for vegetative development, as previously described (Mateo-Bonmatí et al., 2018), but also to ensure proper reproductive development. *ICU11* and *CP2* are expressed in both vegetative and reproductive organs, with *CP2* showing higher expression levels than *ICU11* in the flowers and siliques of wild-type plants (Mateo-Bonmatí et al., 2018).

Similar to the homeotic transformations that we observed in *icu11-5 cp2-1* plants grown with 3% sucrose, the loss-of-function *apetala2* (*ap2*) mutations and the overexpression of *AGAMOUS* (*AG*) and *SEPALLATA3* (*SEP3*) result in the transformation of sepals and petals into carpelloid structures (Mizukami and Ma, 1992; Riechmann and Meyerowitz, 1997; Chen, 2004; Castillejo et al., 2005). Moreover, the weak *emf2-10* allele causes the appearance of carpelloid sepals (Chanvivattana et al., 2004) reminiscent of those of the *icu11-5 cp2-1* double mutant. Indeed, previous studies have described that ICU11 plays a role in repressing *AG*, *SEP1*, *SEP2*, and *SEP3* expression during the vegetative phase (Mateo-Bonmatí et al., 2018; Bloomer et al., 2020). Therefore, based on our observations of *icu11-5 cp2-1*, we propose that ICU11 and CP2 are required to regulate the expression of floral identity genes during reproductive development.

The homeotic transformations of the flowers produced by *icu11-5 cp2-1* and *emf2-3* plants grown on medium supplemented with 3% sucrose impeded self-pollination. Hand pollination of the *icu11-5 cp2-1* double mutant, but not the *emf2-3* single mutant, resulted in a few seeds, only one of which germinated and developed an embryonic flower when grown on growth medium containing 3% sucrose. In this growth condition, *icu11-5 cp2-1* anthers were smaller than those of Col-0, and only 64% contained small but viable pollen grains. When grown under short-day conditions, the mutant *emf2-3* also develops a small shoot with two or three flowers and short siliques that did not produce mature seeds (Chen et al., 1997).

The moderate reduction in pollen viability that we observed by Alexander staining does not explain the extremely low production and viability of *icu11-5 cp2-1* seeds. This clearly suggests the existence of additional problems with either ovule formation, fertilization or embryonic development. Further research would be needed to determine the causes of *icu11-5 cp2-1* reduced fertility.

Data availability statement

The original contributions presented in the study are included in the article/Supplementary Material. Further inquiries can be directed to the corresponding author.

Author contributions

JLM conceived and supervised the study, provided resources, and obtained funding. RN, LJ-V, and JLM designed the methodology. RN, LJ-V, and EM-B performed the experiments. RN, LJ-V, and JLM wrote the original draft. All authors contributed to the article and approved the submitted version.

Funding

The author(s) declare financial support was received for the research, authorship, and/or publication of this article. This work was supported by the Ministerio de Ciencia e Innovación of Spain (PGC2018-093445-B-I00, EQC2018-005181-P and EQC2019-006592-P [MCI/AEI/FEDER, UE]) and the Generalitat Valenciana (PROMETEO/2019/117 and IDIFEDER/2020/019). RN, EM-B, and LJ-V held predoctoral fellowships from the Generalitat Valenciana (GRISOLIAP/2016/131) and the Ministerio de Universidades of Spain (FPU13/00371 and FPU16/03772), respectively.

Acknowledgments

The authors wish to thank JM Serrano and J Castelló for their excellent technical assistance. This manuscript was previously published as a preprint at: https://www.biorxiv.org/content/10.1101/2023.04.20.537354v1.

Conflict of interest

The authors declare that the research was conducted in the absence of any commercial or financial relationships that could be construed as a potential conflict of interest.

Publisher's note

Supplementary material

The Supplementary Material for this article can be found online at: https://www.frontiersin.org/articles/10.3389/fpls.2023.1239093/full#supplementary-material

References

Bancroft, I., Jones, J. D., and Dean, C. (1993). Heterologous transposon tagging of the *DRL1* locus in Arabidopsis. *Plant Cell* 5, 631–368. doi: 10.1105/tpc.5.6.631

Barberon, M., Berthomieu, P., Clairotte, M., Shibagaki, N., Davidian, J. C., and Gosti, F. (2008). Unequal functional redundancy between the two *Arabidopsis thaliana* high-affinity sulphate transporters *SULTR1;1* and *SULTR1;2*. *New Phytol.* 180, 608–619. doi: 10.1111/j.1469-8137.2008.02604.x

Barboza-Barquero, L., Nagel, K. A., Jansen, M., Klasen, J. R., Kastenholz, B., Braun, S., et al. (2015). Phenotype of *Arabidopsis thaliana* semi-dwarfs with deep roots and high growth rates under water-limiting conditions is independent of the *GA5* loss-of-function alleles. *Ann. Bot.* 116, 321–331. doi: 10.1093/aob/mcv099

Barrero, J. M., González-Bayón, R., Del Pozo, J. C., Ponce, M. R., and Micol, J. L. (2007). *INCURVATA2* encodes the catalytic subunit of DNA Polymerase α and interacts with genes involved in chromatin-mediated cellular memory in *Arabidopsis thaliana*. *Plant Cell* 19, 2822–2838. doi: 10.1105/tpc.107.054130

Berná, G., Robles, P., and Micol, J. L. (1999). A mutational analysis of leaf morphogenesis in *Arabidopsis thaliana*. *Genetics* 152, 729–742. doi: 10.1093/genetics/152.2.729

Bloomer, R. H., Hutchison, C. E., Bäurle, I., Walker, J., Fang, X., Perera, P., et al. (2020). The *Arabidopsis* epigenetic regulator ICU11 as an accessory protein of Polycomb Repressive Complex 2. *Proc. Natl. Acad. Sci. U. S. A.* 117, 16660–16666. doi: 10.1073/pnas.1920621117

Bouveret, R., Schönrock, N., Gruissem, W., and Hennig, L. (2006). Regulation of flowering time by *Arabidopsis MSI1*. *Development* 133, 1693–1702. doi: 10.1242/dev.02340

Briggs, G. C., Osmont, K. S., Shindo, C., Sibout, R., and Hardtke, C. S. (2006). Unequal genetic redundancies in *Arabidopsis* – a neglected phenomenon? *Trends Plant Sci.* 11, 492–498. doi: 10.1016/j.tplants.2006.08.005

Brunaud, V., Balzergue, S., Dubreucq, B., Aubourg, S., Samson, F., Chauvin, S., et al. (2002). T-DNA integration into the *Arabidopsis* genome depends on sequences of pre-insertion sites. *EMBO Rep.* 3, 1152–1157. doi: 10.1093/embo-reports/kvf237

Caño-Delgado, A., Yin, Y., Yu, C., Vafeados, D., Mora-García, S., Cheng, J. C., et al. (2004). BRL1 and BRL3 are novel brassinosteroid receptors that function in vascular differentiation in *Arabidopsis*. *Development* 131, 5341–5351. doi: 10.1242/dev.01403

Castillejo, C., Romera-Branchat, M., and Pelaz, S. (2005). A new role of the Arabidopsis *SEPALLATA3* gene revealed by its constitutive expression. *Plant J.* 43, 586–596. doi: 10.1111/j.1365-313X.2005.02476.x

Chandler, C. H., Chari, S., and Dworkin, I. (2013). Does your gene need a background check? How genetic background impacts the analysis of mutations, genes, and evolution. *Trends Genet.* 29, 358–366. doi: 10.1016/j.tig.2013.01.009

Chanvivattana, Y., Bishopp, A., Schubert, D., Stock, C., Moon, Y. H., Sung, Z. R., et al. (2004). Interaction of Polycomb-group proteins controlling flowering in *Arabidopsis*. *Development* 131, 5263–5276. doi: 10.1242/dev.01400

Chen, X. (2004). A microRNA as a translational repressor of *APETALA2* in *Arabidopsis* flower development. *Science* 303, 2022–2025. doi: 10.1126/science.1088060

Chen, L., Cheng, J. C., Castle, L., and Sung, Z. R. (1997). *EMF* genes regulate Arabidopsis inflorescence development. *Plant Cell* 9, 2011–2024. doi: 10.1105/tpc.9.11.2011

Clerkx, E. J., Blankestijn-De Vries, H., Ruys, G. J., Groot, S. P., and Koornneef, M. (2004). Genetic differences in seed longevity of various *Arabidopsis* mutants. *Physiol. Plant* 121, 448–461. doi: 10.1111/j.0031-9317.2004.00339.x

Clough, S. J., and Bent, A. F. (1998). Floral dip: a simplified method for *Agrobacterium*-mediated transformation of *Arabidopsis thaliana*. *Plant J.* 16, 735–743. doi: 10.1046/j.1365-313x.1998.00343.x

Cong, L., Ran, F. A., Cox, D., Lin, S., Barretto, R., Habib, N., et al. (2013). Multiplex genome engineering using CRISPR/Cas systems. *Science* 339, 819–823. doi: 10.1126/science.1231143

Cusack, S. A., Wang, P., Lotreck, S. G., Moore, B. M., Meng, F., Conner, J. K., et al. (2021). Predictive models of genetic redundancy in *Arabidopsis thaliana*. *Mol. Biol. Evol.* 38, 3397-3414. doi: 10.1093/molbev/msab111

Duan, L., Pérez-Ruiz, J. M., Cejudo, F. J., and Dinneny, J. R. (2021). Characterization of *CYCLOPHILLIN38* shows that a photosynthesis-derived systemic signal controls lateral root emergence. *Plant Physiol.* 185, 503–518. doi: 10.1093/plphys/kiaa032

Fernando, V. C. D., Al Khateeb, W., Belmonte, M. F., and Schroeder, D. F. (2018). Role of Arabidopsis *ABF1/3/4* during *det1* germination in salt and osmotic stress conditions. *Plant Mol. Biol.* 97, 149–163. doi: 10.1007/s11103-018-0729-6

Förderer, A., Zhou, Y., and Turck, F. (2016). The age of multiplexity: recruitment and interactions of Polycomb complexes in plants. *Curr. Opin. Plant Biol.* 29, 169–178. doi: 10.1016/j.pbi.2015.11.010

Fu, A., He, Z., Cho, H. S., Lima, A., Buchanan, B. B., and Luan, S. (2007). A chloroplast cyclophilin functions in the assembly and maintenance of photosystem II in *Arabidopsis thaliana*. *Proc. Natl. Acad. Sci. U. S. A.* 104, 15947–15952. doi: 10.1073/pnas.0707851104

Gaj, T., Gersbach, C. A., and Barbas, C. F. (2013). ZFN, TALEN, and CRISPR/Cas-based methods for genome engineering. *Trends Biotechnol.* 31, 397–405. doi: 10.1016/j.tibtech.2013.04.004

Goodrich, J., Puangsomlee, P., Martin, M., Long, D., Meyerowitz, E. M., and Coupland, G. (1997). A Polycomb-group gene regulates homeotic gene expression in *Arabidopsis*. *Nature* 386, 44–51. doi: 10.1038/386044a0

Hafftter, P., Granato, M., Brand, M., Mullins, M. C., Hammerschmidt, M., Kane, D. A., et al. (1996). The identification of genes with unique and essential functions in the development of the zebrafish, *Danio rerio*. *Development* 123, 1–36. doi: 10.1242/dev.123.1.1

Hohenstatt, M. L., Mikulski, P., Komarynets, O., Klose, C., Kycia, I., Jeltsch, A., et al. (2018). PWWP-DOMAIN INTERACTOR OF POLYCOMBS1 interacts with Polycomb-group proteins and histones and regulates Arabidopsis flowering and development. *Plant Cell* 30, 117–133. doi: 10.1105/tpc.17.00117

Huang, C., Yu, Q. B., Lv, R. H., Yin, Q. Q., Chen, G. Y., Xu, L., et al. (2013). The reduced plastid-encoded polymerase-dependent plastid gene expression leads to the delayed greening of the *Arabidopsis fln2* mutant. *PloS One* 8, e73092. doi: 10.1371/journal.pone.0073092

Huq, E., and Quail, P. H. (2002). PIF4, a phytochrome-interacting bHLH factor, functions as a negative regulator of phytochrome B signaling in *Arabidopsis*. *EMBO J.* 21, 2441–2450. doi: 10.1093/emboj/21.10.2441

Iglesias, F. M., Bruera, N. A., Dergan-Dylon, S., Marino-Buslje, C., Lorenzi, H., Mateos, J. L., et al. (2015). The *Arabidopsis* DNA polymerase δ has a role in the deposition of transcriptionally active epigenetic marks, development and flowering. *PloS Genet.* 11, e1004975. doi: 10.1371/journal.pgen.1004975

Islam, M. S., Leissing, T. M., Chowdhury, R., Hopkinson, R. J., and Schofield, C. J. (2018). 2-oxoglutarate-dependent oxygenases. *Annu. Rev. Biochem.* 87, 585–620. doi: 10.1146/annurev-biochem-061516-044724

Jia, Y., Ding, Y., Shi, Y., Zhang, X., Gong, Z., and Yang, S. (2016). The *cbfs* triple mutants reveal the essential functions of *CBFs* in cold acclimation and allow the definition of CBF regulons in *Arabidopsis*. *New Phytol.* 212, 345–353. doi: 10.1111/nph.14088

Jinek, M., Chylinski, K., Fonfara, I., Hauer, M., Doudna, J. A., and Charpentier, E. (2012). A programmable dual RNA-guided DNA endonuclease in adaptive bacterial immunity. *Science* 337, 816–821. doi: 10.1126/science.1225829

Jürgens, G., Mayer, U., Torres Ruiz, R. A., Berleth, T., and Miséra, S. (1991). Genetic analysis of pattern formation in the *Arabidopsis* embryo. *Dev. Supplem.* 113, 27–38. doi: 10.1242/dev.113.Supplement_1.27

Kawai, Y., Ono, E., and Mizutani, M. (2014). Evolution and diversity of the 2-oxoglutarate-dependent dioxygenase superfamily in plants. *Plant J.* 78, 328–343. doi: 10.1111/tpj.12479

Kleinmanns, J. A., Schatlowski, N., Heckmann, D., and Schubert, D. (2017). BLISTER regulates Polycomb-target genes, represses stress-regulated genes and promotes stress responses in *Arabidopsis thaliana*. *Front. Plant Sci.* 8. doi: 10.3389/fpls.2017.01530

Kobayashi, K., Endo, K., and Wada, H. (2016). Multiple impacts of loss of plastidic phosphatidylglycerol biosynthesis on photosynthesis during seedling growth of Arabidopsis. *Front. Plant Sci.* 7. doi: 10.3389/fpls.2016.00336

Koornneef, M., Alonso-Blanco, C., and Vreugdenhil, D. (2004). Naturally occurring genetic variation in *Arabidopsis thaliana*. *Annu. Rev. Plant Biol.* 55, 141–172. doi: 10.1146/annurev.arplant.55.031903.141605

Koornneef, M., Hanhart, C. J., and van der Veen, J. H. (1991). A genetic and physiological analysis of late flowering mutants in *Arabidopsis thaliana*. *Mol. Gen. Genet.* 229, 57–66. doi: 10.1007/BF00264213

Kradolfer, D., Wolff, P., Jiang, H., Siretskiy, A., and Köhler, C. (2013). An imprinted gene underlies postzygotic reproductive isolation in *Arabidopsis thaliana*. *Dev. Cell* 26, 525–535. doi: 10.1016/j.devcel.2013.08.006

Labun, K., Montague, T. G., Krause, M., Torres Cleuren, Y. N., Tjeldnes, H., and Valen, E. (2019). CHOPCHOP v3: expanding the CRISPR web toolbox beyond genome editing. *Nucleic Acids Res.* 47, W171–W174. doi: 10.1093/nar/gkz365

Lee, I., Michaels, S. D., Masshardt, A. S., and Amasino, R. M. (1994). The late-flowering phenotype of *FRIGIDA* and mutations in *LUMINIDEPENDENS* is suppressed in the Landsberg *erecta* strain of *Arabidopsis*. *Plant J.* 6, 903–909. doi: 10.1046/j.1365-313X.1994.6060903.x

Leng, Y. J., Yao, Y. S., Yang, K. Z., Wu, P. X., Xia, Y. X., Zuo, C. R., et al. (2022). Arabidopsis ERdj3B coordinates with ERECTA-family receptor kinases to regulate ovule development and the heat stress response. *Plant Cell* 34, 3665-3684. doi: 10.1093/plcell/koac226

López-González, L., Mouriz, A., Narro-Diego, L., Bustos, R., Martínez-Zapater, J. M., Jarillo, J. A., et al. (2014). Chromatin-dependent repression of the *Arabidopsis* floral integrator genes involves plant specific PHD-containing proteins. *Plant Cell* 26, 3922–3938. doi: 10.1105/tpc.114.130781

Martinez, S., and Hausinger, R. P. (2015). Catalytic mechanisms of Fe(II)- and 2-oxoglutarate-dependent oxygenases. *J. Biol. Chem.* 290, 20702–20711. doi: 10.1074/jbc.R115.648691

Mateo-Bonmatí, E., Esteve-Bruna, D., Juan-Vicente, L., Nadi, R., Candela, H., Lozano, F. M., et al. (2018). *INCURVATA11* and *CUPULIFORMIS2* are redundant

genes that encode epigenetic machinery components in Arabidopsis. *Plant Cell* 30, 1596–1616. doi: 10.1105/tpc.18.00300

Meinke, D. W. (2013). A survey of dominant mutations in *Arabidopsis thaliana*. *Trends Plant Sci.* 18, 84–91. doi: 10.1016/j.tplants.2012.08.006

Méndez-Vigo, B., Martínez-Zapater, J. M., and Alonso-Blanco, C. (2013). The flowering repressor *SVP* underlies a novel *Arabidopsis thaliana* QTL interacting with the genetic background. *PloS Genet.* 9, e1003289. doi: 10.1371/journal.pgen.1003289

Mizukami, Y., and Ma, H. (1992). Ectopic expression of the floral homeotic gene *AGAMOUS* in transgenic Arabidopsis plants alters floral organ identity. *Cell* 71, 119–131. doi: 10.1016/0092-8674(92)90271-D

Mouchel, C. F., Briggs, G. C., and Hardtke, C. S. (2004). Natural genetic variation in *Arabidopsis* identifies *BREVIS RADIX*, a novel regulator of cell proliferation and elongation in the root. *Genes Dev.* 18, 700–714. doi: 10.1101/gad.1187704

Nadi, R., Mateo-Bonmatí, E., Juan-Vicente, L., and Micol, J. L. (2018). The 2OGD superfamily: emerging functions in plant epigenetics and hormone metabolism. *Mol. Plant* 11, 1222–1224. doi: 10.1016/j.molp.2018.09.002

Navarro-Quiles, C., Lup, S. D., Muñoz-Nortes, T., Candela, H., and Micol, J. L. (2023). The genetic and molecular basis of haploinsufficiency in flowering plants. *Trends Plant Sci*. doi: 10.1016/j.tplants.2023.07.009

Nowak, M. A., Boerlijst, M. C., Cooke, J., and Smith, J. M. (1997). Evolution of genetic redundancy. *Nature* 388, 167–171. doi: 10.1038/40618

Nüsslein-Volhard, C., and Wieschaus, E. (1980). Mutations affecting segment number and polarity in *Drosophila*. *Nature* 287, 795–801. doi: 10.1038/287795a0

Ohno, S. (1970). *Evolution by gene duplication* (Heidelberg: Springer Berlin).

Ohtomo, I., Ueda, H., Shimada, T., Nishiyama, C., Komoto, Y., Hara-Nishimura, I., et al. (2005). Identification of an allele of *VAM3/SYP22* that confers a semi-dwarf phenotype in *Arabidopsis thaliana*. *Plant Cell Physiol.* 46, 1358–1365. doi: 10.1093/pcp/pci146

Page, D. R., and Grossniklaus, U. (2002). The art and design of genetic screens: *Arabidopsis thaliana*. *Nat. Rev. Genet.* 3, 124–136. doi: 10.1038/nrg730

Pérez-Pérez, J. M., Candela, H., and Micol, J. L. (2009). Understanding synergy in genetic interactions. *Trends Genet.* 25, 368–376. doi: 10.1016/j.tig.2009.06.004

Pikaard, C. S., and Mittelsten Scheid, O. (2014). Epigenetic regulation in plants. *Cold Spring Harb. Perspect. Biol.* 6, a019315. doi: 10.1101/cshperspect.a019315

Piñeiro, M., Gómez-Mena, C., Schaffer, R., Martínez-Zapater, J. M., and Coupland, G. (2003). EARLY BOLTING IN SHORT DAYS is related to chromatin remodeling factors and regulates flowering in Arabidopsis by repressing *FT*. *Plant Cell* 15, 1552–1562. doi: 10.1105/tpc.012153

Ponce, M. R., Quesada, V., and Micol, J. L. (1998). Rapid discrimination of sequences flanking and within T-DNA insertions in the *Arabidopsis* genome. *Plant J.* 14, 497–501. doi: 10.1046/j.1365-313X.1998.00146.x

Quesada, V., Ponce, M. R., and Micol, J. L. (2000). Genetic analysis of salt-tolerant mutants in *Arabidopsis thaliana*. *Genetics* 154, 421–436. doi: 10.1093/genetics/154.1.421

Riechmann, J. L., and Meyerowitz, E. M. (1997). Determination of floral organ identity by *Arabidopsis* MADS domain homeotic proteins AP1, AP3, PI, and AG is independent of their DNA-binding specificity. *Mol. Biol. Cell* 8, 1243–1259. doi: 10.1091/mbc.8.7.1243

Rustérucci, C., Aviv, D. H., Holt, B. F. 3rd, Dangl, J. L., and Parker, J. E. (2001). The disease resistance signaling components *EDS1* and *PAD4* are essential regulators of the cell death pathway controlled by *LSD1* in Arabidopsis. *Plant Cell* 13, 2211–2224. doi: 10.1105/tpc.010085

Schatlowski, N., Stahl, Y., Hohenstatt, M. L., Goodrich, J., and Schubert, D. (2010). The CURLY LEAF interacting protein BLISTER controls expression of Polycomb-group target genes and cellular differentiation of *Arabidopsis thaliana*. *Plant Cell* 22, 2291–2305. doi: 10.1105/tpc.109.073403

Schönrock, N., Exner, V., Probst, A., Gruissem, W., and Hennig, L. (2006). Functional genomic analysis of CAF-1 mutants in *Arabidopsis thaliana*. *J. Biol. Chem.* 281, 9560–9568. doi: 10.1074/jbc.M513426200

Scortecci, K., Michaels, S. D., and Amasino, R. M. (2003). Genetic interactions between *FLM* and other flowering-time genes in *Arabidopsis thaliana*. *Plant Mol. Biol.* 52, 915–922. doi: 10.1023/a:1025426920923

Sung, Z. R., Belachew, A., Shunong, B., and Bertrand-Garcia, R. (1992). *EMF*, an *Arabidopsis* gene required for vegetative shoot development. *Science* 258, 1645–1647. doi: 10.1126/science.258.5088.1645

Taylor, M. B., and Ehrenreich, I. M. (2015). Higher-order genetic interactions and their contribution to complex traits. *Trends Genet.* 31, 34–40. doi: 10.1016/j.tig.2014.09.001

Tsutsui, H., and Higashiyama, T. (2017). pKAMA-ITACHI vectors for highly efficient CRISPR/Cas9-Mediated gene knockout in *Arabidopsis thaliana*. *Plant Cell Physiol.* 58, 46–56. doi: 10.1093/pcp/pcw191

Wang, L., Xu, D., Scharf, K., Frank, W., Leister, D., and Kleine, T. (2022). The RNA-binding protein RBP45D of Arabidopsis promotes transgene silencing and flowering time. *Plant J.* 109, 1397–1415. doi: 10.1111/tpj.15637

Wilkins, A. S. (1992). *Genetic analysis of animal development*, 2nd Edition. (New York: Wiley-Liss).

Yamamoto, Y. Y., Puente, P., and Deng, X. W. (2000). An *Arabidopsis* cotyledon-specific albino locus: a possible role in 16S rRNA maturation. *Plant Cell Physiol.* 41, 68–76. doi: 10.1093/pcp/41.1.68

Yang, C. H., Chen, L. J., and Sung, Z. R. (1995). Genetic regulation of shoot development in *Arabidopsis*: role of the *EMF* genes. *Dev. Biol.* 169, 421–435. doi: 10.1006/dbio.1995.1158

Yang, Z., Qian, S., Scheid, R. N., Lu, L., Chen, X., Liu, R., et al. (2018). EBS is a bivalent histone reader that regulates floral phase transition in *Arabidopsis*. *Nat. Genet.* 50, 1247–1253. doi: 10.1038/s41588-018-0187-8

Yoo, S. Y., Kim, Y., Kim, S. Y., Lee, J. S., and Ahn, J. H. (2007). Control of flowering time and cold response by a NAC-domain protein in *Arabidopsis*. *PloS One* 2, e642. doi: 10.1371/journal.pone.0000642

Yoshida, N., Yanai, Y., Chen, L., Kato, Y., Hiratsuka, J., Miwa, T., et al. (2001). EMBRYONIC FLOWER2, a novel Polycomb group protein homolog, mediates shoot development and flowering in Arabidopsis. *Plant Cell* 13, 2471–2481. doi: 10.1105/tpc.010227

Yoshimoto, N., Inoue, E., Watanabe-Takahashi, A., Saito, K., and Takahashi, H. (2007). Posttranscriptional regulation of high-affinity sulfate transporters in Arabidopsis by sulfur nutrition. *Plant Physiol.* 145, 378–388. doi: 10.1104/pp.107.105742

Zhao, C., Zhang, Z., Xie, S., Si, T., Li, Y., and Zhu, J. K. (2016). Mutational evidence for the critical role of CBF transcription factors in cold acclimation in Arabidopsis. *Plant Physiol.* 171, 2744–2759. doi: 10.1104/pp.16.00533

Zikherman, J., Hermiston, M., Steiner, D., Hasegawa, K., Chan, A., and Weiss, A. (2009). *PTPN22* deficiency cooperates with the CD45 E613R allele to break tolerance on a non-autoimmune background. *J. Immunol.* 182, 4093–4106. doi: 10.4049/jimmunol.0803317

The unequal functional redundancy of the Arabidopsis *INCURVATA11* and *CUPULIFORMIS2* genes is not dependent on genetic background

Riad Nadi, Lucía Juan-Vicente, Eduardo Mateo-Bonmatí*, and José Luis Micol

Instituto de Bioingeniería, Universidad Miguel Hernández, Campus de Elche, 03202 Elche, Spain

*Current adress: Centro de Biotecnología y Genómica de Plantas (CBGP), Universidad Politécnica de Madrid (UPM) – Instituto Nacional de Investigación y Tecnología Agraria y Alimentaria (INIA)/CSIC, 28223 Pozuelo de Alarcón, Madrid, Spain.

Supplementary Figures and Tables

Supplementary Material not included in this file:

Supplementary Table S2

A Features of sgRNA and its target

sgRNA name: ICU11_sgRNA1

sgRNA sequence: GCGAGGCAAGATTGAAGCTTCGG

Target location: Chr1:8127046. AT1G22950, first exon

Target strand: complementary

sgRNA efficiency: 49.72%

sgRNA predicted off-targets: MM(0):0, MM(1):0, MM(2):0, MM(3):0, MM(4):2

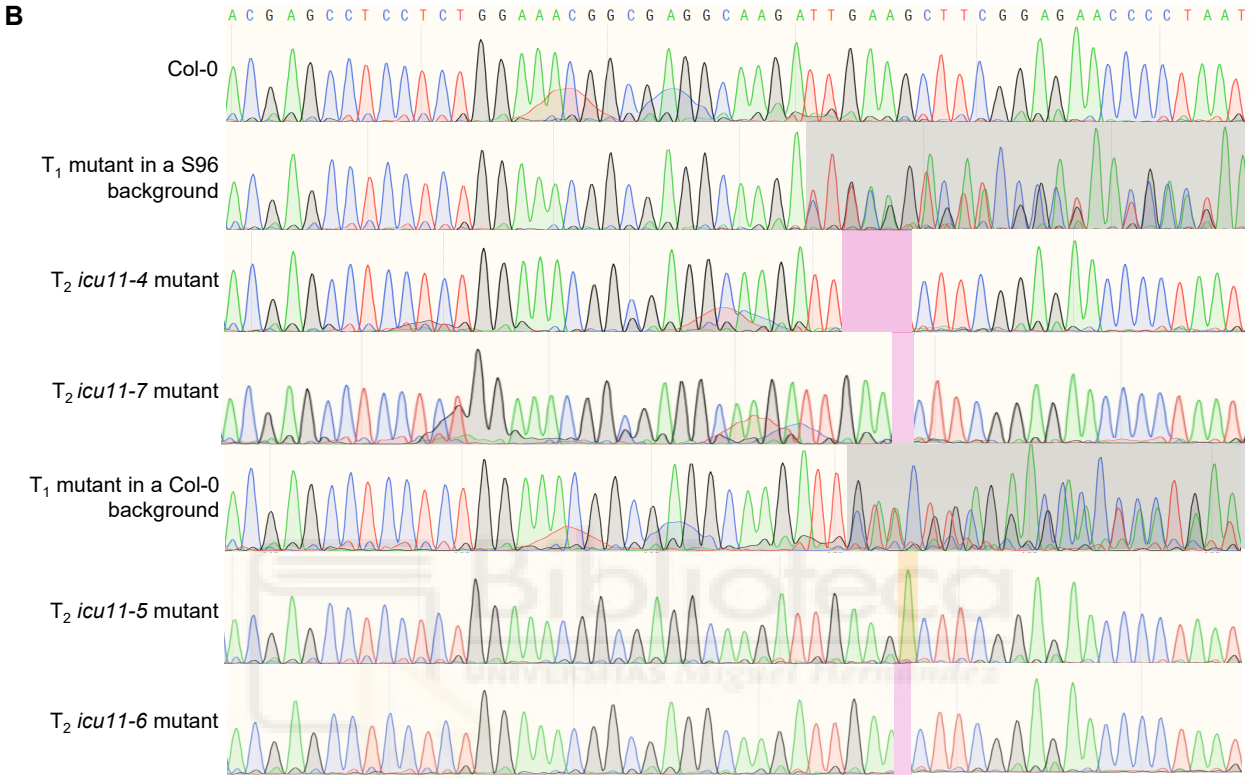

Supplementary Figure S1. Design and effects of the CRISPR/Cas9 mutagenesis of *ICU11*. **(A)** Details of the *ICU11* sgRNA1 target. The PAM sequence is shown in red. On-target mutation efficiency was calculated using the "Rule Set 2" scoring model, which provides values ranging from 0 to 100 (Doench et al., 2016). Possible off-target events are represented according to the number of mismatches [MM (number)]. **(B)** Electropherograms of the *ICU11* sgRNA1 target site in wild-type plants, and T_1 and T_2 transgenic plants. The gray, magenta, and orange shaded areas indicate chimeric, deletion, and insertion mutations, respectively. **(C)** Multiple amino acid sequence alignment of the predicted proteins translated from wild-type and CRISPR/Cas9 alleles showing that all the latter produce truncated proteins. Identical and similar residues are shaded in black and gray, respectively. Numbers indicate residue positions.

A Details of two putative off-targets of ICU11_sgRNA1

	ICU11_sgRNA1 off-target 1	ICU11_sgRNA1 off-target 2
Chromosome	1	3
Position	19132845	2280675
Strand	Forward	Complementary
Gene	Intergenic, between AT1G51590 (*MNS1*) and AT1G51600 (*GATA28*)	First exon of AT3G07170 (*IRP1*)
Mismatches	ICU11-T1: **GCGAGGCAAGATTGAAGCTTCGG** Col-0: **GCGTGGAAATATTGAAACTTTGG**	ICU11-T1: **GCGAGGCAAGATTGAAGCTTCGG** Col-0: **GCGAAGCAAGAATCAAACTTGGG**

B

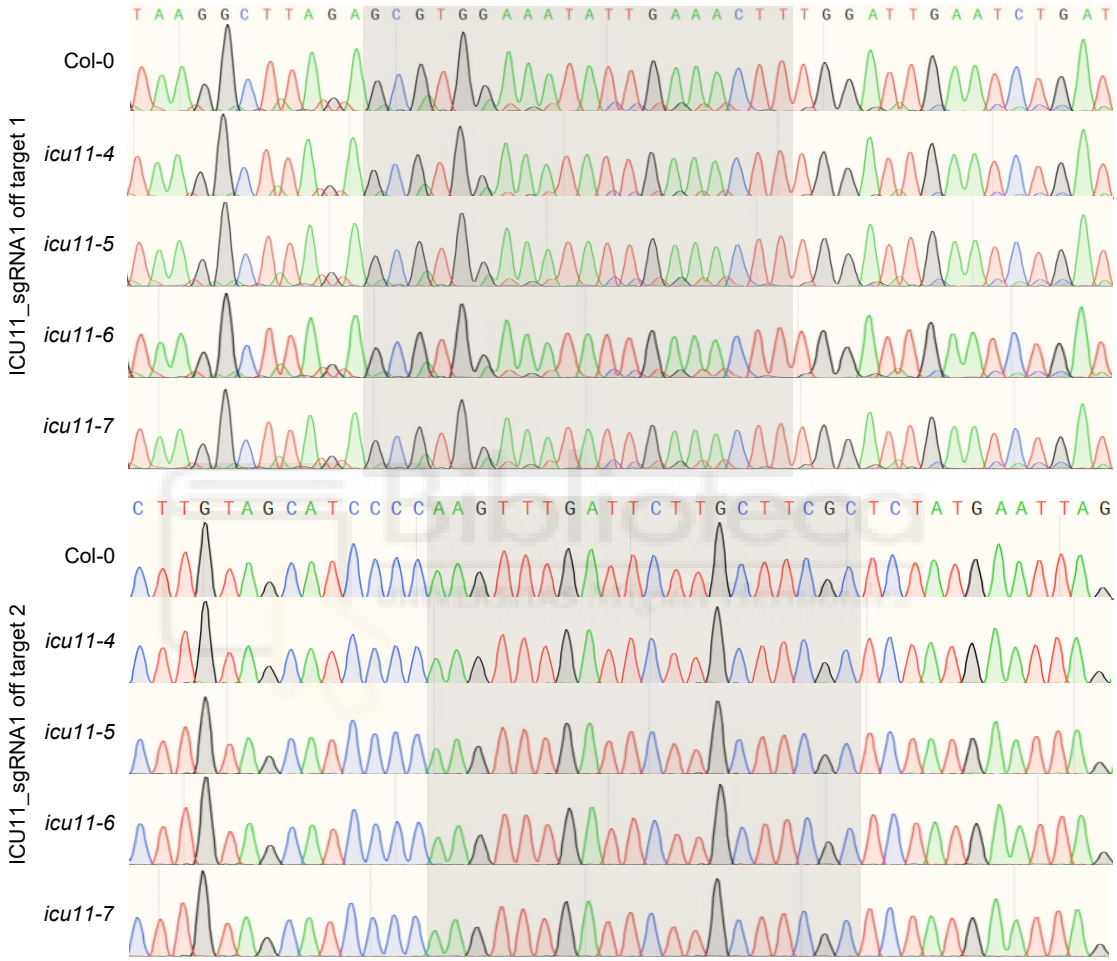

Supplementary Figure S2. Testing of two putative CRISPR/Cas9 off-targets in the new *icu11* mutant lines. **(A)** Off-targets were found using Cas-OFFinder, a bioinformatic tool developed by Bae et al. (2014). Mismatches are shown in red, with the first nucleotide of the PAM sequence (NGG) is in blue. **(B)** Sanger sequencing electropherograms of putative off-targets in T_3 mutant and wild-type plants. The gray shaded area corresponds to the putative off-target sequence.

Supplementary Table S1. Primer sets used in this work

Purpose	Oligonucleotide name(s)	Oligonucleotide sequences (5′ → 3′)	
		Forward primer (L or F)	Reverse primer (R)
Genotyping	ICU11-Off-target1_F/R	TGGTGGGTTTGGTTTGTCTC	CTCGGTCATTGGAGCAACTT
	ICU11-Off-target2_F/R	TGAGTCTGGAAGCAGGAAGG	AATGGGCAAATCAGAGAGTCC
	At1g22950_1F/R	ACCCTAACCTCTCAAACAAACCA	AGACTTTGTTAACCCAATCCGAC
	At1g22950_4F/R	CCTCTCAAACAAACCATCATCA	CGCTCAGTATCAGGGGAATATC
	SAIL_1215_B02_L/R	GAGCGATAACAGTGAGCTTGG	GACATTTTCAAACCATTCATGC
	SAIL_658_E12_L/R	AGAGGCAAGAGACGAAAAAGC	CCTTTGAGCCTGTAGCATCAG
	SAIL_621_G08_L/R	TGAGAGCGAAAGCTTTCATTC	AACAAATGACTGGAGCAGAGC
	gis-5_F/R	GAAGCAAGAACAGGTTTCTATG	AGCTAGTTACACTCGAGGATA
	icu2-1_F/R	TGTTGAAGGAGGTCAGTTATTCT	CACAAGTGTTTTGGATGACTGAA
	clf-2_F/R	ATGGCGTCAGAAGCTTCGCC	CTGGACCTCTCTCCTCCGC
	tfl2-2_F/R	TATCAGCGGTGATCGGTGTG	CGCCGTAATTCTCCCGGTAA
	ebs-1_F/R	TGAAGGTGTGAACAATGCAT	GAAAACTCGACCTGGTGTCG
	fas1-1_F/R	TGAGCTGTTCTTCTGCATCATG	ACTATGGTAGCTGTGAAGAGTG
	AT5G51230_1F/R	TGTAATGGTTCAGAGATCAATAGAA	GTCCGTGCAATCTTGAGAATG
	SALK_131712_L/R	CAGAAGAAGATCGTCCGAGTG	TGAACTTCCCCACTCTTCATG
	SALK_056440_L/R	TGGTCAGATGGGCTAGAATTG	AACGCGTTGCTGTAGAAACTC
	SAIL_826_A06_L/R	AGCAGCAGAAGAAGAAGCATG	TTTGGCCTACAAAGACACCAG
	SALK_021316_L/R	GAGCCGTCTCATCAAACTGAC	TTGCAGGAGCAAATATGGAAC
	SALK_150863_L/R	AGATCGCTTCCAGAGTTAGCC	TTGTCGCAAAAAGCAAAAGAG
	SAIL_223_F05_L/R	GGATCAGCCAAAAGGTTAAGG	TCATTCACTTTGCATCACTCG
	SAIL_809_E03_L/R	GCGTGTACCAGTTTCAAGGAG	TAAAGAGCCCAGTTGTGAAGC
	SALK_045303_L/R	CCAGTTAAGGACAGAACACCG	TCGTCTTTCGATCAAATCCAC
	SALK_022363_L/R	ATCAATGTGGCATCTAGTGGC	ACCCGCCTCTTCTTCATCTAC

Supplementary Table S1 (continued). Primer sets used in this work

Purpose	Oligonucleotide name(s)	Oligonucleotide sequences (5′ → 3′)	
		Forward primer (L or F)	Reverse primer (R)
Genotyping	SAIL_97_E06_L/R	CTTTCCCAGTTTTTACTGCCC	AATCACTCGCTTCTTCCACTG
	SALK_149002_L/R	AATGAAAGCATGCGGATACAC	TCCGTGTTGACTGGAAAGATC
	SALK_130607_L/R	TTTCTCTTGTCCGGTGAAATG	CCTGCAACAATCAGTGTGATG
	SAIL_240_H01_L/R	TTGAGATGAATCTGGAGACCG	AAACGACGACGTATTGGAGTG
	SALK_149692_L/R	TCTTGTGACAGGTGCAACTTG	AAACAAAGCTAGGCACAAGGC
	SALK_080380_L/R	AGGGAACATGTCATCCATGAG	AGGGAGAATCTGAGAACCTGC
	SALK_027726_L/R	ATGGTGTGCGAATCTATGACC	ACGGAGAGGAAAGCTCAAGAC
	LB1[1]	GCCTTTTCAGAAATGGATAAATAGCCTTGCTTCC	
	LbB1.3[2]	ATTTTGCCGATTTCGGAAC	
	Cas9_F/R	GCTTCATCAAGAGACAGCTGG	GGACTTGCCCTTTTCCACTTT
Cloning	ICU11_sgRNA1_F/R	ATTGCGAGGCAAGATTGAAGCTT	AAACAAGCTTCAATCTTGCCTCGC

[1,2]These primers were used for genotyping [1]SAIL and [2]SALK lines, and their sequences were taken from [1]Sessions et al. (2002) and [2]T-DNA Primer Design (http://signal.salk.edu/tdnaprimers.2.html).

SUPPLEMENTARY REFERENCES

Bae, S., Park, J., and Kim, J.S. (2014). Cas-OFFinder: a fast and versatile algorithm that searches for potential off-target sites of Cas9 RNA-guided endonucleases. *Bioinformatics* 30, 1473-1475. doi: 10.1093/bioinformatics/btu048

Cao, X., and Jacobsen, S.E. (2002). Role of the *Arabidopsis DRM* methyltransferases in de novo DNA methylation and gene silencing. *Curr. Biol.* 12, 1138-1144. doi: 10.1016/s0960-9822(02)00925-9

Chan, S.W., Henderson, I.R., Zhang, X., Shah, G., Chien, J.S., and Jacobsen, S.E. (2006). RNAi, DRD1, and histone methylation actively target developmentally important non-CG DNA methylation in *Arabidopsis*. *PLOS Genet.* 2, e83. doi: 10.1371/journal.pgen.0020083

Deng, W., Liu, C., Pei, Y., Deng, X., Niu, L., and Cao, X. (2007). Involvement of the histone acetyltransferase AtHAC1 in the regulation of flowering time via repression of *FLOWERING LOCUS C* in Arabidopsis. *Plant Physiol.* 143, 1660-1668. doi: 10.1104/pp.106.095521

Doench, J.G., Fusi, N., Sullender, M., Hegde, M., Vaimberg, E.W., Donovan, K.F., Smith, I., Tothova, Z., Wilen, C., Orchard, R., Virgin, H.W., Listgarten, J., and Root, D.E. (2016). Optimized sgRNA design to maximize activity and minimize off-target effects of CRISPR-Cas9. *Nat. Biotechnol.* 34, 184-191. doi: 10.1038/nbt.3437

Goll, M.G., Kirpekar, F., Maggert, K.A., Yoder, J.A., Hsieh, C.L., Zhang, X., Golic, K.G., Jacobsen, S.E., and Bestor, T.H. (2006). Methylation of $tRNA^{Asp}$ by the DNA methyltransferase homolog Dnmt2. *Science* 311, 395-398. doi: 10.1126/science.1120976

Jacob, Y., Feng, S., Leblanc, C.A., Bernatavichute, Y.V., Stroud, H., Cokus, S., Johnson, L.M., Pellegrini, M., Jacobsen, S.E., and Michaels, S.D. (2009). ATXR5 and ATXR6 are H3K27 monomethyltransferases required for chromatin structure and gene silencing. *Nat. Struct. Mol. Biol.* 16, 763-768. doi: 10.1038/nsmb.1611

Kim, J.S., Lim, J.Y., Shin, H., Kim, B.G., Yoo, S.D., Kim, W.T., and Huh, J.H. (2019). ROS1-dependent DNA demethylation is required for ABA-inducible *NIC3* expression. *Plant Physiol.* 179, 1810-1821. doi: 10.1104/pp.18.01471

Latrasse, D., Benhamed, M., Henry, Y., Domenichini, S., Kim, W., Zhou, D.X., and Delarue, M. (2008). The MYST histone acetyltransferases are essential for gametophyte development in Arabidopsis. *BMC Plant Biol.* 8, 121. doi: 10.1186/1471-2229-8-121

Lin, W., Sun, L., Huang, R.Z., Liang, W., Liu, X., He, H., Fukuda, H., He, X.Q., and Qian, W. (2020). Active DNA demethylation regulates tracheary element differentiation in *Arabidopsis*. *Sci. Adv.* 6, eaaz2963. doi: 10.1126/sciadv.aaz2963

Pien, S., Fleury, D., Mylne, J.S., Crevillen, P., Inzé, D., Avramova, Z., Dean, C., and Grossniklaus, U. (2008). ARABIDOPSIS TRITHORAX1 dynamically regulates *FLOWERING LOCUS C* activation via histone 3 lysine 4 trimethylation. *Plant Cell* 20, 580-588. doi: 10.1105/tpc.108.058172

Saze, H., Mittelsten Scheid, O., and Paszkowski, J. (2003). Maintenance of CpG methylation is essential for epigenetic inheritance during plant gametogenesis. *Nat. Genet.* 34, 65-69. doi: 10.1038/ng1138

Sessions, A., Burke, E., Presting, G., Aux, G., Mcelver, J., Patton, D., Dietrich, B., Ho, P., Bacwaden, J., Ko, C., Clarke, J.D., Cotton, D., Bullis, D., Snell, J., Miguel, T., Hutchison, D., Kimmerly, B., Mitzel, T., Katagiri, F., Glazebrook, J., Law, M., and Goff, S.A. (2002). A high-throughput Arabidopsis reverse genetics system. *Plant Cell* 14, 2985-2994. doi: 10.1105/tpc.004630

Woo, H.R., Dittmer, T.A., and Richards, E.J. (2008). Three SRA-domain methylcytosine-binding proteins cooperate to maintain global CpG methylation and epigenetic silencing in Arabidopsis. *PLOS Genet.* 4, e1000156. doi: 10.1371/journal.pgen.1000156

Yu, C.W., Chang, K.Y., and Wu, K. (2016). Genome-wide analysis of gene regulatory networks of the FVE-HDA6-FLD complex in *Arabidopsis*. *Front. Plant Sci.* 7, e555. doi: 10.3389/fpls.2016.00555

Yuan, L., Wang, D., Cao, L., Yu, N., Liu, K., Guo, Y., Gan, S., and Chen, L. (2020). Regulation of leaf longevity by DML3-mediated DNA demethylation. *Mol. Plant* 13, 1149-1161. doi: 10.1016/j.molp.2020.06.006

Yun, J.Y., Tamada, Y., Kang, Y.E., and Amasino, R.M. (2012). ARABIDOPSIS TRITHORAX-RELATED3/SET DOMAIN GROUP2 is required for the winter-annual habit of *Arabidopsis thaliana*. *Plant Cell Physiol.* 53, 834-846. doi: 10.1093/pcp/pcs021

Zheng, X., Pontes, O., Zhu, J., Miki, D., Zhang, F., Li, W.X., Iida, K., Kapoor, A., Pikaard, C.S., and Zhu, J.K. (2008). ROS3 is an RNA-binding protein required for DNA demethylation in *Arabidopsis*. *Nature* 455, 1259-1262. doi: 10.1038/nature07305

Supplementary Table S2. Double mutant combinations that rendered additive phenotypes obtained by crossing *icu11-1* to mutants carrying alleles of genes encoding known plant epigenetic machinery components

AGI code	Gene name		Function annotation at TAIR	Mutant (SALK/SAIL code)	Mutant phenotype	First publication describing the mutant
	Full	Abbreviated				
AT3G10010	*DEMETER-LIKE 2*	*DML2*	Encodes a protein with DNA glycosylase activity that is involved in maintaining methylation marks.	*dml2-3* (SALK_131712)	No obvious developmental defects in *dml2-2** (SALK_113573).	Lin et al. (2020)
AT4G34060	*DEMETER-LIKE 3*	*DML3*	Encodes a protein with 5-meC and thymine-DNA glycosylase activity with a preference for CpG and CpHpG sequences. Involved in maintaining methylation marks. Many targets of DML3 are senescence-associated genes (SAGs).	*dml3-1* (SALK_056440)	Delayed leaf senescence.	Yuan et al. (2020)
AT5G25480	*DNA METHYLTRANSFERASE-2*	*DNMT2*	Encodes a DNA methyltransferase homolog. Human Dnmt2 methylates tRNA-Asp and can methylate Arabidopsis tRNA-Asp in vitro.	*dnmt2-2* (SAIL_826_A06)	No obvious developmental defects in *dnmt2** (SALK_136635).	Goll et al. (2006)
AT5G15380	*DOMAINS REARRANGED METHYLASE 1*	*DRM1*	Encodes a methyltransferase involved in the de novo DNA methylation and maintenance of asymmetric methylation of DNA sequences.	*drm1-2* (SALK_021316)	No obvious developmental defects.	Cao et al. (2002) Chan et al. (2006)
AT5G14620	*DOMAINS REARRANGED METHYLASE 2*	*DRM2*	A putative DNA methyltransferase with rearranged catalytic domains; similar to mammalian DNMT3 methyltransferases; contains UBA domains. The 3′-end proximal part of the gene coding region is highly methylated at both adenine and cytosine residues.	*drm2-2* (SALK_150863)	No obvious developmental defects.	Cao et al. (2002) Chan et al. (2006)
AT1G15340	*METHYL-C PG-BINDING DOMAIN 10*	*MBD10*	Protein containing methyl-CpG-binding domain.Has sequence similarity to human MBD proteins.	*mbd10-1* (SAIL_223_F05)	No description.	No publication
AT5G49160	*METHYLTRANSFERASE 1*	*MET1*	Encodes a cytosine methyltransferase MET1. Required for silencing of FWA paternal allele in endosperm. Two lines with RNAi constructs directed against DMT1 have reduced agrobacterium-mediated tumor formation. The mRNA is cell-to-cell mobile.	*met1-4* (SAIL_809_E03)	Late flowering.	Saze et al. (2003)
AT2G36490	*REPRESSOR OF SILENCING 1*	*ROS1*	A repressor of transcriptional gene silencing. Functions by demethylating the target promoter DNA. Interacts physically with RPA2/ROR1. In the ros1 mutants, an increase in methylation is observed in a number of gene promoters. Among the loci affected by ros1, a few (RD29A and At1g76930) are affected in cytosine methylation in all sequence contexts (CpG, CpNpG or CpNpN), although many others are affected primarily in non-CpG contexts. The ros1 mutant is more susceptible to biotrophic pathogens and is repressed in its responsiveness of salyclic acid-dependent defence genes.	*ros1-4* (SALK_045303)	Hypersensitive to ABA.	Kim et al. (2019)
AT5G58130	*REPRESSOR OF SILENCING 3*	*ROS3*	Encodes ROS3 (repressor of silencing 3), a RNA-binding protein required for DNA demethylation.	*ros3-2* (SALK_022363)	Narrow and lobed leaves.	Zheng et al. (2008)
AT5G39550	*VARIANT IN METHYLATION 3*	*VIM3*	Encodes the VIM3/ORTH1 protein that is similar to VIM1. This protein has an N-terminal PHD domain and two RING domains surrounding an SRA domain. The protein has been shown to bind to methylated cytosines of CG, CNG and CNN motifs via its SRA domain but has a preference for the former. This protein functions as an E3 ubiquitin ligase in vitro with members of the UBC8 family E2s. Either of the two RING domains present in the protein can promote ubiquitylation in vitro, but, not the PHD domain. Over-expression of ORTH1/VIM3 leads to decreased levels of FWA methylation, increased levels of FWA transcripts, and delayed flowering. Cen180 repeats are also hypomethylated in plants overexpressing this protein.	*vim3-2* (SAIL_97_E06)	No obvious developmental alterations in *vim3-1** (SALK_088570). The *vim1-2 vim2-2 vim3-1* triple mutant is late flowering.	Woo et al. (2008)
AT2G31650	*ARABIDOPSIS TRITHORAX1*	*ATX1*	Encodes a homolog of trithorax, a histone-lysine N-methyltransferase. Involved in trimethylating histone H3-lysine 4. Involved in the formation, placement, and identity of flower organs. Role in regulation of homeotic genes. Functions as a receptor of phosphatidylinositol 5-phosphate. Localizes to cytoplasm, plasma membrane and nuclei, shifting to nuclei in the presence of PI5P.	*atx1-2* (SALK_149002)	Slight early flowering.	Pien et al. (2008)
AT5G09790	*ARABIDOPSIS TRITHORAX-RELATED PROTEIN 5*	*ATXR5*	Encodes a SET-domain protein, a H3K27 monomethyltransferases required for chromatin structure and gene silencing. Regulates heterochromatic DNA replication. Contains a PCNA-binding domain. ATXR5 accumulates preferentially during the late G1 or S phase, suggesting that it plays a role in cell-cycle regulation or progression. A plant line expressing an RNAi construct directed against this gene has reduced agrobacterium-mediated tumor formation.	*atxr5* (SALK_130607)	No obvious developmental alterations. The *atxr5 atxr6* double mutant has a reduced leaf size.	Jacob et al. (2009)

AT5G24330	*ARABIDOPSIS TRITHORAX-RELATED PROTEIN 6*	*ATXR6*	Encodes a SET-domain protein, a H3K27 monomethyltransferases required for chromatin structure and gene silencing. Regulates heterochromatic DNA replication. Contains a PCNA-binding domain. ATXR6 accumulates preferentially during the late G1 or S phase, suggesting that it plays a role in cell-cycle regulation or progression.	*atxr6* (SAIL_240_H01)	No obvious developmental defects. The double mutant *atxr5 atxr6* has a reduced leaf size.	Jacob et al. (2009)
AT5G42400	*ARABIDOPSIS TRITHORAX-RELATED PROTEIN 7*	*ATXR7*	Encodes ATXR7 (ARABIDOPSIS TRITHORAX-RELATED7), required for histone H3-K4 methylation and for transcriptional activation of Flowering Locus C.	*atxr7-1* (SALK_149692)	Early flowering.	Yun et al. (2012)
AT1G79000	*HISTONE ACETYLTRANSFERASE OF THE CBP FAMILY 1*	*HAC1*	Homologous to CREB-binding protein, a co-activator of transcription with histone acetyl-transferase activity. No single prior lysine acetylation is sufficient to block HAC1 acetylation of the H3 or H4 peptides, suggesting that HAC1, HAC5, and HAC12 can acetylate any of several lysines present in the peptides. HAM2 acetylates histone H4 lysine 5. A plant line expressing an RNAi construct targeted against HAC1 has reduced rates of agrobacterium-mediated root transformation.	*hac1-3* (SALK_080380)	Late flowering and reduced fertility.	Deng et al. (2007)
AT5G63110	*HISTONE DEACETYLASE 6*	*HDA6*	RPD3-like histone deacetylase. HDA6 mutations specifically increase the expression of auxin-responsive transgenes, suggesting a role in transgene silencing.	*hda6-6* and *hda6-7*	Early flowering.	Yu et al. (2016)
AT5G64610	*HISTONE ACETYLTRANSFERASE OF THE MYST FAMILY 1*	*HAM1*	Encodes an enzyme with histone acetyltransferase activity. HAM1 primarily acetylate histone H4, but also display some ability to acetylate H3. Prior acetylation of lysine 5 on histone H4 reduces radioactive acetylation by either HAM1. HAM1 acetylates histone H4 lysine 5.	*ham1-1* (SALK_027726)	No obvious developmental defects. The *ham1-1 ham2-1* double mutant is lethal.	Latrasse et al. (2008)

*These phenotypes correspond to the allele previously described in the reference indicated in the column headed as "Mutant phenotype", but not the one that we used for crosses in this work (shown in column E).

X.- OTRAS PUBLICACIONES

Overlapping roles of Arabidopsis INCURVATA11 and CUPULIFORMIS2 as Polycomb Repressive Complex 2 accessory proteins

Riad Nadi[1,*], Lucía Juan-Vicente[1,*], Samuel Daniel Lup[1], Yolanda Fernández[2], Vicente Rubio[2], and José Luis Micol[1]

[1]Instituto de Bioingeniería, Universidad Miguel Hernández, Campus de Elche, 03202 Elche, Spain
[2]Centro Nacional de Biotecnología, CNB-CSIC, Madrid 28049, Spain
*These authors contributed equally to this work.

Corresponding author: J.L. Micol (telephone: 34 96 665 85 04; email: jlmicol@umh.es)

Running head: ICU11 and CP2 as PRC2 accessory proteins

Keywords: 2OGD, ICU11, CP2, PRC2 accessory proteins, TAP, BiFC, RNA-seq, H3K36me3, H3K27me3, functional redundancy.

Word count (total): 11884.

Figures: 5 Supplemental Figures: 4 Supplemental Tables: 6
Supplemental Data Sets: 8

ABSTRACT

Polycomb Repressive Complex 2 (PRC2) is methyl transferase that plays a key role in epigenetic repression of gene expression in plants and animals. Its core components have all been identified in *Arabidopsis thaliana*, with an expanding list of accessory proteins, some of which facilitate the recruitment of PRC2 to specific chromatin regions. INCURVATA11 (ICU11) is a 2-oxoglutarate and Fe^{2+}-dependent dioxygenase that was previously shown to be a likely PRC2 accessory protein. In Tandem Affinity Purification (TAP)-based screens for interacting partners of ICU11 and its redundant paralog CUPULIFORMIS2 (CP2), we discovered that ICU11 interacts with four PRC2 core components, including EMBRYONIC FLOWER 2 (EMF2), and with the accessory proteins EMF1, TELOMERE REPEAT BINDING 1 (TRB1), TRB2, and TRB3. CP2 did not interact with PRC2 core components, nor with TRB1, TRB2, or TRB3, but did interact with TRB4 and TRB5. Both ICU11 and CP2 interacted with the nuclear proteins NAC DOMAIN CONTAINING PROTEIN 50 (NAC050), NAC052 and COP9 SIGNALOSOME SUBUNIT 1 (CSN1). Bimolecular Fluorescence Complementation (BiFC) assays revealed that ICU11 and CP2 both interact with the PRC2 core components CURLY LEAF and SWINGER, and the accessory proteins LIKE HETEROCHROMATIN PROTEIN 1, TRB1, and TRB3. ICU11 and CP2 did not interact with each other. We also conducted RNA-seq analyses of the lethal embryonic flowers of the *emf2-3* single mutant and the *icu11-5 cp2-1* double mutant, which revealed strong similarities between their transcriptomic profiles and with those of single mutants affected in genes encoding PRC2 core components. A significant proportion of the genes mis-regulated in *icu11-5 cp2-1* are known to harbor H3K27me3 repressive marks in the wild type. Our results provide further evidence that ICU11 acts as a PRC2 accessory protein, and strongly suggest that CP2 plays a similar role.

INTRODUCTION

The first gene encoding a Polycomb group (PcG) protein was discovered by the characterization of a mutation in the fruit fly *Drosophila melanogaster* (Lewis, 1947). PcG proteins are highly conserved among eukaryotes and epigenetically repress the expression of genes controlling growth, development, and environmental adaptation (Jiao et al., 2020; Xiao and Wagner, 2015). PcG proteins form part of two heteromultimeric Polycomb Repressive Complexes (PRCs), which perform different epigenetic activities: PRC1 is a histone H2A ubiquitin ligase, whereas PRC2 is a histone H3 lysine 27 (H3K27) methyltransferase (Bratzel et al., 2010).

Plant PRCs function in many critical developmental stages and events, such as the transition from embryo to seedling (Bouyer et al., 2011), gametophyte and seed development (Roszak and Köhler, 2011), and vernalization and flowering induction (Pazhouhandeh et al., 2011; Tian et al., 2019; Whittaker and Dean, 2017). In Arabidopsis (*Arabidopsis thaliana*), PRC2 comprises eight core components: CURLY LEAF (CLF: Goodrich et al., 1997), SWINGER (SWN; Chanvivattana et al., 2004), MEDEA (MEA; Grossniklaus et al., 1998), FERTILIZATION INDEPENDENT SEED 2 (FIS2; Luo et al., 1999), EMBRYONIC FLOWER 2 (EMF2; Yoshida et al., 2001), VERNALIZATION2 (VRN2; Gendall et al., 2001), FERTILIZATION-INDEPENDENT ENDOSPERM (FIE; Ohad et al., 1999), and MULTICOPY SUPRESSOR OF IRA (inhibitory regulator of the RAS-cAMP pathway) 1 (MSI1; Hennig et al., 2003; Köhler et al., 2003). The Arabidopsis PRC1 core components include three B Lymphoma Mo-MLV Insertion Region 1 (BMI1) homologs (BMI1A, BMI1B, and BMI1C) and two RING FINGER proteins (RING1A and RING1B) (Sanchez-Pulido et al., 2008).

Accessory proteins facilitate the recruitment of PRC1 and PRC2 to specific chromatin regions; for example, the plant-specific proteins EMBRYONIC FLOWER 1 (EMF1) and LIKE HETEROCHROMATIN PROTEIN 1 (LHP1) interact with each other and with PRC1 and PRC2 core components (Bratzel et al., 2010; Calonje et al., 2008; Derkacheva et al., 2013; Godwin and Farrona, 2022; Mozgova and Hennig, 2015; Scortecci et al., 2003). LHP1 contributes to the maintenance of the tri-methylated H3K27 (H3K27me3) chromatin repressive state through the continuous recruitment of PRC2 to regions enriched with the H3K27me3 mark (Ramirez-Prado et al., 2019; Turck et al., 2007; Zhang et al., 2007). EMF1 contributes to H3K27me3 deposition at a subgroup of PRC2 target genes, and is also required for histone H2A monoubiquitination by PRC1 (Kim et al., 2012).

Lack of vegetative development and the formation of flower-like organs immediately after germination—the so-called embryonic flowers—is a conspicuous phenotype that was first observed in *emf1* mutants (Aubert et al., 2001; Sung et al., 1992; Yang et al., 1995; Yoshida et al., 2001). Embryonic flowers are also produced by the *telomere repeat binding1-2* (*trb1-2*) *trb2-1 trb3-2* triple mutant (Yang et al., 2013; Zhou et al., 2018). Arabidopsis TRB1, TRB2, and

TRB3 bind to telomeric repeat DNA sequences to maintain chromosome ends (Klepikova et al., 2016; Lee and Cho, 2016; Nadi et al., 2023; Schubert et al., 2006), and are thought to recruit the PRC2 complex to certain genes for H3K27me3 deposition (Zhou et al., 2018).

The 2-oxoglutarate and Fe(II)-dependent dioxygenase (2OGD, also called 2ODD) domain characterizes the second largest protein superfamily in the plant kingdom (Martinez and Hausinger, 2015) and is represented by about 150 genes in Arabidopsis (Kawai et al., 2014; Nadi et al., 2018). 2OGD proteins catalyze oxidative reactions using 2-oxoglutarate (also called α-ketoglutarate) and molecular oxygen as co-substrates, and Fe^{2+} as a cofactor (Islam et al., 2018). Phylogenetic analyses of plant 2OGDs grouped them into the DOXA, DOXB, DOXC, and JUMONJI (JMJ) protein classes, with demonstrated functions that include DNA and RNA demethylation, collagen hydroxylation, a diverse range of metabolic processes, and histone demethylation, respectively (Islam et al., 2018; Kawai et al., 2014). Two Arabidopsis DOXB-type 2OGDs, INCURVATA11 (ICU11) and CUPULIFORMIS2 (CP2), are redundant components of the epigenetic machinery (Mateo-Bonmatí et al., 2018; Nadi et al., 2023). Whereas *icu11* mutants exhibit a mild morphological phenotype consisting of hyponastic leaves and early flowering, and *cp2* mutants are phenotypically wild type, *icu11 cp2* double mutants skip vegetative development and develop embryonic flowers immediately after germination, culminating in plant death 20–40 days after stratification (Mateo-Bonmatí et al., 2018; Nadi et al., 2023).

Based on co-immunoprecipitation (co-IP) analyses, ICU11 was proposed to be a PRC2 accessory protein, probably involved in H3K36me3 demethylation at the *FLOWERING LOCUS C* (*FLC*) floral repressor gene (Bloomer et al., 2020). Here, we provide further evidence for ICU11 as a PRC2 accessory protein through experimental approaches complementary to co-IP, including an *in vitro* tandem affinity purification (TAP)-based screen and *in vivo* heterologous bimolecular fluorescence complementation (BiFC) assays. We also used these approaches to identify several interacting partners of CP2, some of which are PRC2 core components or accessory proteins. Furthermore, using RNA sequencing (RNA-seq), we identified many genes that are upregulated in the lethal embryonic flowers of the *icu11-5 cp2-1* double mutant and involved in flower development, as previously shown by microarray analysis in the *emf2-3* single mutant (Kim et al., 2010). Taken together, our results confirm that ICU11 is a PRC2 accessory protein and strongly suggest that CP2 also plays this role.

RESULTS

ICU11 interacts with PRC2 core components and accessory proteins in a TAP-based screen

To identify interactors of ICU11 and CP2, we carried out a TAP-based screen followed by liquid chromatography electrospray ionization and tandem mass spectrometry (LC-ESI-MS/MS). Specifically, we used C-terminal translational fusions of ICU11 and CP2 to the GS^{Rhino} tag, consisting of protein G, a streptavidin-binding peptide, and rhinovirus 3C protease cleavage sites. We transformed PSB-D Arabidopsis cell cultures with *Agrobacterium tumefaciens* carrying the aforehead mentioned translational fusions. In line with previous results obtained using co-IP assays followed by tandem mass spectrometry (Bloomer et al., 2020), we determined that ICU11 interacts with the PRC2 core components EMF2, FIE, SWN, and MSI1, as well as the PRC2 accessory proteins EMF1, TRB1, TRB2, and TRB3 (Supplemental Figure S1, Supplemental Table S1 and Supplemental Dataset DS1). TRB1, TRB2, and TRB3 are components of the PWWPs-EPCRs-ARIDs-TRBs (PEAT) complexes that recruit PRC2 to telobox-related motifs present at telomeres (Godwin and Farrona, 2022; Scortecci et al., 2003; Tan et al., 2018; Zhou et al., 2016; Zhou et al., 2018). We also identified MSI1 and SWN as interactors of ICU11 in one of our TAP-based replicates (Supplemental Dataset DS1). In contrast to Bloomer et al. (2020), we did not identify CLF or LHP1 as ICU11 interactors.

Among the best-represented interactors of ICU11, we also noticed three paralogous proteins, which are predicted to be nuclear: the AT5G66000 hypothetical protein and the AT3G17460 and AT4G35510 uncharacterized proteins with a PHD finger domain. AT5G66000 was previously detected as an interactor of EMF1, CLF, and ICU11 in the co-IP assays performed by Bloomer et al. (2020), in which these authors also detected AT3G17460 as an ICU11 interactor, and AT4G35510 as an interactor of CLF but not ICU11.

CP2 interacts with TRB4, TRB5, and other nuclear proteins in a TAP-based screen

We also performed a TAP-based screen to identify CP2 interactors, from which we detected no PRC2 core component. CP2 strongly interacted with TRB4 and TRB5 (Supplemental Figure S1 and Supplemental Table S1), two poorly characterized members of the TRB family; however, their TRB1, TRB2, and TRB3 paralogs were not detected as CP2 interactors. We excluded any possible ambiguity in the interactions of ICU11 and CP2 with the TRB proteins by checking that the peptides identified from each TRB were protein-specific, the only exception being one peptide whose sequence matches an identical region in TRB2 and TRB3 (Supplemental Figure S3). Other nuclear proteins identified as interactors of CP2 but not of ICU11 were DEVELOPMENT RELATED MYB-LIKE1 (DRMY1) and DRMY PARALOG 1 (DP1; Supplemental Figure S1 and Supplemental Table S1), which belong to the single repeat MYB family of transcription factors. Whereas the *dp1* mutant is indistinguishable from the wild type,

drmy1 loss-of-function mutants exhibit pleotropic defects in root, vegetative, and floral development, but not in flowering time (Wu et al., 2018; Yanhui et al., 2006; Zhu et al., 2020). Another interactor of CP2 but not of ICU11 was INOSITOL REQUIRING 80 (INO80; Supplemental Figure S1 and Supplemental Table S1), a nuclear chromatin remodeling factor conserved among eukaryotes. Depletion of INO80 represses photomorphogenesis and causes multiple developmental defects including reduced plant size, late flowering, abnormal shape of reproductive organs, reduced pollen grain number per anther, and smaller siliques (Kang et al., 2019; Yang et al., 2020; Zhang et al., 2015).

Another CP2 interactor we identified was the JMJ-type 2OGD protein INCREASE IN BONSAI METHYLATION 1 (IBM1; Supplemental Figure S1 and Supplemental Table S1), a known H3K9me2/1 demethylase (Miura et al., 2009). Several *ibm1* alleles perturb leaf and flower morphogenesis and reduce fertility. The depletion of IBM1 increases H3K9me marks and DNA methylation in the CHG and CHH genomic contexts (Saze et al., 2008).

Nuclear proteins that interact with both ICU11 and CP2 in TAP-based screens

Our TAP assays also revealed nuclear proteins that interact with both ICU11 and CP2 (Supplemental Figure S1, Supplemental Table S1 and Supplemental Dataset DS1). Two of these were the paralogous transcription factors NAC050 and NAC052, which associate with the histone demethylase JMJ14 in the negative regulation of flowering through the removal of the H3K4me3 mark at flowering regulator genes such as *FLC* (Ning et al., 2015). Neither NAC050 nor NAC052 was identified as an ICU11 interactor by Bloomer et al. (2020). By contrast, JMJ14 was identified as an ICU11 interactor by Bloomer et al. (2020) but was not detected in our TAP assays.

We also identified COP9 SIGNALOSOME SUBUNIT 1 (CSN1), also named FUSCA 6 (FUS6), a member of the CONSTITUTIVE PHOTOMORPHOGENESIS 9 (COP9) signalosome complex, which maintains skotomorphogenesis by repressing photomorphogenesis (Qin et al., 2020; Wang et al., 2002), and is required for the proper development of floral organs (Wang et al., 2003). CSN1 was not detected by Bloomer et al. (2020).

Neither of our two TAP-based screens revealed any interaction between ICU11 and CP2, despite their shared interactors.

ICU11 and CP2 interact with PRC2 core components and accessory proteins in BiFC assays

To obtain additional and independent evidence for the results of our TAP-based screens, we performed heterologous BiFC assays through the transient transformation of *Nicotiana benthamiana* leaves (Kerppola, 2006; Martin et al., 2009). The co-infiltration of such leaves with constructs encoding the N-terminal half of enhanced yellow fluorescence protein (EYFP)

fused to ICU11 (nEYFP-ICU11) and the C-terminal half of EYFP fused to CLF (cEYFP-CLF), SWN (cEYFP-SWN), or LHP1 (cEYFP-LHP1) all produced strong nuclear EYFP signals (Figure 1A–I), which is consistent with the known nucleoplasmic colocalization of ICU11 (Mateo-Bonmatí et al., 2018), CLF (Schubert et al., 2006), SWN (Wang et al., 2006), and LHP1 (Zemach et al., 2006). We established that nEYFP-CP2 interacts with cEYFP-CLF, cEYFP-SWN, and cEYFP-LHP1 (Figure 1P–X). All co-infiltrations of nEYFP-ICU11 or nEYFP-CP2 with cEYFP-TRB1 or cEYFP-TRB3 resulted in strong EYFP signals (Figure 1J–O, Y–AD), consistent with the known subnuclear localization of TRB1 and TRB3 (Zhou et al., 2016). As a positive control, both coinfiltrations of cEYFP-LHP1 with nEYFP-UBP12 and nEYFP-UBP13 rendered strong nuclear signals, as previously described (Supplemental Figure S3A-F; Derkacheva et al., 2016). The absence of interaction between ICU11 and CP2 was confirmed by coinfiltration of *Nicotiana benthamiana* leaves with nEYFP-ICU11 and cEYFP-CP2 (Supplemental Figure S3G-I). nEYFP-ICU11 and nEYFP-CP2 were used as negative controls (Supplemental Figure S3O-Q).

The transcriptomic profile of the *icu11-5 cp2-1* double mutant resemble that of the *emf2-3* single mutant

We previously used both RNA-seq and reverse transcription-quantitative PCR (RT-qPCR) to show that the *icu11-1* mutant, in the Arabidopsis S96 genetic background, transcriptionally misregulates hundreds of genes (Mateo-Bonmatí et al., 2018). As *ICU11* and *CP2* encode putative PRC2 accessory proteins and the morphological phenotype of their double mutant combinations (namely, embryonic flowers) resembles that of the *emf1* and *emf2* single mutants, we compared the transcriptome of the *icu11-5 cp2-1* double mutant with that of the PRC2 strong loss-of-function mutant *emf2-3*. We used clustered regularly interspaced short palindromic repeat (CRISPR)/CRISPR-associated nuclease 9 (Cas9)-mediated mutagenesis to obtain the *icu11-5* and *icu11-6* alleles of *ICU11* in a Col-0 genetic background to avoid possible differences in gene expression due to the genetic background (Nadi et al., 2023).

We performed RNA-seq analyses of the Col-0, *icu11-5* and *cp2-1* seedlings, and the *icu11-5 cp2-1* and *emf2-3* embryonic flowers, which were all collected 10 das; Col-0 inflorescences were also collected 40 das for RNA-seq (Figure 2, Supplemental Table S2 and Supplemental Dataset DS2). We only identified 23 upregulated genes and 5 downregulated genes in the *cp2-1* mutant relative to Col-0; the morphological phenotype of this mutant is indistinguishable from the wild type. We also identified 738 upregulated genes and 78 downregulated genes in the *icu11-5* mutant, whose morphological phenotype is relatively weak. By contrast, the number of de-regulated genes in the *icu11-5 cp2-1* and *emf2-3* embryonic flowers was similar: these plants showed 3199 upregulated genes and 1770 downregulated genes, and 2520 upregulated genes and 1774 downregulated genes,

Nadi *et al*., Figure 1

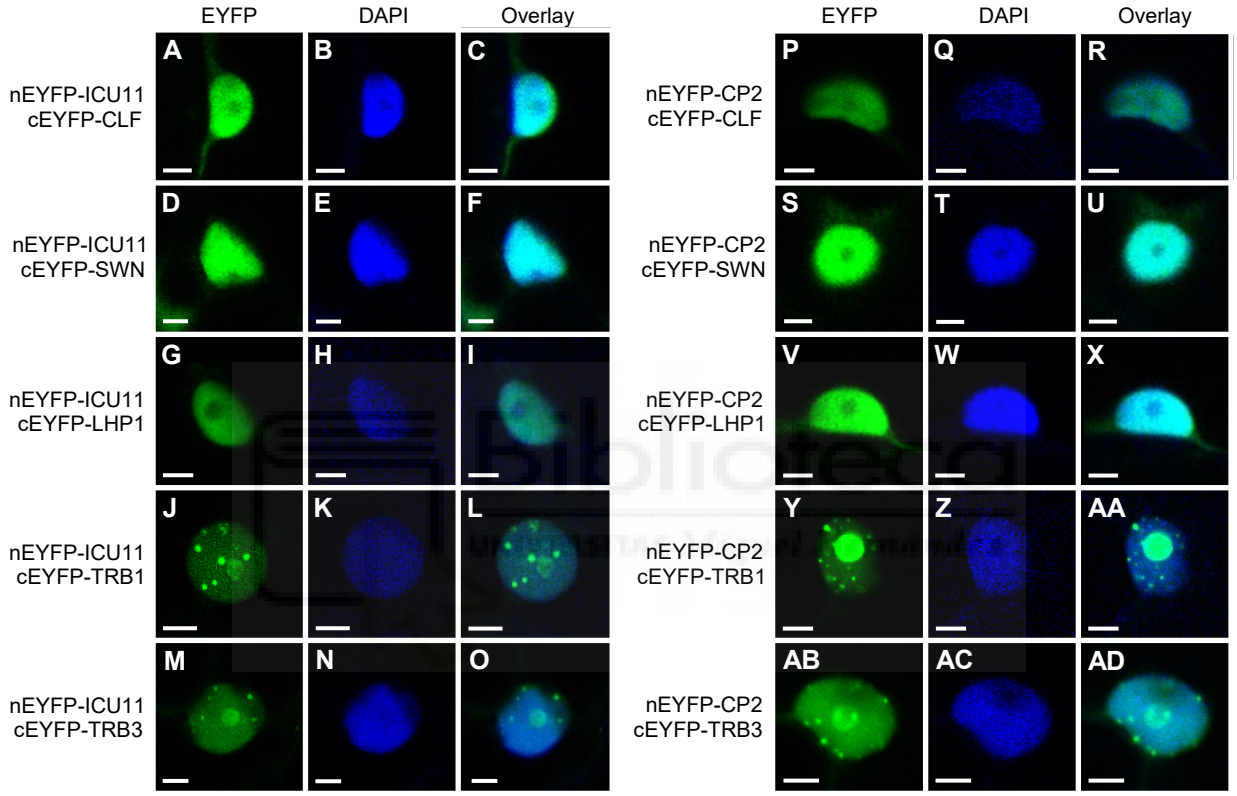

Figure 1. *In vivo* interactions of ICU11 and CP2 with proteins with known epigenetic roles. Bimolecular fluorescence complementation assays showing interaction between the indicated proteins. Individual nuclei of *Nicotiana benthamiana* leaves co-infiltrated with the constructs *nEYFP-ICU11* or *nEYFP-CP2* with *cEYFP-CLF*, *cEYFP-LHP1*, *cEYFP-TRB1*, or *cEYFP-TRB3*. Fluorescent signals correspond to EYFP (A, D, G, J, M, P, S, V, Y, AB), DAPI (B, E, H, K, N, Q, T, W, Z, AC), and their overlay (C, F, I, L, O, R, U, X, AA, AD). Scale bars, 5 μm.

Nadi *et al.*, Figure 2

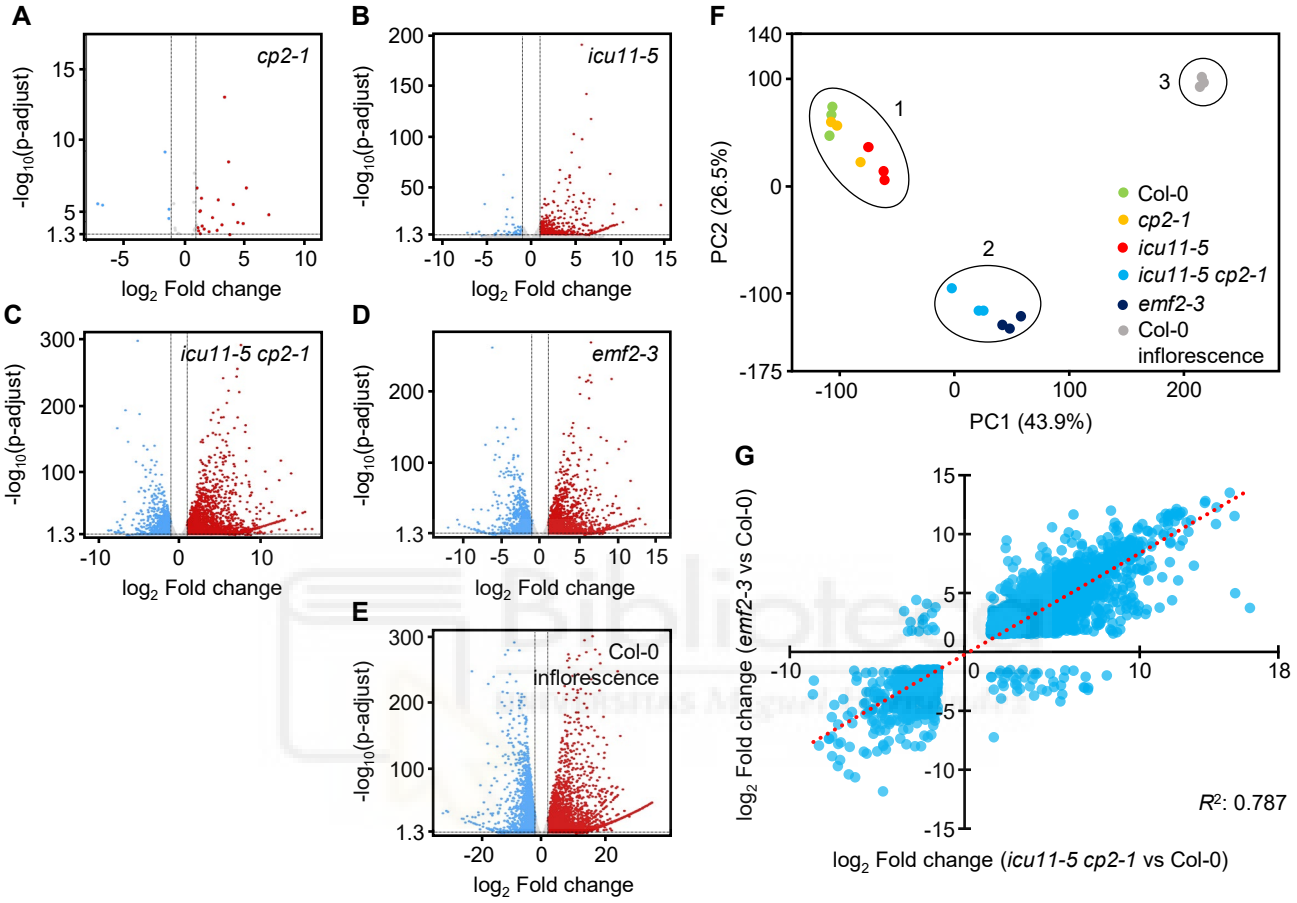

Figure 2. Transcriptomic profiling of *icu11-5 cp2-1* and *emf2-3* embryonic flowers. (A–E) Volcano plots representing differentially expressed genes (DEGs) in *cp2-1* (A) and *icu11-5* (B) seedlings; *icu11-5 cp2-1* (C) and *emf2-3* (D) embryonic flowers; and Col-0 (E) inflorescences, all compared to Col-0 seedlings. Blue and red dots indicate significantly downregulated and upregulated genes, respectively, with a Benjamini and Hochberg corrected *p*-value < 0.05. Total RNA was extracted from three biological samples collected 10 (A–D) or 40 (E) das. (F) Principal component analysis of the transcriptomic profiles showing three clusters: (1) Col-0, *cp2-1*, and *icu11-5* seedlings; (2) *icu11-5 cp2-1*, and *emf2-3* embryonic flowers; and (3) Col-0 inflorescences. Each dot represents a biological replicate. (G) Scatterplot showing the positive correlation between the relative expression levels of DEGs of the *icu11-5 cp2-1* double mutant and those of the *emf2-3* single mutant, both relative to Col-0 seedlings. Log_2 values ranging from –1.5 to 1.5 were not plotted. The best-fit line is shown as a red dashed line, and the R^2 value is indicated.

respectively, when compared to Col-0 seedlings. Moreover, the Col-0 inflorescences showed the expected strong transcriptomic differences when compared to Col-0 seedlings, with 5431 upregulated genes and 3084 downregulated genes, in agreement with similar data previously published (Klepikova et al., 2016).

Genes encoding MADS-box transcription factors, such as *AGAMOUS* (*AG*) and *SEEDSTICK* (*STK*), are flower organ identity genes repressed by PRC2 (Petrella et al., 2020; Schubert et al., 2006). In the present study, *AG*, *SHATTERPROOF 2* (*SHP2*), and *STK* were found upregulated in in *icu11-5* seedlings, *icu11-5 cp2-1* and *emf2-3* embryonic flowers, and Col-0 inflorescences, but not in *cp2-1* seedlings, which we confirmed using RT-qPCR. Among the genes upregulated in *cp2-1* seedlings, we found *EARLY ARABIDOPSIS INDUCED 1* (*EARLI1*), which encodes a proline-rich family protein involved in lignin biosynthesis and flowering time control (Shi et al., 2011); *PIRIN 1* (*PRN1*), a cupin-fold protein involved in seed germination, development, and the response to abscisic acid and light (Orozco-Nunnelly et al., 2014); and *RIBONUCLEASE 1* (*RNS1*), a protein that functions in cell death and the generation of tRNA-derived fragments, which are involved in the regulation of gene expression, RNA degradation, and the inhibition of protein synthesis (Goodman et al., 2022; Megel et al., 2019) (Supplemental Figure S4).

A principal component analysis identified different patterns of transcriptional misregulation, with three main clusters: one formed by the seedlings of Col-0, *cp2-1,* and to a certain extent *icu11-5*; another one consisting of the *icu11-5 cp2-1* and *emf2-3* embryonic flowers; and the last one representing the transcriptome of the Col-0 inflorescence (Figure 2F). The transcriptomes of *icu11-5 cp2-1* and *emf2-3* were similar (R^2 = 0.787; Figure 2G).

A protein domain enrichment analysis revealed that *icu11-5* seedlings*, icu11-5 cp2-1* and *emf2-3* embryonic flowers and Col-0 inflorescences share an upregulation of genes in the Mitogen-Activated Protein Kinase (MAPK) cascade, an important conserved mechanism in eukaryotes that triggers the intracellular transduction response to a range of developmental and environmental signals (Jagodzik et al., 2018; Plotnikov et al., 2011; Supplemental Datasets DS3 to DS7). The *icu11-5 cp2-1* and *emf2-3* transcriptomes also had similar Gene Ontology (GO) enrichment of biological processes profiles, among the most significant of which for the upregulated genes included response to phytohormones, abiotic stresses, and transcriptional regulation (Supplemental Datasets DS5 and DS7). We also observed that most enriched GO terms in the downregulated genes in the *icu11-5 cp2-1* and *emf2-3* embryonic flowers and the Col-0 inflorescence are related to photosynthesis, chloroplast organization and biosynthesis, and sucrose biosynthesis (Supplemental Datasets DS5 and DS7).

Regarding the protein domain enrichment analysis, the genes upregulated in *icu11-5* were enriched in those encoding proteins harboring the keratin-like (K-box) and MADS-box domains (Supplemental Dataset DS3), which are associated with the regulation of flowering

time (Alvarez-Buylla et al., 2000). The same categories were also enriched in the upregulated genes of *icu11-5 cp2-1* and *emf2-3* embryonic flowers, and Col-0 inflorescences, which also encompassed 13 other categories, including Non Apical Meristem (NAM), a FAD-binding domain, and WRKY domains, which are also related to the regulation of flowering (Aida et al., 1997; Liu et al., 2008; Martignago et al., 2019; Singh et al., 2014; Spedaletti et al., 2008). The genes upregulated in *icu11-5 cp2-1* and *emf2-3* embryonic flowers were significantly enriched in genes encoding transcription factors containing the APETALA2/ETHYLENE-RESPONSIVE ELEMENT BINDING FACTOR (AP2/ERF) domain (Drews et al., 1991; Feng et al., 2020; Okamuro et al., 1997; Supplemental Datasets DS5-DS7).

The transcriptomic profile of *icu11-5 cp2-1* resembles that of mutants affected in genes encoding PRC2 core components or accessory proteins

Venn diagrams of the Differentially Expressed Genes (DEGs) of *icu11-5* and *cp2-1* seedlings and *icu11-5 cp2-1* embryonic flowers, all compared with Col-0 seedlings*,* showed no overlap between the genes downregulated in *icu11-5* and *cp2-1*, and only eight genes were upregulated in both *icu11-5* and *cp2-1*. We also found that 78% and 58% of the genes upregulated and downregulated in *icu11-5*, respectively, are coregulated in the *icu11-5 cp2-1* double mutant (Figure 3A, D).

We conducted comparative analyses of the published transcriptomic profiles of mutants carrying mutant alleles of genes encoding PRC2 core components or accessory proteins, which exhibit morphological phenotypes ranging from wild type to callus-like, as is the case for *clf-29 swn-21* (Wang et al., 2016; Yang et al., 2013). The *trb1-2 trb2-1 trb3-2* triple mutant exhibits an embryonic flower phenotype (Zhou et al., 2018); we determined that 56% of the 411 upregulated genes and 40% of the 31 downregulated genes in *icu11-5* are similarly upregulated or downregulated in *trb1-2 trb2-1 trb3-2* (Figure 3B, E). The morphological phenotypes of *trb1-2 trb2-1 trb3-2*, *emf2-3,* and *icu11-5 cp2-1* are similar, and their transcriptomic profiles included 530 and 275 genes that are similarly upregulated or downregulated, respectively. Only 548 (17%) and 337 (19%) genes were exclusively upregulated and downregulated, respectively, in *icu11-5 cp2-1* but not in *emf2-3, clf29 swn-21, or trb1-2 trb2-1 trb3-2* (Figure 3C, F).

Hierarchical clustering of the *icu11-5* and *icu11-5 cp2-1* transcriptomic profiles and those of mutants affected in genes encoding PRC2 core components and accessory components, as well as PRC1 core components, revealed that *icu11-5 cp2-1* showed a high transcriptomic similarity to *emf2-3,* and to a lesser extent with *trb1-2 trb2-1 trb3-2.* The *icu11-5* mutant clustered with the mutans affected in PcG genes with milder morphological phenotypes, such as *clf-29* (Figure 3G).

Nadi *et al.*, Figure 3

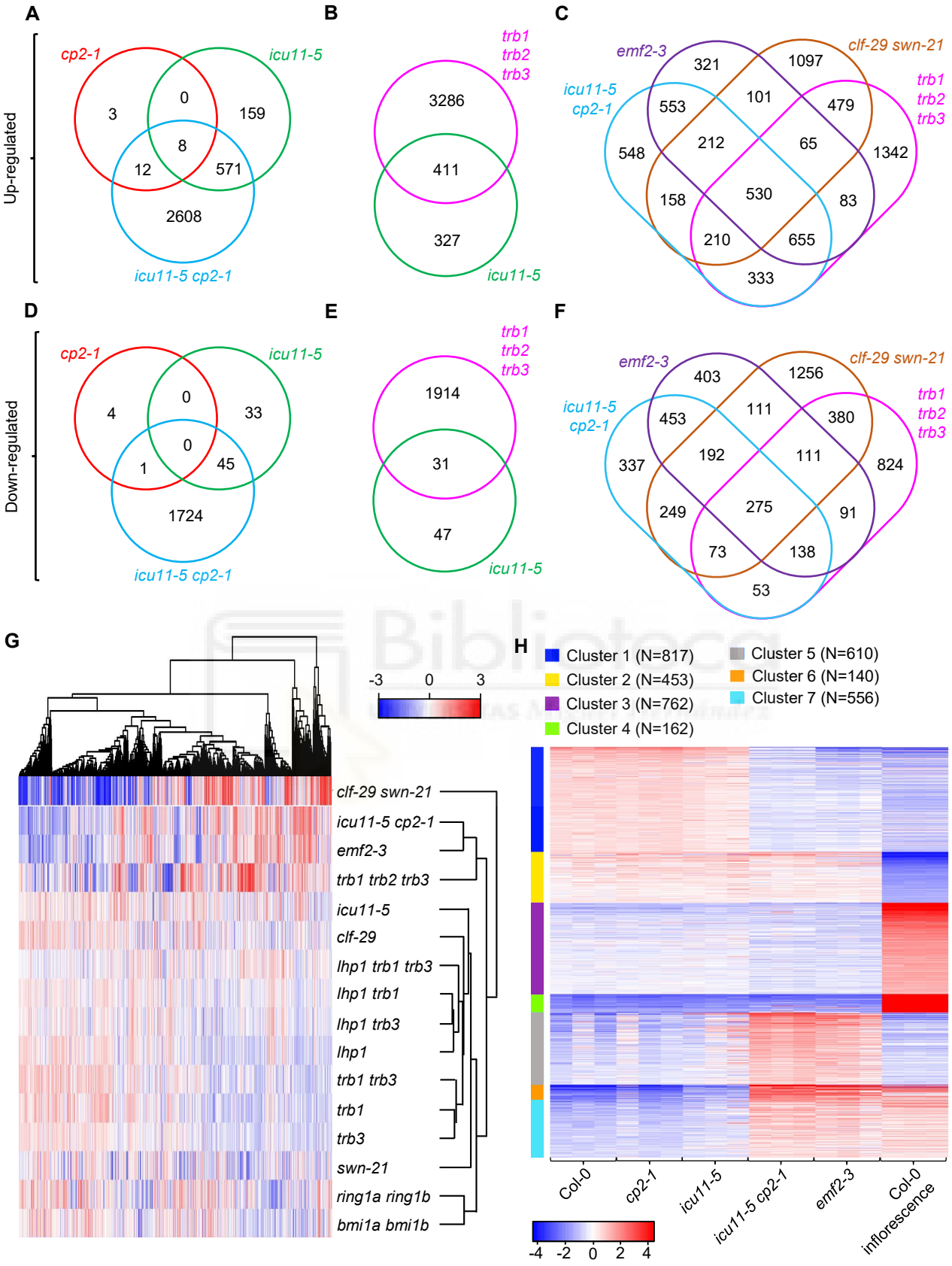

Figure 3. Comparison of differential expression in the *icu11-5 cp2-1* double mutant and in mutants lacking function of PRC2 core components or accessory proteins. (A–F) Venn diagrams showing the overlap between upregulated (A–C) and downregulated (D–F) genes in *cp2-1* and *icu11-5* seedlings and *icu11-5 cp2-1* embryonic flowers (A, D), *icu11-5* seedlings and *trb1 trb2 trb3* embryonic flowers (B, E), and *icu11-5 cp2-1*, *emf2-3* and *trb1 trb2 trb3* embryonic flowers and *clf-29 swn-21* callus-like seedlings (C, F). The abbreviations *trb1*, *trb2*, *trb3*, and *lhp1* stand for the

Nadi *et al*., Figure 3

alleles *trb1-2*, *trb2-1*, *trb3-2*, and *lhp1-4*, respectively. (G) Heatmap showing the normalized $\log_2$ fold-change of genes misregulated in the plants studied. Genes represented in red and blue are upregulated and downregulated, respectively. (H) k-means transcriptional clustering of the genotypes under study. Seven clusters and normalized read counts of the 3500 most variable genes were used. N is the number of genes per cluster. The color scale indicates the range of normalized $\log_2$ fold-change of the 3500 genes.

To ascertain which set of the genes misregulated in *icu11-5 cp2-1* contributes to its embryonic flower phenotype, we performed k-clustering with the 3500 most variably expressed genes and a k value of 7 (Figure 3H). Clusters 2, 3, and 4 harbored 453, 762, and 162 genes, respectively, for which the Col-0 inflorescence presented significantly different expression levels compared to the remaining samples. Cluster 2 genes were repressed in Col-0 inflorescences, suggesting that these genes are important for vegetative development. On the contrary, 924 genes from clusters 3 and 4 were highly expressed in Col-0 inflorescences, suggesting a role in reproductive development instead. We identified 817 genes from cluster 1 (downregulated) and 556 genes from cluster 7 (upregulated) as being coregulated in the *icu11-5 cp2-1* and *emf2-3* embryonic flowers and Col-0 inflorescences in comparison to Col-0 seedlings. Moreover, cluster 5 contained 610 genes that are highly expressed in *icu11-5 cp2-1* and *emf2-3* but not in the remaining samples (Figure 3H). The embryonic flower phenotype of *icu11-5 cp2-1* and *emf2-3* is therefore likely to be a direct consequence of the misregulation of genes composing clusters 1, 5, and 7. Cluster 6 comprised 140 genes that are downregulated in Col-0 and *cp2-1* seedlings, moderately downregulated in *icu11-5* seedlings, and upregulated in *icu11-5 cp2-1* and *emf2-3* embryonic flowers, as well as in Col-0 inflorescences (Figure 3H).

GO and protein domain enrichment analyses of each k-cluster revealed that the categories enriched in cluster 5 are related to responses to different stimuli, regulation of metabolic processes, and regulation of transcription, being mainly represented by WRKY, NAC, and the Ethylene Responsive Factor (ERF) transcription factors. In cluster 6, only the positive regulation of transcription mediated by RNA polymerase II category was enriched, represented by 10 MADS-box genes (Supplemental Data Set 8B). In cluster 1, we observed enrichment in processes related to photosynthesis, while cluster 7 included more enriched categories related to responses to biotic and abiotic stresses. In conclusion, our RNA-seq analyses provide evidence of the substantial alteration of transcript levels in the *icu11-5 cp2-1* double mutant compared to the profiles of the *icu11-5* and *cp2-1* single mutants. Additionally, the transcriptomic profile of *icu11-5 cp2-1* resembles that of mutants affected in genes encoding the PRC2 core components and accessory proteins, in particular the *emf2-3* mutant. Finally, some of the misregulated genes in the *icu11-5 cp2-1* embryonic flowers are expressed as they are in the wild-type reproductive organs of Col-0 inflorescences.

Genes misregulated in the *icu11-5 cp2-1* double mutant are enriched in PRC2 targets and genes marked with H3K27me3

A previous report suggested that ICU11 is a H3K36me3 demethylase, based on the substantial decrease of the H3K27me3 repressive mark seen in the *icu11-1* mutant (Bloomer et al., 2020). We performed a comparative analysis of the genes misregulated in *icu11-5, icu11-5 cp2-1*,

and *emf2-3* with genes known to be marked by H3K27me3, H2AK121ub, and H3K36me3 in Col-0, which are deposited by PRC2, PRC1 and SET DOMAIN-CONTAINING GROUP 8 (SDG8), respectively (Li et al., 2015; Merini et al., 2017; Sanders et al., 2017; Yang et al., 2014; Zhou et al., 2017). We determined that the genes marked with H3K27me3 and H2AK121ub in Col-0 are significantly overrepresented among the DEGs of *icu11-5, icu11-5 cp2-1*, and *emf2-3*; however, genes marked with H3K36me3 in Col-0 were underrepresented among the DEGs of these mutants (Figure 4A and Supplemental Table S3). Genes individually targeted by the TRB1, EMF1, and LHP1 accessory proteins of PRC2 and by both CLF and SWN (Kim et al., 2012; Shu et al., 2019; Veluchamy et al., 2016; Zhou et al., 2018) were significantly enriched among the genes misregulated in *icu11-5, icu11-5 cp2-1,* and *emf2-3*. The TRB1 targets, however, were underrepresented among the downregulated genes in *icu11-5* and *icu11-5 cp2-1*. Taken together, these data suggest that most genes misregulated in the *icu11-5 cp2-1* double mutant are direct targets of PRC2 or its accessory proteins. Indeed, genes that were marked with H3K27me3 and H2AK121ub in Col-0 seedlings were overrepresented among those misregulated in *icu11-5 cp2-1*. It is of note that genes marked with H3K36me3 in Col-0 were underrepresented among those misregulated in *icu11-5, icu11-5 cp2-1,* and *emf2-3*.

Nadi *et al.*, Figure 4

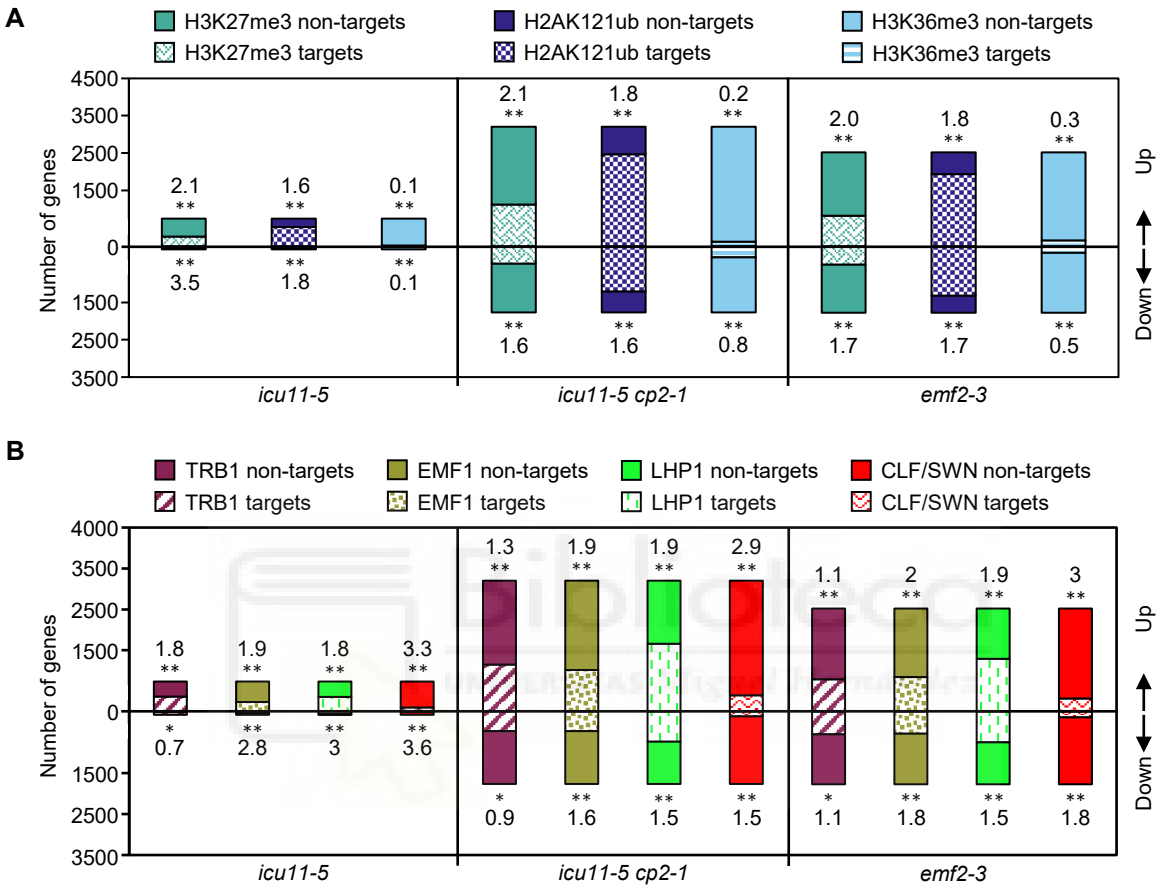

Figure 4. Integrated comparison of the chromatin immunoprecipitation-seq data and transcriptomic profiles in *icu11-5*, *icu11-5 cp2-1*, and *emf2-3* and lists of genome-wide histone mark distributions or protein targets in Col-0. (A) Overlapping fraction of upregulated and downregulated genes in the indicated mutants with genes marked by H3K27me3, H2AK121ub, and H3K36me3 in Col-0. (B) Overlapping fraction of upregulated and downregulated genes in the indicated mutants with genes bound by the TRB1, EMF1, LHP1, CLF, and SWN proteins in Col-0. Numbers indicate the enrichment factor of overlapping fractions [(number of common genes × number of total Arabidopsis genes)/(number of genes in list 1 × number of genes in list 2)], where enrichment factors > 1 or < 1 indicate more or less overlap than expected between the two independent gene lists, respectively. Asterisks indicate a significant overlap between the RNA-seq and ChIP-seq lists in a Fisher's exact test (*P < 0.05 and **P < 0.01).

DISCUSSION

The TAP- and BiFC-based protein-protein interaction profiles of ICU11 and CP2 partially overlap, pointing to their roles as PRC2 accessory proteins

We previously showed that *ICU11* and *CP2* are close paralogs whose encoded proteins behave as components of the epigenetic machinery of Arabidopsis, which display unequal functional redundancy (Mateo-Bonmatí et al., 2018; Nadi et al., 2023). A co-IP analysis indicated that ICU11 is a PRC2 accessory protein (Bloomer et al., 2020). Very recently, both ICU11 and CP2 were shown by co-IP followed by mass spectrometry to interact with the PRC2 accessory proteins TRB1, TRB2 and TRB3, although this result was not discussed by the authors (Wang et al., 2023).

Here, we aimed to define the ICU11 and CP2 interactomes and their potential overlap in order to ascertain their epigenetic activities. We confirmed the physical interactions between ICU11 and the core components and accessory proteins of PRC2, through experimental approaches that are complementary to co-IP: TAP-based screens, and heterologous BiFC-based assays. Through these techniques, we also provide evidence that CP2 is likely to play a role as a PRC2 accessory protein, as ICU11 appears to do.

Our TAP-based screens revealed different protein-protein interaction profiles for ICU11 and CP2, despite their unequal functional redundancy; however, in our BiFC assays, ICU11 and CP2 showed similar *in vivo* interaction profiles. Other examples of partially or completely divergent results obtained from different methods of studying protein-protein interactions have been published for Arabidopsis. One of these examples is given by the pentatricopeptide repeat proteins SLOW GROWTH 2 (SLO2) and MITOCHONDRIAL EDITING FACTOR 57 (MEF57), which appeared to interact in mitochondria based on a BiFC assay, but did not interact using co-IP assays (Andrés-Colás et al., 2017). The Arabidopsis circadian clock regulators SPINDLY (SPY) and PSEUDO-RESPONSE REGULATOR 5 (PRR5) interacted in co-IP followed by mass spectrometry, as well as in co-IP followed by the identification of interactors by Western Blot and BiFC assays, but not in yeast two-hybrid (Y2H) assays; in addition interaction between SPY and GIGANTEA (GI) was detected using Y2H but not by co-IP either followed by mass spectrometry or Western Blot (Wang et al., 2020).

Taken together, our results indicate that CP2 can bind to TRBs and other proteins related to PRC2, and suggest that CP2 has the potential to bind to ICU11 interactors with less affinity than ICU11. A similar observation has been made in budding yeast (*Saccharomyces cerevisiae*), in a protein fragment complementation assay that was performed for 56 pairs of redundant paralogs. For 22 such pairs, one paralog had weaker detectable interactions than the other because of lower abundance or affinity; when the latter was lost, the former compensated for its function by binding to the same partners (Diss et al., 2017). It is of note that for compensating pairs, there was no detectable change in the level of expression of the

functional paralog when the other was deleted. The same appears to hold for *CP2* in an *icu11* background, as *CP2* is not upregulated in the *icu11-5* mutant (this work) or in *icu11-1* (Mateo-Bonmatí et al., 2018). Another example is provided in human T cells by the retinoblastoma-associated protein p130, which binds to EARLY 2 FACTOR (E2F) transcription factors to control cell proliferation by gene repression. When p130 is depleted, its paralogous p107 gains new interactions with E2F proteins to compensate for the absence of p130 (Mulligan et al., 1998).

In addition to their morphological phenotypes, the molecular phenotypes of the *icu11-5 cp2-1* and *emf2-3* embryonic flowers are similar

Our RNA-seq analyses revealed that about 21% of Arabidopsis genes were significantly misregulated in the *icu11-5 cp2-1* lethal embryonic flowers. Alongside its synergistic morphological phenotype, the *icu11-5 cp2-1* double mutant also had six times more misregulated genes than the *icu11-5* single mutant, overlapping to a large extent with misregulated genes in mutants affected in the PcG genes with strongly aberrant phenotypes, such as the *emf2-3* embryonic flowers and the *clf-29 swn-21* callus-like seedlings (Wang et al., 2016). Like in the *emf1* and *emf2* single mutants, in which many genes related to photosynthesis are repressed (Moon et al., 2003), ICU11 and CP2 appear to be involved in the positive regulation of photosynthesis, photosystem II assembly, the response to light stimulus, and auxin biosynthesis and signaling. Except for the latter, the downregulation of these genes in *icu11-5 cp2-1* and *emf2-3* embryonic flowers is also shown in wild-type Col-0 inflorescences (Kim et al., 2010; Moon et al., 2003).

During vegetative growth, ICU11 and/or CP2 seem to negatively regulate hundreds of genes to ensure the proper repression of genes that induce flowering, the formation of flower organs, the response to phytohormones, and abiotic stress. Genes encoding homeobox, MADS-box, and MYB, AP2/ERF and NAM/NAC domain transcription factors were enriched among the *icu11-5 cp2-1* upregulated DEGs. These genes were also highly expressed in Col-0 inflorescence meristems, where they play a crucial role in floral meristem development (Jofuku et al., 1994; Zhang et al., 2014; Zhang et al., 2009). Our k-mean clustering analysis of the most differentially regulated genes allowed the identification of a set of 1573 genes (clusters 1, 6, and 7 in Figure 3) that are expressed similarly in the *icu11-5 cp2-1* and *emf2-3* embryonic flowers and Col-0 inflorescences. Another set encompassed 1377 genes (clusters 2, 3, and 4) that are exclusively differentially expressed in Col-0 inflorescences. Finally, a set of 610 genes (cluster 5) comprised those highly upregulated only in *icu11-5 cp2-1* and *emf2-3,* and slightly upregulated in the *icu11-5* single mutant seedlings. This last set of genes was characterized by GO enrichment related to the responses to chemicals, oxygen-containing compounds, drugs, chitin and inorganic substances and stimuli, the regulation of metabolic

and biosynthetic processes, with 54 genes involved in regulation of transcription. Taken together, our results explain the embryonic flower phenotypes of *icu11-5 cp2-1* and *emf2-3*, given that there are 696 and 817 common up- and down-regulated genes with the wild-type inflorescence, respectively (clusters 1, 6, and 7), but also their failure to form a proper inflorescence, as expected from the 1377 genes that behave differently in the Col-0 inflorescences (clusters 2, 3, and 5). In conclusion, the similarity of not only the morphological but also the molecular phenotypes of *icu11-5 cp2-1* and *emf2-3* provides further support for the hypothesis that both ICU11 and CP2 are PRC2 accessory proteins.

Our interactomic and transcriptomic data suggest that CP2 can replace ICU11

Bloomer et al. (2020) proposed that ICU11 is a H3K36me3 demethylase. The depletion of a protein involved in the removal of an activating mark is expected to yield predominantly upregulated genes, which is in line with the pattern of misregulation detected here. This pattern has also been observed for lack-of-function alleles of the *JMJ17* and *JMJ14* genes, whose encoded proteins remove the H3K4me1/2/3 activating marks (Huang et al., 2019; Ning et al., 2015). The H3K36me3 mark antagonizes the deposition of H3K27me3 by PRC2 (Yang et al., 2014), which may explain the requirement of ICU11 for the deposition of the latter mark at the *FLC* locus by PRC2 during vernalization (Bloomer et al., 2020). It is therefore reasonable to assume that the transcriptomic profile of *icu11-5 cp2-1* is similar to that of a strong PcG mutant, such as *emf2-3*, because PRC2 cannot deposit H3K27me3 when the H3K36me3 mark cannot be removed.

Our comparison of the transcriptional misregulation of *icu11-5, icu11-5 cp2-1* and *emf2-3* with published chromatin immunoprecipitation (ChIP)-seq data reveals that genes marked by H3K27me3 and H2AK121ub or targeted by PRC2 core components and accessory proteins are overrepresented among the genes misregulated in these three mutants; the morphological and transcriptomic alterations observed for these genotypes are likely to be due to defective PRC2 repression on a substantial set of genes. If ICU11 and CP2 targets are not marked with H3K36me3 in Col-0, this would explain the underrepresentation of H3K36me3 marked genes among the differentially expressed genes in *icu11-5* and *icu11-5 cp2-1*.

We propose that ICU11 interacts with PRC2 core and accessory proteins, some of which recruit ICU11 to their target genes, so ICU11 can demethylate H3K36me3 and PRC2 can deposit H3K27me3 afterwards (Figure 5A). In the *icu11* mutants, although CP2 has less affinity for PRC2 core and accessory proteins, it can substitute ICU11 and demethylate H3K36me3 (Figure 5B). In the *icu11-5 cp2-1* double mutant, the H3K36me3 mark cannot be removed, leading to an impairment of PRC2 repression, resulting in the characteristic embryonic flower phenotype (Figure 5C). Since this does not explain the wild-type function of CP2, further research will be required to assess the specific function of CP2.

Nadi *et al.*, Figure 5

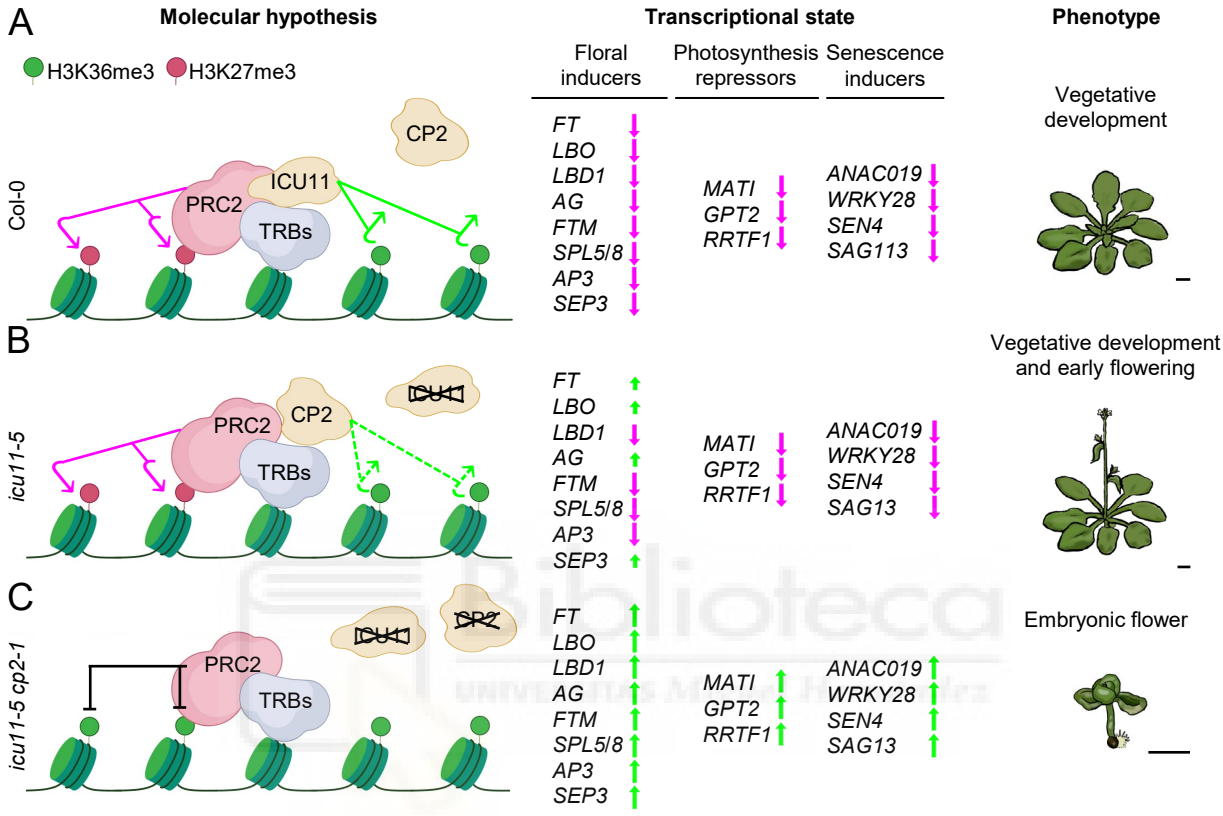

Figure 5. Model of the molecular role of ICU11 and CP2 and the effects of their depletion on transcription and phenotype in Arabidopsis. (A) In the wild-type Col-0, ICU11 may bind to the TRB1, TRB2, and TRB3 accessory proteins of PRC2, which recruit ICU11 to its target loci to remove the H3K36me3 activation mark. This enables PRC2 to deposit the repressive mark H3K27me3, leading to the repression of flower development genes, senescence inducers, and photosynthesis repressor genes, promoting proper vegetative development. (B) In the *icu11-5* mutant, CP2 can only partially compensate for the absence of ICU11 because of its lower affinity for TRB proteins and its less efficient removal of H3K36me3, decreasing the PRC2 repressive capacity, which results in an early flowering phenotype. (C) In the *icu11-5 cp2-1* double mutant, the presence of H3K36me3 at the target loci of ICU11 and CP2 impedes the deposition of H3K27me3, leading to an upregulation of floral and senescence inducers and photosynthetic repressors, resulting in the embryonic flower phenotype. ✕: full or partial depletion of a protein. ↗: H3K36me3 removal. ↘: H3K27me3 deposition. ⊥: inhibition of PRC2-mediated H3K27me3 deposition. ↑: transcriptional activation. ↓: transcriptional repression. Scale bars indicate 2 mm.

TRB and NAC proteins may recruit both ICU11 and CP2

ICU11 was previously described as a putative H3K36me3 demethylase, required for the removal of H3K36me3 during vernalization to allow the deposition of H3K27me3 (Bloomer et al., 2020). The interaction of both ICU11 and CP2 with TRB1, TRB2, and TRB3 suggests that these TRB proteins may recruit ICU11 and CP2 to their chromatin targets (Zhou et al., 2018). This hypothesis is reinforced by the similar embryonic flower phenotypes and transcriptomic profiles of the *icu11 cp2* double mutants and the *trb1-2 trb2-1 trb3-2* triple mutant.

The Arabidopsis genome encodes 21 2OGD proteins of the JMJ class, some of which are known to be involved in histone demethylation (Lu et al., 2008; Nadi et al., 2018). The H3K4 demethylase JMJ14 interacts with the NAC050 and NAC052 transcription factors through its phenylalanine/tyrosine-rich C-terminal (FYRC) domain, and plays an essential role in controlling flowering time (Ning et al., 2015). Here, we showed that ICU11 and CP2 also interact with NAC050 and NAC052, even though unlike JMJ14, ICU11 and CP2 do not have FYRC or FYRN domains. It is of note that neither NAC050 nor NAC052 were identified as ICU11 interactors by Bloomer et al. (2020), although JMJ14 was. NAC050 and/or NAC052 might recruit ICU11 and CP2 to their targets.

We also found three paralogous nuclear proteins that were not previously described as ICU11 interactors: At5g66000, At3g17460 and AT4G35510. At3g17460 and At4g35510 have a PHD domain. Bloomer et al. (2020) showed that the protein encoded by At5g66000 interacts with ICU11, EMF1 and CLF, that At3g17460 interacts with ICU11 and that At4g335510 interacts with CLF. We also showed that CP2 interacts with DRMY1 and DP1. Given that both ICU11 and CP2 lack any known DNA- or chromatin-binding domain, our results indicate they interact with proteins that may mediate their interaction with DNA or chromatin. Taken together, our interactome and transcriptome data confirm that ICU11 is a PRC2 accessory protein, and strongly suggest that CP2 also does this role for the correct deposition of H3K27me3 by PRC2.

METHODS

Plant materials, culture conditions, and crosses

The Nottingham Arabidopsis Stock Center (NASC) provided seeds for the wild-type *Arabidopsis thaliana* (L.) Heynh. accession Columbia-0 (Col-0, N1092), and the mutants *cp2-1* (N861581, in the Col-0 genetic background) and *emf2-3* (N16240, in Col-0). The *icu11-5* (in Col-0) single mutant was obtained using CRISPR/Cas9 mutagenesis and was described previously by Nadi et al. (2023). The presence and position of all mutations were confirmed by PCR amplification using gene-specific primers and, if required, Sanger sequencing (Supplemental Table S4).

Unless otherwise stated, plants were grown under sterile conditions in 150-mm Petri plates containing 100 ml half-strength Murashige and Skoog (MS) agar medium with 1% (w/v) sucrose at 20°C ± 1°C, 60–70% relative humidity, and continuous illumination at ~75 µmol m^{-2} s^{-1}, as previously described (Ponce et al., 1998). The crosses were performed as previously described (Quesada et al., 2000). Unless otherwise stated, all plants studied in this work were homozygous for the indicated mutations.

Gene constructs

All inserts were PCR amplified using Phusion High Fidelity Polymerase (Thermo Fisher Scientific, Waltham, MA, USA), primers containing *att*B sites at their 5′ ends (Supplemental Table S4), and Col-0 complementary DNA (cDNA) as a template. The PCR products were purified using an Illustra GFX PCR and Gel Band Purification Kit (Cytiva, Marlborough, MA, USA) and then cloned into the pGEM-T Easy221 vector and transferred to *Escherichia coli* DH5α cells, as previously described (Mateo-Bonmatí et al., 2018).

Tandem affinity purification assays

To obtain the GSRhino-TAP-tagged ICU11 or CP2 fusions (Supplemental Table S5), the pGEM-T Easy221 vector harboring the *ICU11* or *CP2* full-length coding sequences without their stop codons, together with the vectors pEN-L4-2-R1 and pEN-R2-GSrhinotag-L3, were recombined into the pKCTAP destination vector, as previously described (Van Leene et al., 2015). PSB-D Arabidopsis cell suspension cultures were transformed with *Agrobacterium tumefaciens* cells carrying the constructs and the TAP purification of the GSRhino-TAP-tagged ICU11 and CP2 fusions was performed as previously described (García-León et al., 2018; Van Leene et al., 2015). Two independent TAP assays were performed for each fusion protein. Proteins were identified using nano liquid chromatography–mass spectrometry (LC–MS)/MS at the Centro Nacional de Biotecnología (CNB, Madrid). Tandem mass spectra were searched against the Araport11 annotation of the Arabidopsis genome (Cheng et al., 2017) using the MASCOT search engine (Perkins et al., 1999). Experimental background proteins were

subtracted based on 40 TAP experiments performed on wild-type cultures and cultures accumulating GSRhino-TAP-tagged GUS, RFP, and GFP fusion proteins (Van Leene et al., 2010).

BiFC assays in *Nicotiana benthamiana* leaves and confocal microscopy

To obtain translational fusions for the BiFC assays, the pGEM-T Easy221 vector harboring the full-length *ICU11*, *CP2*, *TRB1*, *TRB2*, *TRB3*, *CLF*, *LHP1*, and *SWN* coding sequences, including their stop codons, were individually recombined with the pSITE-nEYFP-C1 or pSITE-cEYFP-C1 vectors (Martin et al., 2009). The nEYFP-UBP12 and nEYFP-UBP13 constructs were kindly provided by Dr. Claudia Köhler (Max Planck Institute, Postdam, Germany) Derkacheva et al., 2016). The BiFC constructs (Supplemental Table S5) were transformed into Agrobacterium (*Agrobacterium tumefaciens*) strain GV3101 (C58C1 Rif^R) cells, which were the grown in suspension as previously described (Derkacheva et al., 2016; Goodin et al., 2002). Briefly, the cells were grown overnight and resuspended in infiltration medium (10 mM $MgCl_2$, 150 µg/ml acetosyringone, and 10 mM MES-KOH, pH 5.6) to a final optimal density (OD_{600}) ≤ 1. After 3 h at room temperature, the Agrobacterium cell suspension was used to infiltrate the leaf abaxial surface of three- to five-week-old *Nicotiana benthamiana* plants. Leaf tissue samples were water-mounted for confocal visualization 48 h after infiltration.

Confocal microscopy was performed with a Nikon D-Eclipse C1 confocal microscope equipped with a Nikon DS-Ri1 camera and processed with the operator software EZ-C1 (Nikon, Tokyo, Japan). YFP was excited at 488 nm with an argon ion laser, and the emission signal was collected between 520 nm and 582 nm. The nuclei of the infiltrated leaves were stained with a 0.2 µg ml^{-1} 4′,6-diamidino-2-phenylindole (DAPI) solution (Sony Biotechnology, San José, CA, USA). DAPI was excited at 408 nm with a diode laser, and detected with a 450/35 nm filter.

RNA-seq analyses

Total RNA was isolated from 100 mg of pooled aerial tissues from Col-0, *icu11-5, cp2-1, icu11-5 cp2-1,* or *emf2-3* seedlings, collected 10 das using TRIzol (Thermo Fisher Scientific). The RNA quality of the samples was checked with a 2100 Bioanalyzer (Agilent Technologies, Santa Clara, CA, USA), and its RNA integrity number (RIN) was always ≥ 6.8. More than 10 µg of RNA per sample was sent to Novogene (Cambridge, UK) for library preparation and massive sequencing on an Illumina Novaseq 6000 (Illumina, San Diego, CA, USA).

Raw reads were pre-processed using fastp (v.0.21.0; Chen et al., 2018) with default parameters for read trimming, adapter removal, and low-quality read filtering. Pre-processed reads were then aligned to the TAIR10 reference genome (Lamesch et al., 2012) using HISAT2 (v.2.2.0; Kim et al., 2019), with argument "—dta-cufflinks" for downstream compatibility

(Supplemental Table S6). Cufflinks (v.2.2.1; Trapnell et al., 2012) was then used for transcript assembly using the TAIR10 structural annotation for reference, and transcripts were quantified with htseq-count to generate read count files (v.0.11.5; Anders et al., 2015). Read counts were normalized with DESeq2 (v.1.30.0; Love et al., 2014), which was then used to detect DEGs) between the sample and control pairs using the combined criteria |log2-fold-change| > 1 and *p*.adj value < 0.05. Volcano plots were obtained with the volcano plot tool of Galaxy (www.usegalaxy.org; The Galaxy Community, 2022). For principal component analysis we used NetworAnalyst tool (Zhou et al., 2019).

Both GO and Protein Domain enrichment analyses of the DEGs were performed using DAVID Bioinformatics tool (v.6.8; Huang da et al., 2009) with default parameters. Heatmaps were obtained using the heatmap.2 function from the gplots R package (v.20 3.0.1) using a total of 11116 genes that were misregulated in at least one of the genotypes under study. Additional RNA-seq data were downloaded from the Gene Expression Omnibus (https://www.ncbi.nlm.nih.gov/geo/) under accession number SRP056594 and from the European Nucleotide Archive (https://www.ebi.ac.uk/ena/browser/) under accession numbers ERP022017 and ERP009986. A principal component analysis and k-means clustering was performed using normalized counts on the iDEP 9.1 web 133 application (Ge et al., 2018). ChIP-seq data for cross analysis with RNA-seq were obtained from work published by Kim et al. (2012), Li et al. (2015), Merini and Calonje (2015), Sanders et al. (2017), Shu et al. (2019), Veluchamy et al. (2016), Zhou et al. (2017), and Zhou et al. (2018).

RNA isolation, cDNA synthesis, and qPCR

For the RT-qPCR, three biological replicates of seedling aerial tissues were collected 10 das and immediately frozen in liquid nitrogen. Total RNA was extracted using TRIzol (Thermo Fisher Scientific). The removal of contaminating DNA, cDNA synthesis, and qPCR were performed as previously described (Mateo-Bonmatí et al., 2018). Each reaction was performed in triplicate and the relative quantification of gene expression was performed using the $2^{-\Delta\Delta C_T}$ method (Livak and Schmittgen, 2001; Schmittgen and Livak, 2008) with the *ACTIN2* gene (At3g18780) as a control. All PCR reactions were performed on an Applied Biosystems Step One Plus System (Thermo Fisher Scientific). All PCR primers are listed in Supplemental Table S4; for the mean ΔCT statistical comparisons, a Mann-Whitney *U* test was performed.

Accession numbers

Sequence data from this article can be found at The Arabidopsis Information Resource (http://www.arabidopsis.org) under the following accession numbers: *ICU11* (At1g22950), *CP2* (At3g18210), *EMF2* (AT5G51230), *SWN* (AT4g02020), *CLF* (AT2g23380), *TFL2/LHP1* (At5g17690), *AG* (At4g18960), *SHP2* (AT2g42830), *STK* (AT4g09960), *EARLI1* (AT4g12480),

PRN1 (AT3g59220), *RNS1* (AT2g02990), *TRB1* (AT1g49950), *TRB2* (AT5g67580), *TRB3* (AT3g49850), *TRB4* (AT1g17520), and *TRB5* (AT1g72740). The raw RNA-seq data were deposited in the Sequence Read Archive (SRA, https://www.ncbi.nlm.nih.gov/sra) database under the following accession number: PRJNA1081349.

AUTHOR CONTRIBUTIONS

J.L.M. conceived and supervised the study, provided resources, and obtained funding. R.N., L.J.-V., and J.L.M. designed the methodology. R.N., L.J.-V., S.D.L, Y.F., and V.R. performed the research. R.N., L.J.-V. and J.L.M. wrote the original draft. All authors reviewed and edited the manuscript.

ACKNOWLEDGMENTS

The authors wish to thank C. Köhler and I. Fudal for providing constructs, M.R. Ponce for critical reading of the manuscript, J.M. Serrano and J. Castelló for their excellent technical assistance, and S. Vivo and C. Torralbo for their help in BiFC assays. Research in the laboratory of J.L.M. was supported by grants from the Ministerio de Ciencia e Innovación of Spain (PGC2018-093445-B-I00 and PID2021-127725NB-I00 [MCI/AEI/FEDER, UE]) and the Generalitat Valenciana (CIPROM/2022/2). R.N. and L.J.-V. held predoctoral fellowships from the Generalitat Valenciana (GRISOLIAP/2016/131) and the Ministerio de Universidades of Spain (FPU16/03772), respectively.

COMPETING INTERESTS

The authors declare no competing financial interests.

Supplemental material

Supplemental Figure S1. Diagram of the protein-protein interactions of ICU11 and CP2 detected in tandem affinity purification (TAP)-based screens.

Supplemental Figure S2. Peptides from TRB proteins identified using Liquid Chromatography Electrospray Ionization and Tandem Mass Spectrometry (LC-ESI-MS/MS) in ICU11 and CP2 TAP-based screens.

Supplemental Figure S3. Controls used for the Bimolecular Fluorescence Complementation (BiFC) assays.

Supplemental Figure S4. Validation by reverse transcription-quantitative PCR (RT-qPCR) of some of the genes found to be upregulated in our RNA-seq analyses.

Supplemental Table S1. Selected ICU11 and CP2 interactors identified in TAP-based screens.

Supplemental Table S2. Number of differentially expressed genes in *cp2-1* and *icu11-5* seedlings, *icu11-5 cp2-1* and *emf2-3* embryonic flowers, and Col-0 inflorescences, compared to the Col-0 seedlings.

Supplemental Table S3. Enrichment of overlapping fractions of chromatin immunoprecipitation (ChIP)-seq and transcriptomic profiles and their statistical significance.

Supplemental Table S4. Primer sets used in this work.

Supplemental Table S5. TAP and BiFC constructs.

Supplemental Table S6. Quality control summary of the RNA-seq analyses

Supplemental Data Set DS1. Protein identification in ICU11 and CP2 TAP-based screens.

Supplemental Data Set DS2. Differentially expressed genes in the RNA-seq analyses of *icu11-5* and *cp2-1* seedlings, *icu11-5 cp2-1* and *emf2-3* embryonic flowers, and Col-0 inflorescences.

Supplemental Data Set DS3. Protein domains and biological process gene ontology terms enriched among genes deregulated in *icu11-5* seedlings.

Supplemental Data Set DS4. Protein domains and biological process gene ontology terms enriched among genes deregulated in *cp2-1* seedlings.

Supplemental Data Set DS5. Protein domains and biological process gene ontology terms enriched among genes deregulated in *icu11-5 cp2-1* embryonic flowers.

Supplemental Data Set DS6. Protein domains and biological process gene ontology terms enriched among genes deregulated in *emf2-3* embryonic flowers.

Supplemental Data Set DS7. Protein domains and biological process gene ontology terms enriched among genes deregulated in Col-0 inflorescences.

Supplemental Data Set DS8. Biological process gene ontology enrichment analysis from k-means gene clustering.

REFERENCES

Aida, M., Ishida, T., Fukaki, H., Fujisawa, H., and Tasaka, M. (1997). Genes involved in organ separation in Arabidopsis: an analysis of the *cup-shaped cotyledon* mutant. Plant Cell 9:841-857.

Alvarez-Buylla, E.R., Pelaz, S., Liljegren, S.J., Gold, S.E., Burgeff, C., Ditta, G.S., Ribas de Pouplana, L., Martínez-Castilla, L., and Yanofsky, M.F. (2000). An ancestral MADS-box gene duplication occurred before the divergence of plants and animals. Proc. Natl. Acad. Sci. USA 97:5328-5333.

Anders, S., Pyl, P.T., and Huber, W. (2015). HTSeq—a Python framework to work with high-throughput sequencing data. Bioinformatics 31:166-169.

Andrés-Colás, N., Zhu, Q., Takenaka, M., De Rybel, B., Weijers, D., and Van Der Straeten, D. (2017). Multiple PPR protein interactions are involved in the RNA editing system in *Arabidopsis* mitochondria and plastids. Proc. Natl. Acad. Sci. USA 114:8883-8888.

Aubert, D., Chen, L., Moon, Y.H., Martin, D., Castle, L.A., Yang, C.H., and Sung, Z.R. (2001). EMF1, a novel protein involved in the control of shoot architecture and flowering in Arabidopsis. Plant Cell 13:1865-1875.

Bloomer, R.H., Hutchison, C.E., Bäurle, I., Walker, J., Fang, X., Perera, P., Velanis, C.N., Gümüs, S., Spanos, C., Rappsilber, J., et al. (2020). The *Arabidopsis* epigenetic regulator ICU11 as an accessory protein of Polycomb Repressive Complex 2. Proc. Natl. Acad. Sci. USA 117:16660-16666.

Bouyer, D., Roudier, F., Heese, M., Andersen, E.D., Gey, D., Nowack, M.K., Goodrich, J., Renou, J.P., Grini, P.E., Colot, V., et al. (2011). Polycomb repressive complex 2 controls the embryo-to-seedling phase transition. PLOS Genet. 7:e1002014.

Bratzel, F., López-Torrejón, G., Koch, M., del Pozo, J.C., and Calonje, M. (2010). Keeping cell identity in *Arabidopsis* requires PRC1 RING-finger homologs that catalyze H2A monoubiquitination. Curr. Biol. 20:1853-1859.

Calonje, M., Sanchez, R., Chen, L., and Sung, Z.R. (2008). EMBRYONIC FLOWER1 participates in Polycomb group–mediated *AG* gene silencing in *Arabidopsis*. Plant Cell 20:277-291.

Chanvivattana, Y., Bishopp, A., Schubert, D., Stock, C., Moon, Y.H., Sung, Z.R., and Goodrich, J. (2004). Interaction of Polycomb-group proteins controlling flowering in *Arabidopsis*. Development 131:5263-5276.

Chen, S., Zhou, Y., Chen, Y., and Gu, J. (2018). fastp: an ultra-fast all-in-one FASTQ preprocessor. Bioinformatics 34:i884-i890.

Cheng, C.Y., Krishnakumar, V., Chan, A.P., Thibaud-Nissen, F., Schobel, S., and Town, C.D. (2017). Araport11: a complete reannotation of the *Arabidopsis thaliana* reference genome. Plant J. 89:789-804.

Derkacheva, M., Liu, S., Figueiredo, D.D., Gentry, M., Mozgova, I., Nanni, P., Tang, M., Mannervik, M., Köhler, C., and Hennig, L. (2016). H2A deubiquitinases UBP12/13 are part of the *Arabidopsis* polycomb group protein system. Nat. Plants 2:e16126.

Derkacheva, M., Steinbach, Y., Wildhaber, T., Mozgová, I., Mahrez, W., Nanni, P., Bischof, S., Gruissem, W., and Hennig, L. (2013). *Arabidopsis* MSI1 connects LHP1 to PRC2 complexes. EMBO J. 32:2073-2085.

Diss, G., Gagnon-Arsenault, I., Dion-Coté, A.M., Vignaud, H., Ascencio, D.I., Berger, C.M., and Landry, C.R. (2017). Gene duplication can impart fragility, not robustness, in the yeast protein interaction network. Science 355:630-634.

Drews, G.N., Bowman, J.L., and Meyerowitz, E.M. (1991). Negative regulation of the Arabidopsis homeotic gene *AGAMOUS* by the *APETALA2* product. Cell 65:991-1002.

Feng, K., Hou, X.L., Xing, G.M., Liu, J.X., Duan, A.Q., Xu, Z.S., Li, M.Y., Zhuang, J., and Xiong, A.S. (2020). Advances in AP2/ERF super-family transcription factors in plant. Crit. Rev. Biotechnol. 40:750-776.

García-León, M., Iniesto, E., and Rubio, V. (2018). Tandem affinity purification of protein complexes from Arabidopsis cell cultures. Methods Mol. Biol. 1794:297-309.

Ge, S.X., Son, E.W., and Yao, R. (2018). iDEP: an integrated web application for differential expression and pathway analysis of RNA-Seq data. BMC Bioinform. 19:534.

Gendall, A.R., Levy, Y.Y., Wilson, A., and Dean, C. (2001). The *VERNALIZATION 2* gene mediates the epigenetic regulation of vernalization in *Arabidopsis*. Cell 107:525-535.

Godwin, J., and Farrona, S. (2022). The importance of networking: plant Polycomb Repressive Complex 2 and its interactors. Epigenomes 6.

Goodin, M.M., Dietzgen, R.G., Schichnes, D., Ruzin, S., and Jackson, A.O. (2002). pGD vectors: versatile tools for the expression of green and red fluorescent protein fusions in agroinfiltrated plant leaves. Plant J. 31:375-383.

Goodman, H.L., Kroon, J.T.M., Tomé, D.F.A., Hamilton, J.M.U., Alqarni, A.O., and Chivasa, S. (2022). Extracellular ATP targets Arabidopsis RIBONUCLEASE 1 to suppress mycotoxin stress-induced cell death. New Phytol. 235:1531-1542.

Goodrich, J., Puangsomlee, P., Martin, M., Long, D., Meyerowitz, E.M., and Coupland, G. (1997). A Polycomb-group gene regulates homeotic gene expression in *Arabidopsis*. Nature 386:44-51.

Grossniklaus, U., Vielle-Calzada, J.P., Hoeppner, M.A., and Gagliano, W.B. (1998). Maternal control of embryogenesis by *MEDEA*, a *Polycomb* group gene in *Arabidopsis*. Science 280:446-450.

Hennig, L., Taranto, P., Walser, M., Schönrock, N., and Gruissem, W. (2003). *Arabidopsis* MSI1 is required for epigenetic maintenance of reproductive development. Development 130:2555-2565.

Huang da, W., Sherman, B.T., and Lempicki, R.A. (2009). Bioinformatics enrichment tools: paths toward the comprehensive functional analysis of large gene lists. Nucleic Acids Res. 37:1-13.

Huang, Y., Jiang, L., Liu, B.Y., Tan, C.F., Chen, D.H., Shen, W.H., and Ruan, Y. (2019). Evolution and conservation of polycomb repressive complex 1 core components and putative associated factors in the green lineage. BMC Genom. 20:533.

Islam, M.S., Leissing, T.M., Chowdhury, R., Hopkinson, R.J., and Schofield, C.J. (2018). 2-Oxoglutarate-dependent oxygenases. Annu. Rev. Biochem. 87:585-620.

Jagodzik, P., Tajdel-Zielinska, M., Ciesla, A., Marczak, M., and Ludwikow, A. (2018). Mitogen-activated protein kinase cascades in plant hormone signaling. Front. Plant Sci. 9:1387.

Jiao, H., Xie, Y., and Li, Z. (2020). Current understanding of plant Polycomb group proteins and the repressive histone H3 Lysine 27 trimethylation. Biochem. Soc. Trans. 48:1697-1706.

Jofuku, K.D., den Boer, B.G., Van Montagu, M., and Okamuro, J.K. (1994). Control of Arabidopsis flower and seed development by the homeotic gene *APETALA2*. Plant Cell 6:1211-1225.

Kang, H., Zhang, C., An, Z., Shen, W.H., and Zhu, Y. (2019). AtINO80 and AtARP5 physically interact and play common as well as distinct roles in regulating plant growth and development. New Phytol. 223:336-353.

Kawai, Y., Ono, E., and Mizutani, M. (2014). Evolution and diversity of the 2-oxoglutarate-dependent dioxygenase superfamily in plants. Plant J. 78:328-343.

Kerppola, T.K. (2006). Design and implementation of bimolecular fluorescence complementation (BiFC) assays for the visualization of protein interactions in living cells. Nat. Protoc. 1:1278-1286.

Kim, D., Paggi, J.M., Park, C., Bennett, C., and Salzberg, S.L. (2019). Graph-based genome alignment and genotyping with HISAT2 and HISAT-genotype. Nat. Biotechnol. 37:907-915.

Kim, S.Y., Lee, J., Eshed-Williams, L., Zilberman, D., and Sung, Z.R. (2012). EMF1 and PRC2 cooperate to repress key regulators of Arabidopsis development. PLOS Genet. 8:e1002512.

Kim, S.Y., Zhu, T., and Sung, Z.R. (2010). Epigenetic regulation of gene programs by EMF1 and EMF2 in Arabidopsis. Plant Physiol. 152:516-528.

Klepikova, A.V., Kasianov, A.S., Gerasimov, E.S., Logacheva, M.D., and Penin, A.A. (2016). A high resolution map of the *Arabidopsis thaliana* developmental transcriptome based on RNA-seq profiling. Plant J. 88:1058-1070.

Köhler, C., Hennig, L., Bouveret, R., Gheyselinck, J., Grossniklaus, U., and Gruissem, W. (2003). *Arabidopsis* MSI1 is a component of the MEA/FIE *Polycomb* group complex and required for seed development. EMBO J. 22:4804-4814.

Lamesch, P., Berardini, T.Z., Li, D., Swarbreck, D., Wilks, C., Sasidharan, R., Muller, R., Dreher, K., Alexander, D.L., Garcia-Hernandez, M., et al. (2012). The Arabidopsis Information Resource (TAIR): improved gene annotation and new tools. Nucleic Acids Res. 40:D1202-D1210.

Lee, W.K., and Cho, M.H. (2016). Telomere-binding protein regulates the chromosome ends through the interaction with histone deacetylases in *Arabidopsis thaliana*. Nucleic Acids Res. 44:4610-4624.

Lewis, P.H. (1947). New mutants report. Drosoph. Inf. Serv. 21:69.

Li, Y., Mukherjee, I., Thum, K.E., Tanurdzic, M., Katari, M.S., Obertello, M., Edwards, M.B., McCombie, W.R., Martienssen, R.A., and Coruzzi, G.M. (2015). The histone methyltransferase SDG8 mediates the epigenetic modification of light and carbon responsive genes in plants. Genome Biol. 16:e79.

Liu, H., Yu, X., Li, K., Klejnot, J., Yang, H., Lisiero, D., and Lin, C. (2008). Photoexcited CRY2 interacts with CIB1 to regulate transcription and floral initiation in *Arabidopsis*. Science 322:1535-1539.

Livak, K.J., and Schmittgen, T.D. (2001). Analysis of relative gene expression data using real-time quantitative PCR and the $2^{-\Delta\Delta CT}$ method. Methods 25:402-408.

Love, M.I., Huber, W., and Anders, S. (2014). Moderated estimation of fold change and dispersion for RNA-seq data with DESeq2. Genome Biol. 15:550.

Lu, F., Li, G., Cui, X., Liu, C., Wang, X.J., and Cao, X. (2008). Comparative analysis of JmjC domain-containing proteins reveals the potential histone demethylases in *Arabidopsis* and rice. J. Integr. Plant Biol. 50:886-896.

Luo, M., Bilodeau, P., Koltunow, A., Dennis, E.S., Peacock, W.J., and Chaudhury, A.M. (1999). Genes controlling fertilization-independent seed development in *Arabidopsis thaliana*. Proc. Natl. Acad. Sci. USA 96:296-301.

Martignago, D., Bernardini, B., Polticelli, F., Salvi, D., Cona, A., Angelini, R., and Tavladoraki, P. (2019). The four FAD-dependent histone demethylases of Arabidopsis are differently involved in the control of flowering time. Front. Plant Sci. 10:e669.

Martin, K., Kopperud, K., Chakrabarty, R., Banerjee, R., Brooks, R., and Goodin, M.M. (2009). Transient expression in *Nicotiana benthamiana* fluorescent marker lines provides enhanced definition of protein localization, movement and interactions *in planta*. Plant J. 59:150-162.

Martinez, S., and Hausinger, R.P. (2015). Catalytic mechanisms of Fe(II)- and 2-oxoglutarate-dependent oxygenases. J. Biol. Chem. 290:20702-20711.

Mateo-Bonmatí, E., Esteve-Bruna, D., Juan-Vicente, L., Nadi, R., Candela, H., Lozano, F.M., Ponce, M.R., Pérez-Pérez, J.M., and Micol, J.L. (2018). *INCURVATA11* and *CUPULIFORMIS2* are redundant genes that encode epigenetic machinery components in Arabidopsis. Plant Cell 30:1596-1616.

Megel, C., Hummel, G., Lalande, S., Ubrig, E., Cognat, V., Morelle, G., Salinas-Giegé, T., Duchêne, A.M., and Maréchal-Drouard, L. (2019). Plant RNases T2, but not Dicer-like proteins, are major players of tRNA-derived fragments biogenesis. Nucleic Acids Res. 47:941-952.

Merini, W., and Calonje, M. (2015). PRC1 is taking the lead in PcG repression. Plant J. 83:110-120.

Merini, W., Romero-Campero, F.J., Gomez-Zambrano, A., Zhou, Y., Turck, F., and Calonje, M. (2017). The Arabidopsis Polycomb repressive complex 1 (PRC1) components AtBMI1A, B, and C impact gene networks throughout all stages of plant development. Plant Physiol. 173:627-641.

Miura, A., Nakamura, M., Inagaki, S., Kobayashi, A., Saze, H., and Kakutani, T. (2009). An *Arabidopsis* jmjC domain protein protects transcribed genes from DNA methylation at CHG sites. EMBO J. 28:1078-1086.

Moon, Y.H., Chen, L., Pan, R.L., Chang, H.S., Zhu, T., Maffeo, D.M., and Sung, Z.R. (2003). *EMF* genes maintain vegetative development by repressing the flower program in Arabidopsis. Plant Cell 15:681-693.

Mozgova, I., and Hennig, L. (2015). The Polycomb group protein regulatory network. Annu. Rev. Plant Biol. 66:269-296.

Mulligan, G.J., Wong, J., and Jacks, T. (1998). p130 is dispensable in peripheral T lymphocytes: evidence for functional compensation by p107 and pRB. Mol. Cell. Biol. 18:206-220.

Nadi, R., Juan-Vicente, L., Mateo-Bonmatí, E., and Micol, J.L. (2023). The unequal functional redundancy of Arabidopsis *INCURVATA11* and *CUPULIFORMIS2* is not dependent on genetic background. Front. Plant Sci.

Nadi, R., Mateo-Bonmatí, E., Juan-Vicente, L., and Micol, J.L. (2018). The 2OGD superfamily: emerging functions in plant epigenetics and hormone metabolism. Mol. Plant 11:1222-1224.

Ning, Y.Q., Ma, Z.Y., Huang, H.W., Mo, H., Zhao, T.T., Li, L., Cai, T., Chen, S., Ma, L., and He, X.J. (2015). Two novel NAC transcription factors regulate gene expression and flowering time by associating with the histone demethylase JMJ14. Nucleic Acids Res. 43:1469-1484.

Ohad, N., Yadegari, R., Margossian, L., Hannon, M., Michaeli, D., Harada, J.J., Goldberg, R.B., and Fischer, R.L. (1999). Mutations in *FIE*, a WD Polycomb group gene, allow endosperm development without fertilization. Plant Cell 11:407-415.

Okamuro, J.K., Caster, B., Villarroel, R., Van Montagu, M., and Jofuku, K.D. (1997). The AP2 domain of *APETALA2* defines a large new family of DNA binding proteins in *Arabidopsis*. Proc. Natl. Acad. Sci. USA 94:7076-7081.

Orozco-Nunnelly, D.A., Muhammad, D., Mezzich, R., Lee, B.S., Jayathilaka, L., Kaufman, L.S., and Warpeha, K.M. (2014). Pirin1 (PRN1) is a multifunctional protein that regulates quercetin, and impacts specific light and UV responses in the seed-to-seedling transition of *Arabidopsis thaliana*. PLOS One 9:e93371.

Pazhouhandeh, M., Molinier, J., Berr, A., and Genschik, P. (2011). MSI4/FVE interacts with CUL4-DDB1 and a PRC2-like complex to control epigenetic regulation of flowering time in *Arabidopsis*. Proc. Natl. Acad. Sci. USA 108:3430-3435.

Perkins, D.N., Pappin, D.J., Creasy, D.M., and Cottrell, J.S. (1999). Probability-based protein identification by searching sequence databases using mass spectrometry data. Electrophoresis 20:3551-3567.

Petrella, R., Caselli, F., Roig-Villanova, I., Vignati, V., Chiara, M., Ezquer, I., Tadini, L., Kater, M.M., and Gregis, V. (2020). BPC transcription factors and a Polycomb Group protein confine the expression of the ovule identity gene *SEEDSTICK* in Arabidopsis. Plant J. 102:582-599.

Plotnikov, A., Zehorai, E., Procaccia, S., and Seger, R. (2011). The MAPK cascades: signaling components, nuclear roles and mechanisms of nuclear translocation. Biochim. Biophys. Acta 1813:1619-1633.

Ponce, M.R., Quesada, V., and Micol, J.L. (1998). Rapid discrimination of sequences flanking and within T-DNA insertions in the *Arabidopsis* genome. Plant J. 14:497-501.

Qin, N., Xu, D., Li, J., and Deng, X.W. (2020). COP9 signalosome: discovery, conservation, activity, and function. J. Integr. Plant Biol. 62:90-103.

Quesada, V., Ponce, M.R., and Micol, J.L. (2000). Genetic analysis of salt-tolerant mutants in *Arabidopsis thaliana*. Genetics 154:421-436.

Ramirez-Prado, J.S., Latrasse, D., Rodriguez-Granados, N.Y., Huang, Y., Manza-Mianza, D., Brik-Chaouche, R., Jaouannet, M., Citerne, S., Bendahmane, A., Hirt, H., et al. (2019). The Polycomb protein LHP1 regulates *Arabidopsis thaliana* stress responses through the repression of the MYC2-dependent branch of immunity. Plant J. 100:1118-1131.

Roszak, P., and Köhler, C. (2011). Polycomb group proteins are required to couple seed coat initiation to fertilization. Proc. Natl. Acad. Sci. USA 108:20826-20831.

Sanchez-Pulido, L., Devos, D., Sung, Z.R., and Calonje, M. (2008). RAWUL: a new ubiquitin-like domain in PRC1 Ring finger proteins that unveils putative plant and worm PRC1 orthologs. BMC Genom. 9:308.

Sanders, D., Qian, S., Fieweger, R., Lu, L., Dowell, J.A., Denu, J.M., and Zhong, X. (2017). Histone lysine-to-methionine mutations reduce histone methylation and cause developmental pleiotropy. Plant Physiol. 173:2243-2252.

Saze, H., Shiraishi, A., Miura, A., and Kakutani, T. (2008). Control of genic DNA methylation by a jmjC domain–containing protein in *Arabidopsis thaliana*. Science 319:462-465.

Scortecci, K., Michaels, S.D., and Amasino, R.M. (2003). Genetic interactions between *FLM* and other flowering-time genes in *Arabidopsis thaliana*. Plant Mol. Biol. 52:915-922.

Schmittgen, T.D., and Livak, K.J. (2008). Analyzing real-time PCR data by the comparative C_T method. Nat. Protoc. 3:1101-1108.

Schubert, D., Primavesi, L., Bishopp, A., Roberts, G., Doonan, J., Jenuwein, T., and Goodrich, J. (2006). Silencing by plant Polycomb-group genes requires dispersed trimethylation of histone H3 at lysine 27. EMBO J. 25:4638-4649.

Shi, Y., Zhang, X., Xu, Z.Y., Li, L., Zhang, C., Schläppi, M., and Xu, Z.Q. (2011). Influence of EARLI1-like genes on flowering time and lignin synthesis of *Arabidopsis thaliana*. Plant Biol. 13:731-739.

Shu, J., Chen, C., Thapa, R.K., Bian, S., Nguyen, V., Yu, K., Yuan, Z.C., Liu, J., Kohalmi, S.E., Li, C., et al. (2019). Genome-wide occupancy of histone H3K27 methyltransferases CURLY LEAF and SWINGER in *Arabidopsis* seedlings. Plant Direct 3:e00100.

Singh, V., Roy, S., Singh, D., and Nandi, A.K. (2014). *Arabidopsis FLOWERING LOCUS D* influences systemic-acquired-resistance-induced expression and histone modifications of *WRKY* genes. J. Biosci. 39:119-126.

Spedaletti, V., Polticelli, F., Capodaglio, V., Schininà, M.E., Stano, P., Federico, R., and Tavladoraki, P. (2008). Characterization of a lysine-specific histone demethylase from *Arabidopsis thaliana*. Biochemistry 47:4936-4947.

Sung, Z.R., Belachew, A., Shunong, B., and Bertrand-Garcia, R. (1992). *EMF*, an *Arabidopsis* gene required for vegetative shoot development. Science 258:1645-1647.

Tan, L.M., Zhang, C.J., Hou, X.M., Shao, C.R., Lu, Y.J., Zhou, J.X., Li, Y.Q., Li, L., Chen, S., and He, X.J. (2018). The PEAT protein complexes are required for histone deacetylation and heterochromatin silencing. EMBO J. 37:e98770.

The-Galaxy-Community. (2022). The Galaxy platform for accessible, reproducible and collaborative biomedical analyses: 2022 update. Nucleic Acids Res. 50:W345-W351.

Tian, Y., Zheng, H., Zhang, F., Wang, S., Ji, X., Xu, C., He, Y., and Ding, Y. (2019). PRC2 recruitment and H3K27me3 deposition at *FLC* require FCA binding of *COOLAIR*. Sci. Adv. 5:eaau7246.

Trapnell, C., Roberts, A., Goff, L., Pertea, G., Kim, D., Kelley, D.R., Pimentel, H., Salzberg, S.L., Rinn, J.L., and Pachter, L. (2012). Differential gene and transcript expression analysis of RNA-seq experiments with TopHat and Cufflinks. Nat. Protoc. 7:562-578.

Turck, F., Roudier, F., Farrona, S., Martin-Magniette, M.L., Guillaume, E., Buisine, N., Gagnot, S., Martienssen, R.A., Coupland, G., and Colot, V. (2007). Arabidopsis TFL2/LHP1 specifically associates with genes marked by trimethylation of histone H3 lysine 27. PLOS Genet. 3:e86.

Van Leene, J., Eeckhout, D., Cannoot, B., De Winne, N., Persiau, G., Van De Slijke, E., Vercruysse, L., Dedecker, M., Verkest, A., Vandepoele, K., et al. (2015). An improved toolbox to unravel the plant cellular machinery by tandem affinity purification of *Arabidopsis* protein complexes. Nat. Protoc. 10:169-187.

Van Leene, J., Hollunder, J., Eeckhout, D., Persiau, G., Van De Slijke, E., Stals, H., Van Isterdael, G., Verkest, A., Neirynck, S., Buffel, Y., et al. (2010). Targeted interactomics reveals a complex core cell cycle machinery in *Arabidopsis thaliana*. Mol. Syst. Biol. 6:397.

Veluchamy, A., Jégu, T., Ariel, F., Latrasse, D., Mariappan, K.G., Kim, S.K., Crespi, M., Hirt, H., Bergounioux, C., Raynaud, C., et al. (2016). LHP1 regulates H3K27me3 spreading and shapes the three-dimensional conformation of the Arabidopsis genome. PLOS One 11:e0158936.

Wang, D., Tyson, M.D., Jackson, S.S., and Yadegari, R. (2006). Partially redundant functions of two SET-domain polycomb-group proteins in controlling initiation of seed development in *Arabidopsis*. Proc. Natl. Acad. Sci. USA 103:13244-13249.

Wang, H., Liu, C., Cheng, J., Liu, J., Zhang, L., He, C., Shen, W.H., Jin, H., Xu, L., and Zhang, Y. (2016). Arabidopsis flower and embryo developmental genes are repressed in seedlings by different combinations of Polycomb group proteins in association with distinct sets of cis-regulatory elements. PLOS Genet. 12:e1005771.

Wang, M., Zhong, Z., Gallego-Bartolomé, J., Feng, S., Shih, Y.H., Liu, M., Zhou, J., Richey, J.C., Ng, C., Jami-Alahmadi, Y., et al. (2023). Arabidopsis TRB proteins function in H3K4me3 demethylation by recruiting JMJ14. Nat. Commun. 14:1736.

Wang, X., Feng, S., Nakayama, N., Crosby, W.L., Irish, V., Deng, X.W., and Wei, N. (2003). The COP9 signalosome interacts with SCF^{UFO} and participates in Arabidopsis flower development. Plant Cell 15:1071-1082.

Wang, X., Kang, D., Feng, S., Serino, G., Schwechheimer, C., and Wei, N. (2002). CSN1 N-terminal–dependent activity is required for Arabidopsis development but not for Rub1/Nedd8 deconjugation of cullins: a structure-function study of CSN1 subunit of COP9 signalosome. Mol. Biol. Cell 13:646-655.

Wang, Y., He, Y., Su, C., Zentella, R., Sun, T.P., and Wang, L. (2020). Nuclear localized *O*-fucosyltransferase SPY facilitates PRR5 proteolysis to fine-tune the pace of *Arabidopsis* circadian clock. Mol. Plant 13:446-458.

Whittaker, C., and Dean, C. (2017). The *FLC* locus: a platform for discoveries in epigenetics and adaptation. Annu. Rev. Cell. Dev. Biol. 33:555-575.

Wu, P., Peng, M., Li, Z., Yuan, N., Hu, Q., Foster , C., Saski, C., Wu, G., Sun, D., and Luo, H. (2018). DRMY1, a Myb-Like protein, regulates cell expansion and seed production in *Arabidopsis thaliana*. Plant Cell Physiol. 60:285-302.

Xiao, J., and Wagner, D. (2015). Polycomb repression in the regulation of growth and development in *Arabidopsis*. Curr. Opin. Plant Biol. 23:15-24.

Yang, C., Bratzel, F., Hohmann, N., Koch, M., Turck, F., and Calonje, M. (2013). VAL- and AtBMI1-mediated H2Aub initiate the switch from embryonic to postgerminative growth in *Arabidopsis*. Curr. Biol. 23:1324-1329.

Yang, C., Yin, L., Xie, F., Ma, M., Huang, S., Zeng, Y., Shen, W.H., Dong, A., and Li, L. (2020). AtINO80 represses photomorphogenesis by modulating nucleosome density and H2A.Z incorporation in light-related genes. Proc. Natl. Acad. Sci. USA 117:33679-33688.

Yang, C.H., Chen, L.J., and Sung, Z.R. (1995). Genetic regulation of shoot development in *Arabidopsis*: role of the *EMF* genes. Dev. Biol. 169:421-435.

Yang, H., Howard, M., and Dean, C. (2014). Antagonistic roles for H3K36me3 and H3K27me3 in the cold-induced epigenetic switch at *Arabidopsis FLC*. Curr. Biol. 24:1793-1797.

Yanhui, C., Xiaoyuan, Y., Kun, H., Meihua, L., Jigang, L., Zhaofeng, G., Zhiqiang, L., Yunfei, Z., Xiaoxiao, W., Xiaoming, Q., et al. (2006). The MYB transcription factor superfamily of Arabidopsis: expression analysis and phylogenetic comparison with the rice MYB family. Plant Mol. Biol. 60:107-124.

Yoshida, N., Yanai, Y., Chen, L., Kato, Y., Hiratsuka, J., Miwa, T., Sung, Z.R., and Takahashi, S. (2001). EMBRYONIC FLOWER2, a novel Polycomb group protein homolog, mediates shoot development and flowering in Arabidopsis. Plant Cell 13:2471-2481.

Zemach, A., Li, Y., Ben-Meir, H., Oliva, M., Mosquna, A., Kiss, V., Avivi, Y., Ohad, N., and Grafi, G. (2006). Different domains control the localization and mobility of LIKE HETEROCHROMATIN PROTEIN1 in *Arabidopsis* nuclei. Plant Cell 18:133-145.

Zhang, C., Cao, L., Rong, L., An, Z., Zhou, W., Ma, J., Shen, W.H., Zhu, Y., and Dong, A. (2015). The chromatin-remodeling factor AtINO80 plays crucial roles in genome stability maintenance and in plant development. Plant J. 82:655-668.

Zhang, L., Wang, L., Yang, Y., Cui, J., Chang, F., Wang, Y., and Ma, H. (2014). Analysis of *Arabidopsis* floral transcriptome: detection of new florally expressed genes and expansion of Brassicaceae-specific gene families. Front. Plant Sci. 5:802.

Zhang, X., Germann, S., Blus, B.J., Khorasanizadeh, S., Gaudin, V., and Jacobsen, S.E. (2007). The *Arabidopsis* LHP1 protein colocalizes with histone H3 Lys27 trimethylation. Nat. Struct. Mol. Biol. 14:869-871.

Zhang, Y., Cao, G., Qu, L.J., and Gu, H. (2009). Characterization of *Arabidopsis MYB* transcription factor gene *AtMYB17* and its possible regulation by LEAFY and AGL15. J. Genet. Genom. 36:99-107.

Zhou, G., Soufan, O., Ewald, J., Hancock, R.E.W., Basu, N., and Xia, J. (2019). NetworkAnalyst 3.0: a visual analytics platform for comprehensive gene expression profiling and meta-analysis. Nucleic Acids Res. 47:W234-W241.

Zhou, Y., Hartwig, B., James, G.V., Schneeberger, K., and Turck, F. (2016). Complementary activities of TELOMERE REPEAT BINDING proteins and Polycomb Group complexes in transcriptional regulation of target genes. Plant Cell 28:87-101.

Zhou, Y., Romero-Campero, F.J., Gómez-Zambrano, A., Turck, F., and Calonje, M. (2017). H2A monoubiquitination in *Arabidopsis thaliana* is generally independent of LHP1 and PRC2 activity. Genome Biol. 18:e69.

Zhou, Y., Wang, Y., Krause, K., Yang, T., Dongus, J.A., Zhang, Y., and Turck, F. (2018). Telobox motifs recruit CLF/SWN-PRC2 for H3K27me3 deposition via TRB factors in *Arabidopsis*. Nat. Genet. 50:638-644.

Zhu, M., Chen, W., Mirabet, V., Hong, L., Bovio, S., Strauss, S., Schwarz, E.M., Tsugawa, S., Wang, Z., Smith, R.S., et al. (2020). Robust organ size requires robust timing of initiation orchestrated by focused auxin and cytokinin signalling. Nat. Plants 6:686-698.

Overlapping roles of Arabidopsis INCURVATA11 and CUPULIFORMIS2 as Polycomb Repressive Complex 2 accessory proteins

Riad Nadi[1,*], Lucía Juan-Vicente[1,*], Samuel Daniel Lup[1], Yolanda Fernández[2], Vicente Rubio[2], and José Luis Micol[a]

[1]Instituto de Bioingeniería, Universidad Miguel Hernández, Campus de Elche, 03202 Elche, Spain; [2]Centro Nacional de Biotecnología, CNB-CSIC, Madrid, Spain. *These authors contributed equally to this work.

Supplemental Figures and Tables

Supplemental Material included in this file:

Supplemental Figures S1-S4

Supplemental Tables S1-S6

Supplemental Material not included in this file:

Supplemental Datasets DS1-DS8

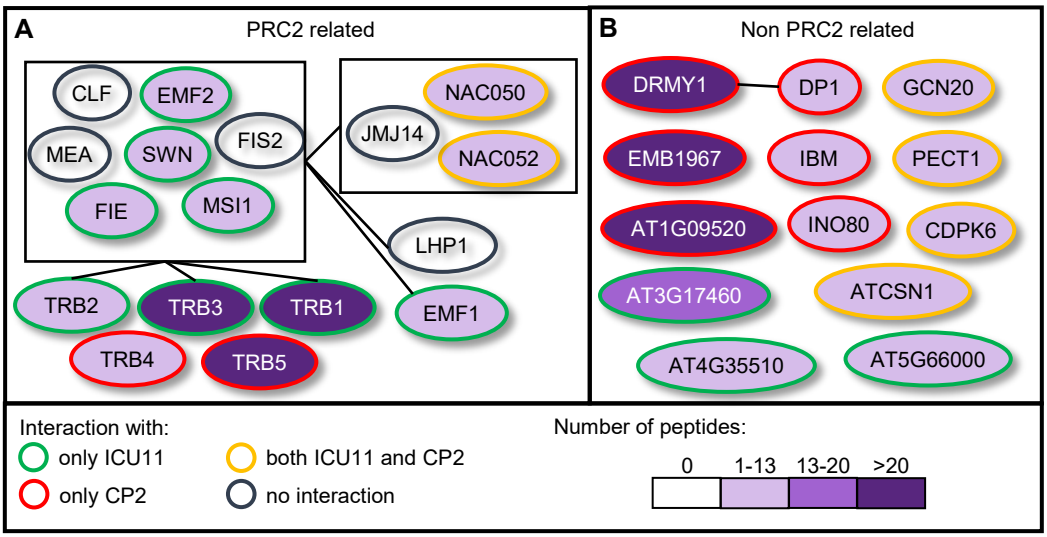

Supplemental Figure S1. Diagram of the protein-protein interactions of ICU11 and CP2 detected in Tandem Affinity Purification (TAP)-based screens. Proteins that interacted with ICU11 and CP2 in TAP assays, classified as (A) known to be related to the PRC2, or (B) not related. Proteins are represented as ellipses outlined in green, red, yellow, and black lines, depending upon their interaction with only ICU11, only CP2, both ICU11 and CP2, or no interaction with ICU11 or CP2, respectively. Black lines indicate previously known interactions. The violet color intensity scale represents the maximum number of peptides from each protein identified as detailed in Supplemental Table S1. Boxes represent the previously described complexes or groups of interacting proteins, and include some that we found not to interact with ICU11 or CP2 (the CLF, MEA and FIS2 core components of PRC2, and the JMJ14 accessory protein).

AT1G49950 (TRB1; 53.33%)

MGAPKQKWTQEEESALKSGVIKHGPGKWRTILKDPEFSGVLYLRSNVDLKDKWRNMSVMANGWGSREKSRLAVKRTFSL
PKQEENSLALTNSLQSDEENVDATSGLQVSSNPPPRRPNVRLDSLIMEAIATLKEPGGCNKTTIGAYIEDQYHAPPDFK
RLLSTKLKYLTSCGKLVKVKRKYRIPNSTPLSSHRRKGLGVFGGKQRTSSLPSPKTDIDEVNFQTRSQIDTEIARMKSM
NVHEAAAVAAQAVAEAEAAMAEAEEAAKEAEAAEAEAEAAQAFAEEASKTLKGRNICKMMIRA

AT5G67580 (TRB2; 42.14%)

MGAPKQKWTPEEEAALKAGVLKHGTGKWRTILSDTEFSLILKSRSNVDLKDKWRNISVTALWGSRKKAKLALKRTPPGT
KQDDNNTALTIVALTNDDERAKPTSPGGSGGGSPRTCASKRSITSLDKIIFEAITNLRELRGSDRTSIFLYIEENFKTP
PNMKRHVAVRLKHLSSNGTLVKIKHKYRFSSNFIPAGARQKAPQLFLEGNNKKDPTKPEENGANSLTKFRVDGELYMIK
GMTAQEAAEAAARAVAEAEFAITEAEQAAKEAERAEAEAEAAQIFAKAAMKALKFRIRNHPW

AT3G49850 (TRB3; 50.51%)

MGAPKLKWTPEEETALKAGVLKHGTGKWRTILSDPVYSTILKSRSNVDLKDKWRNISVTALWGSRKKAKLALKRTPLSG
SRQDDNATAITIVSLANGDVGGQQIDAPSPPAGSCEPPRPSTSVDKIILEAITSLKRPFGPDGKSILMYIEENFKMQPD
MKRLVTSRLKYLTNVGTLVKKKHKYRISQNYMAEGEGQRSPQLLLEGNKENTPKPEENGVKNLTKSQVGGEVMIMGMTE
KEAAAAAAARAVAEAEFAMAEAEEAAREADKAEAEAEAAHIFAKAAMKAVKYRMHSQTR

AT1G17520 (TRB4; 30.74%)

MGNQKLKWTAEEEEALLAGVRKHGPGKWKNILRDPELAEQLSSRSNIDLKDKWRNLSVAPGIQGSKDKIRTPKIKAAAF
HLAAAAAAAIVTPTHSGHSSPVATLPRSGSSDLSIDDSFNIVVDPKNAPRYDGMIFEALSNLTDANGSDVSAIFNFIEQ
RQEVPPNFRRMLSSRLRRLAAQGKLEKVSHLKSTQNFYKMNDNSLVQRTPHVARPKESNTKSRQQTNSQGPSISQQIVE
ASITAAYKLVEVENKLDVSKGAAEEIERLMKLAEEADEMLVIAREMHEECSQGKIMYLN

AT1G72740 (TRB5; 41.81%)

MGNQKLKWTAEEEEALLAGIRKHGPGKWKNILRDPEFADQLIHRSNIDLKDKWRNLSVPPGTQSLTNKARPAKVKEEGD
TPAADANDAVTIPRPIPTIPPPPGRRTLPSELIPDENTKNAPRYDGVIFEALSALADGNGSDVSSIYHFIEPRHEVPPN
FRRILSTRLRRLAAQSKLEKVSTFKSIQNFYKIPDPSGTKIGVPKPKETHTKLRQANNQTSADSQQMIEEAAITAACKV
VEAENKIDVAKLAAEEFEKMTKIAEENRKLLVIATEMHELCSCGETMLLA

Supplemental Figure S2. Peptides from TRB proteins identified using Liquid Chromatography Electrospray Ionization and Tandem Mass Spectrometry (LC-ESI-MS/MS) in ICU11 and CP2 TAP-based screens. Arabidopsis Genome Initiative (AGI) gene identifiers (AtNgNNNNN) are shown, together with the corresponding protein name and peptide coverage (in percentage) for each protein. Full-length protein sequences were obtained from The Arabidopsis Information Resource (TAIR; https://www.arabidopsis.org/). All the peptides identified were protein-specific and are shaded in black; the only exception was the peptide shaded in red, which is identical in TRB2 and TRB3. Peptide coverage is shown as a percentage, and was calculated by dividing the total number of residues of each protein by those of the peptides.

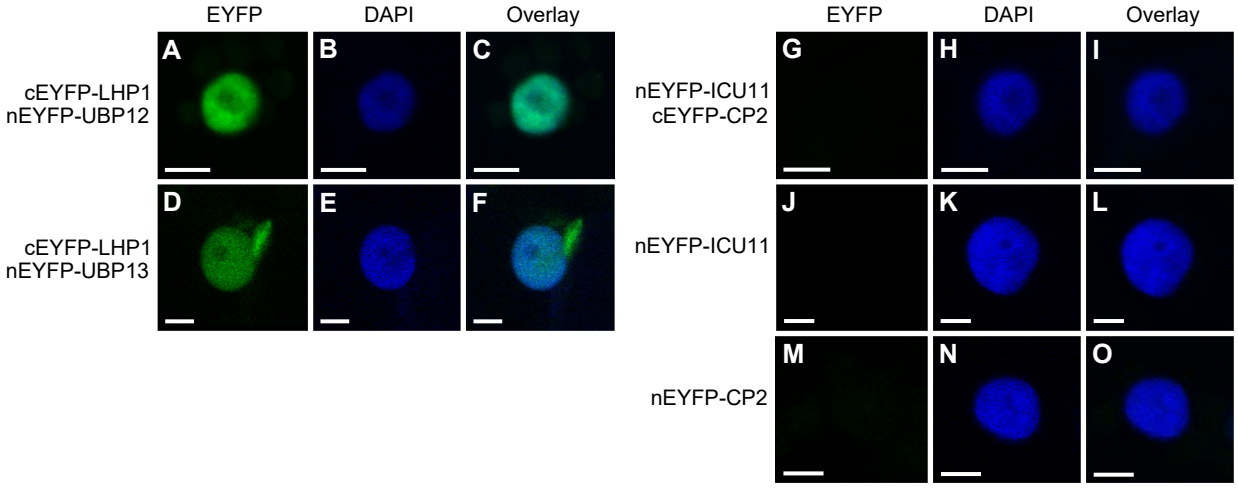

Supplemental Figure S3. Controls used for the Bimolecular Fuorescence Complementation (BiFC) assays. (A–F) Nuclei of *Nicotiana benthamiana* leaf cells showing BiFC of *nEYFP-UBP12* and *nEYFP-UBP13* with *cEYFP-LHP1*, which were used as positive controls. (G–O) Nuclei of *Nicotiana benthamiana* leaf cells showing no BiFC after (G–I) co-infiltration with both *nEYFP-ICU11* and *nEYFP-CP2*, or infiltration with (J–L) only *nEYFP-ICU11* or (M–O) only *cEYFP-CP2*, which were used as negative controls. Fluorescent signals correspond to EYFP (A, D, G, J, M), the DAPI nuclear dye (B, E, H, K, N), and their overlay (C, F, I, L, O). Scale bars, 5 μm.

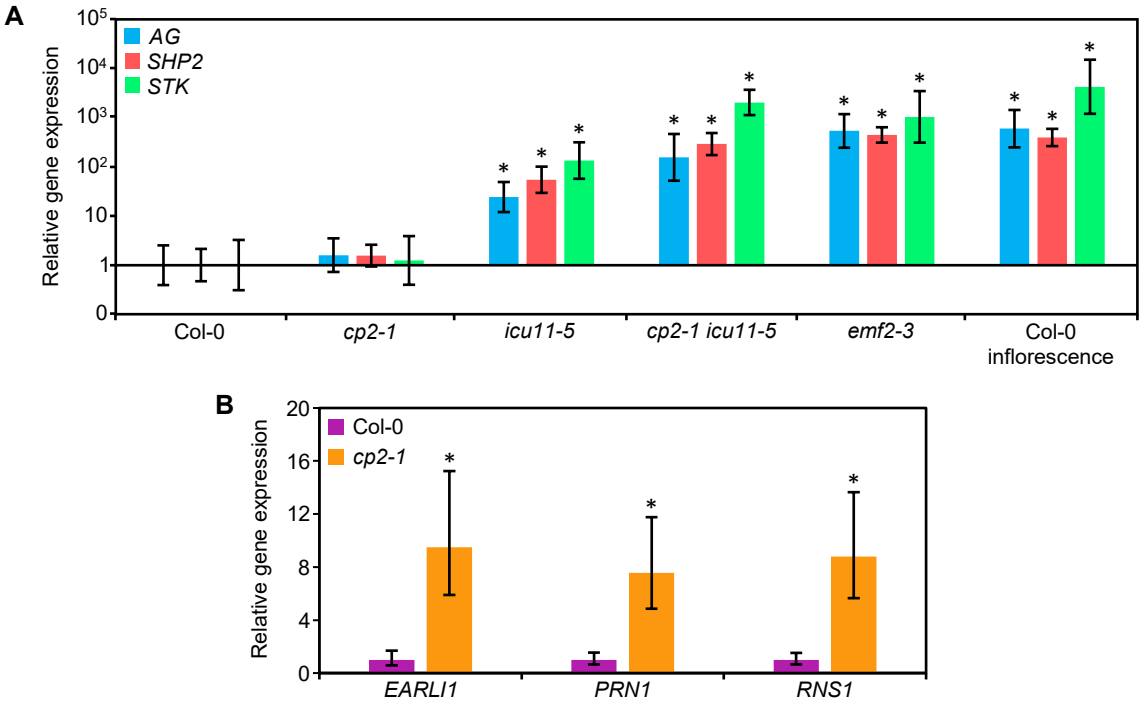

Supplementary Figure S4. Validation by reverse transcription-quantitative PCR (RT-qPCR) of some of the genes found to be upregulated in our RNA-seq analyses. (A) Relative expression of the *AGAMOUS* (*AG*), *SHATTERPROOF 2* (*SHP2*) and *SEEDSTICK* (*STK*) in the aerial tissues of Col-0 (only error bars are visible), *cp2-1* and *icu11-5* seedlings, and *cp2-1 icu11-5* and *emf2-3* embryonic flowers collected 10 das, as well as Col-0 inflorescences collected 40 das. (B) Relative expression of *EARLY ARABIDOPSIS ALUMINUM INDUCED 1* (*EARLI1*), *PIRIN 1* (*PRN1*) and *RIBONUCLEASE 1* (*RNS1*) in aerial tissues of Col-0 and *cp2-1* plants, collected 10 das. Values are means ± standard deviation. Asterisks indicate $2^{-\Delta\Delta C_T}$ values significantly differing from those of Col-0 in a Mann-Whitney *U* test (**P* < 0.01; *n* = 3).

Supplemental Table S1. Selected ICU11 and CP2 interactors identified by TAP-based screens

Sample	Interactor	Full name and/or annotation	Protein score
GSRhino-TAP-tagged ICU11	TRB1[a]	PRC2 accessory protein	962
	TRB3[a]	PRC2 accessory protein	713
	AT3G17460[a]	Nuclear protein with PHD domain	653
	TRB2[a]	PRC2 accessory protein	415
	NAC052[b]	NAC DOMAIN CONTAINING PROTEIN 52; transcription factor	208
	NAC050[b]	NAC DOMAIN CONTAINING PROTEIN 50; transcription factor	158
	ALDH4[b]	ALDEHYDE DEHYDROGENASE 4	115
	EMF1[a]	PRC2 accessory protein	111
	CDPK3[b]	CALCIUM DEPENDENT PROTEIN KINASE 6	133
	AT4G35510	Nuclear protein with PHD domain	104
	AT5G66000[a]	Nuclear protein with PHD domain	92
	GCN20	GENERAL CONTROL NON-REPRESSIBLE 20	87
	EMF2[a]	PRC2 core component	85
	PECT1	PHOSPHORYLETHANOLAMINE CYTIDYLYLTRANSFERASE 1	79
	FIE[a]	PRC2 core component	71
	SWN[a]	PRC2 core component	61
	CSN1	COP9 signalosome complex subunit 1	65
	MSI1[a]	PRC2 core component	45
GSRhino-TAP-tagged CP2	AT1G09520	Hypothetical nuclear protein	1618
	TRB5	TELOMERE REPEAT BINDING FACTOR 5	1067
	DRMY1	DEVELOPMENT RELATED MYB-LIKE1; transcription factor	763
	EMB1967	EMBRYO DEFECTIVE 1967	643
	TRB4	TELOMERE REPEAT BINDING FACTOR 4	374
	IBM1	IMBIBITION-INDUCIBLE 1; transcription factor	324
	RICE1	RISC-INTERACTING CLEARING 3′-5′ EXORIBONUCLEASE 1	197
	DGR1b	DUF642 L-GALL RESPONSIVE GENE 1	181
	CPK3b	CALCIUM DEPENDENT PROTEIN KINASE 3	168
	DP1	DRMY1 PARALOG 1; transcription factor	164
	INO80	INOSITOL REQUIRING80	124

[a]Proteins that were identified in Bloomer et al. (2020).[b]Proteins that were identified in both GSRhino-TAP-tagged ICU11 and CP2 fusions TAP assays. The Protein Score is calculated by the Mascot search engine (Perkins et al., 1999) for each protein; it is based on the probability that peptide mass matches are non-random events. If the Protein Score is equal to or greater than the Mascot Significance Level calculated for the database search, the protein match is considered to be statistically non-random at the 95% confidence interval. The Protein Score is reported as $-10\text{Log}_{10}(P)$ where P is the probability that the observed match is a random event.

Supplemental Table S2. Number of differentially expressed genes in *cp2-1* and *icu11-5* seedlings, *icu11-5 cp2-1* and *emf2-3* embryonic flowers, and Col-0 inflorescences, compared to Col-0 seedlings

Genes	Seedlings		Embryonic flowers		Col-0
	cp2-1	*icu11-5*	*icu11-5 cp2-1*	*emf2-3*	inflorescence
Up-regulated	23	738	3199	2520	5431
Down-regulated	5	78	1770	1774	3084
Total	28	816	4969	4294	8515

All samples were compared to Col-0 seedlings to detect differentially expressed genes which were filtered using padj < 0.05 and |log2FC| > 1.

Supplemental Table S3. Enrichment of overlapping fractions of ChIP-seq and transcriptomic profiles and their statistical significance

Genotype	Mis-regulation	Criterion	Epigenetic marks			Genes bound by			
			H3K27me3	H2AK121ub	H3K36me3	TRB1	EMF1	LHP1	CLF/SWN
icu11-5	Up-regulated	Enrichment factor	2.1	1.6	0.1	1.8	1.9	1.8	3.3
		Fisher's exact test (p-value)	1.309e-35	9.433e-53	1.775e-49	2.022e-36	2.356e-23	2.020e-37	4.153e-27
	Down-regulated	Enrichment factor	3.5	1.8	0.1	0.7	2.8	3	3.6
		Fisher's exact test (p-value)	1.848e-16	3.618e-10	2.986e-07	0.042	5.020e-10	7.706e-25	1.118e-04
icu11-5 cp2-1	Up-regulated	Enrichment factor	2.1	1.8	0.2	1.3	1.9	1.9	2.9
		Fisher's exact test (p-value)	1.808e-160	0.000e+00	7.624e-184	2.979e-23	2.941e-106	1.201e-213	7.910e-94
	Down-regulated	Enrichment factor	1.6	1.6	0.8	0.9	1.6	1.5	1.5
		Fisher's exact test (p-value)	4.350e-28	6.844e-106	9.150e-06	0.045	8.317e-28	3.405e-39	2.972e-06
emf2-3	Up-regulated	Enrichment factor	2.0	1.8	0.3	1.1	2	1.9	3
		Fisher's exact test (p-value)	6.627e-96	5.331e-278	7.833e-98	2.964e-04	2.626e-101	6.249e-157	2.213e-75
	Down-regulated	Enrichment factor	1.7	1.7	0.5	1.1	1.8	1.5	1.8
		Fisher's exact test (p-value)	6.914e-35	7.839e-167	4.799e-37	0.003	4.498e-46	1.521e-43	5.821e-12

Enrichment factors > 1 and < 1 indicate more and less overlap than expected of two independent gene lists, respectively. These data are complementary to those shown in Figure 4.

Supplemental Table S4. Primer sets used in this work

Purpose	Oligonucleotide name(s)	Oligonucleotide sequences (5′ → 3′)	
		Forward primer (F or L)	Reverse primer (R)
Genotyping	At1g22950_1F/R	ACCCTAACCTCTCAAACAAACCA	AGACTTTGTTAACCCAATCCGAC
	At1g22950_4F/R	CCTCTCAAACAAACCATCATCA	CGCTCAGTATCAGGGGAATATC
	SAIL_1215_B02_L/R	GAGCGATAACAGTGAGCTTGG	GACATTTTCAAACCATTCATGC
	AT5G51230_1F/R	TGTAATGGTTCAGAGATCAATAGAA	GTCCGTGCAATCTTGAGAATG
	LB1[a]		GCCTTTTCAGAAATGGATAAATAGCCTTGCTTCC
RT-qPCR	qEARLI1_F/R	GATGCTCTCAGACTCGGTG	CGTCGAGGTCAACCAAACCT
	qRNS1_F/R	CGTTTTGGGAGCACGAATGG	ATCCCGGCTTTGGTTAGAGC
	qATPIRIN1_F/R	GAAGGAAGGTGAAGGAGCTG	TCTGTGAGGATGATCTGGGA
	qACTIN2_F/R	CACTTGCACCAAGCAGCATGAAGA	AATGGAACCACCGATCCAGACACT
	qAG_F/R	CCGATCCAAGAAGAATGAGCTCTT	CATTTTCAGCTATCTTTGCACGAA
	qSTK_F/R	TCAATCTCCCTTTTCTGCGCGTTT	TCAGGTCCAAGAAGCATGAGTTGC
	qSHP2_F/R	TCCGATCCAAGAAGCACGAGATGT	TCGTTTTGCAGCTCGATTTCCCTT
	qOTC_F/R	TGAAGGGACAAAGGTTGTGTATGTT	CGCAGACAAAGTGGAATGGA
Cloning[b]	TAP-CP2_Stop_F/R	ggggacaagtttgtacaaaaaagcaggctCTATGTCAAGTGAGCAGCGAGAAG	ggggaccactttgtacaagaaagctgggtTCAAGCTTGGGTTTGACGTGG
	TAP-CP2_No Stop_F/R	ggggacaagtttgtacaaaaaagcaggctCTATGTCAAGTGAGCAGCGAGAAG	ggggaccactttgtacaagaaagctgggtCAGCTTGGGTTTGACGTGGTTTA
	TAP-ICU11_Stop_F/R	ggggacaagtttgtacaaaaaagcaggctTCATGTGCAATCAAACTCCTCTTAG	ggggaccactttgtacaagaaagctgggtTTACTCGGCACATGATTTTGAAGC
	TAP-ICU11_No Stop_F/R	ggggacaagtttgtacaaaaaagcaggctTCATGTGCAATCAAACTCCTCTTAG	ggggaccactttgtacaagaaagctgggtGCTCGGCACATGATTTTGAAGC
	TRB1_EYFP_Cter_F/R	gggacaagtttgtacaaaaaagcaggctTAATGGGTGCTCCTAAGCAGAAAT	ggggaccactttgtacaagaaagctgggtTCAGGCACGGATCATCATTTTG

Supplemental Table S4 (continued). Primer sets used in this work

Purpose	Oligonucleotide name(s)	Oligonucleotide sequences (5′ → 3′)	
		Forward primer (F)	Reverse primer (R)
Cloning[b]	TRB3_EYFP_Cter_F/R	gggacaagtttgtacaaaaaagcaggctTAATGGGAGCTCCAAAGCTGAAG	ggggaccactttgtacaagaaagctgggtTTACCGAGTTTGGCTATGCATT
	LHP1_EYFP_Cter_F/R	gggacaagtttgtacaaaaaagcaggctTAATGAAAGGGGCAAGTGGTGCT	ggggaccactttgtacaagaaagctgggtTTAAGGCGTTCGATTGTACTTGA
	SWN_EYFP_Cter_F/R	gggacaagtttgtacaaaaaagcaggctTAATGGTGACGGACGATAGCAAC	ggggaccactttgtacaagaaagctgggtTCAATGAGATTGGTGCTTTCTG
	CLF_EYFP_Cter_F/R	gggacaagtttgtacaaaaaagcaggctTAATGGCGTCAGAAGCTTCGCC	ggggaccactttgtacaagaaagctgggtCTAAGCAAGCTTCTTGGGTCTA

[a]Sequence taken from http://signal.salk.edu/tdnaprimers.2.html. [b] The *att*B1 and *att*B2 sequences are represented in lower case.

Supplemental Table S5. TAP and BiFC constructs

Assay	Construct	Insert size (pb)[a]	Coordinates[b]	Destination vector
TAP	GSRhino-TAP-tagged ICU11	1,252	Chr1:8125294-8127168	pKCTAP
	GSRhino-TAP-tagged CP2	1,243	Chr3: 6238266-6240396	pKCTAP
BiFC	nEYFP-ICU11	1,255	Chr1:8125291-8127168	pSITE-nEYFP-C1
	nEYFP-CP2	1,246	Chr3: 6238263-6240396	pSITE-nEYFP-C1
	cEYFP-CLF	2,769	Chr2: 9955570-9960117	pSITE-cEYFP-C1
	cEYFP-SWN	2,632	Chr4: 886692-891473	pSITE-cEYFP-C1
	cEYFP-LHP1	1,399	Chr5: 5827504-5829537	pSITE-cEYFP-C1
	cEYFP-TRB1	1,177	Chr1: 1531806-1534305	pSITE-cEYFP-C1
	cEYFP-TRB2	1,132	Chr2: 13732247-13734361	pSITE-cEYFP-C1
	cEYFP-TRB3	949	Chr3: 18489451-18490731	pSITE-cEYFP-C1

[a]The inserts were amplified from Col-0 cDNA using the *att*B primers shown in Supplemental Table S4. [b]TAIR10 Arabidopsis genome coordinates.

Supplemental Table S6. Quality control summary of RNA-seq analyses

Sample[a]	Number of clean reads	Q30 bases (%)[b]	Read alignment rate (%)
Col-0 #1	53209306	95.78	98.81
Col-0 #2	91762216	95.63	98.41
Col-0 #3	61794508	95.58	98.51
cp2-1 #1	65083932	95.77	97.65
cp2-1 #2	73028616	94.71	98.26
cp2-1 #3	69311310	95.78	98.51
icu11-5 #1	65576476	95.77	98.39
icu11-5 #2	53564942	94.56	98.22
icu11-5 #3	61220290	95.52	98.09
cp2-1 icu11-5 #1	68890358	95.82	98.24
cp2-1 icu11-5 #2	75598942	94.34	98.16
cp2-1 icu11-5 #3	67551250	95.77	98.12
emf2-3 #1	55526214	95.45	98.38
emf2-3 #2	56487776	95.44	98.36
emf2-3 #3	66034456	94.22	98.39
Col-0 inflorescence #1	56192392	95.61	98.16
Col-0 inflorescence #2	55011404	95.78	98.29
Col-0 inflorescence #3	54861298	95.56	98.30

[a]Each line corresponds to a different biological replicate. [b]The Q30 quality score indicates the percentage of bases whose correct base recognition rates are greater than 99.9% for the total bases.

XI.- AGRADECIMIENTOS

XI.- AGRADECIMIENTOS

La realización de esta Tesis ha sido posible gracias a la financiación del trabajo que se realiza en el laboratorio de José Luis Micol por la Generalitat Valenciana (GJIDI/2018/A/214, PROMETEO/2019/117, IDIFEDER/2020/019 e IDIFEDER/2021/033) y el Ministerio de Ciencia e Innovación (EQC2018-005181-P, EQC2019-006592-P, BIO2014-53063-P y PGC2018-093445-B-I00). Durante mi periodo predoctoral he sido beneficiario de un contrato predoctoral Santiago Grisolía (GrisolíaP/2016/131).

Gracias en primer lugar a mi director de Tesis, José Luis Micol, por depositar su confianza en mí y permitirme realizar esta Tesis en su laboratorio; y por ayudarme a aprender cómo superar los diversos problemas a los cuales me he enfrentado durante estos años.

A María Rosa, por su inestimable apoyo, enseñanzas y sugerencias que me permitieron mejorar como investigador.

A todos los profesores del Área de Genética en especial a Sara Jover, Raquel Sarmiento, Héctor Candela, José Manuel Pérez, Victor Quesada y Pedro Robles por las interesantes charlas científicas, y no científicas, que hemos tenido en las diferentes estancias de nuestro instituto y durante las prácticas. También les agradezco su disposición a ayudarme con las dudas que me han surgido.

A Juan Castelló, José Manuel Serrano y Maria José Ñiguez, los excelentes técnicos de nuestro laboratorio, que siempre lo han mantenido en inmejorables condiciones, facilitando así nuestro día a día. José Manuel, siempre serán escasas las palabras que describen como me has acogido fuera del laboratorio, cómo hiciste que un extranjero de otra cultura se sintiera como en su casa “tienes un alma altruista, tienes un alma universal”.

Rosana Martínez Fitor, hemos coincidido solo dos años, pero dos minutos son suficientes para apreciar tu bondad. ¡Verte es sinónimo de alegría, buen humor y energía!

A los doctores David Wilson, Rosa Micol y Tamara Muñoz: hemos coincidido poco tiempo, pero suficiente para aprender de vosotros que defender una tesis y llevar a cabo una investigación es cuestión de ponerle mucho trabajo y dedicación.

A Eduardo Mateo-Bonmatí, me enseñaste desde el protocolo más sencillo hasta el más sencillo, no es un error, sino que contigo lo difícil parece fácil. Aprovecho estas palabras para decirte que eres un auténtico ejemplo a seguir y desearte una brillante carrera científica. Edu, tampoco me has abandonado fuera del lab; como verdaderos ilicitanos, Aida y tú me habéis acogido como miembro de la familia, hemos compartido buenos momentos, pádel, Elche CF, Nit de l’Albá, playa, etc. Es un honor haberme cruzado en tu camino y simplemente hasta siempre.

A mis compañeros presentes, y mis amigos: Alejandro, Sergio, Samuel, Sara, Adrián, Àngela (y su familia) y al ¡wea de Uri! Cada uno de vosotros merece un Oscar del mejor compañero de trabajo, dado que siempre habéis estado dispuestos a ayudar y echar un cable ¡Mil gracias!

Lucía (con acento) y Carla, han sido muchos años y muchos recuerdos, hemos compartido muchas alegrías y unas cuantas penas. En mí habéis grabado vuestros nombres y formas de ser, he disfrutado de cada uno de los momentos que hemos pasado juntos dentro de lab, de lunes a viernes, y fuera del lab en los findes.

A la administración y los profesores del Instituto Agronómico Mediterráneo de Zaragoza y la Universitad de Lleida, que me proporcionaron una excelente oportunidad de realizar el Máster y dar mis primeros pasos en la universidad española.

A mis profesores de la Universidad Saad Dahleb en Argelia, por su capacidad de transmisión de conocimiento a pesar de las dificultades, en especial a doña Fatiha Briki por enseñarme el rigor en el trabajo y darme la oportunidad de enseñar a su lado. Desde lo más profundo de mi alma, deseo que pronto te encuentres la libertad y nos juntemos de nuevo, siempre proclamando libertad de expresión y democracia.

A mis amigos que dejé en Argelia, en especial a Imad, me alegro mucho de mantener los vínculos y os deseo lo mejor en vuestras vidas.

A mis abuelos, que perdí sin poder verlos por última vez, ni darles un último beso, y a mi tío Ali que he perdído debido al maldito Covid-19. ¡Os quiero!

A mi gran familia, grande no solo en número de miembros sino por los valores que se transmiten de cada generación a la siguiente. Orgulloso de tener tías, tíos, primas y primos que siempre han apoyado y animado mis pasos.

A mis padres, Saad y Dalila, nunca dejaré de valorar la magnitud de vuestro sacrificio y vuestra dedicación. Eternamente agradecido, ¡os quiero!

A mi hermanito, que ya es un joven empezando su vida, aprovecho estas palabras para desearte una vida plena, llena de éxitos. Siempre podrás contar conmigo y siempre estaré a tu lado.

A mi mujer, Karima, más de trece años apoyándome y llenando mi vida de alegría, soportándome en los momentos difíciles. Contigo todo parece al alcance de mano.

Por último a mi pequeño, a mi hijo Malik, en solo dos años me has llenado de alegría para el resto de mi vida, ¡te dedico esta tesis y te deseo lo mejor de este mundo!